The interaction of healthy and cancerous cells with nano- and microtopography

Patricia Davidson

L'interaction de cellules saines et cancéreuses avec la micro et la nanotopographie de surface

The interaction of healthy and cancerous cells with nano- and microtopography

Patricia Marie Lyne Hazel DAVIDSON

Doctorat
Chimie des Matériaux

Université de Haute Alsace et
Institut de Science des Matériaux de Mulhouse (IS2M), CNRS LRC 7228
Mulhouse, France

Thèse dirigée par Dr. Karine ANSELME

Soutenue le 28 juin 2011

Président du jury	Dr. Claus FÜTTERER	University of Leipzig
Membre du jury	Dr. Manuel Thery	CEA, Grenoble
Membre du jury	Dr. Michel BORNENS	Institut Curie, Paris (invité)
Rapporteur	Dr. Matthew J. DALBY	University of Glasgow
Rapporteur	Dr. Joachim P. SPATZ	Max Planck Institute for Metals Research, Stuttgart
Co-directeur	Dr. Günter REITER	Institute of Physics, Freiburg University
Directeur	Dr. Karine ANSELME	Institut de Science des Matériaux de Mulhouse

Titre: L'interaction de cellules saines et cancéreuses avec la micro et la nanotopographie de surface

Résumé

L'objet de cette thèse est l'étude comparative de la réponse de cellules saines et malignes à la micro- et la nano-topographie de surface. L'interaction avec des stries de profondeur nanométrique est étudiée grâce à une méthode statistique. Nous démontrons que les cellules saines s'alignent plutôt sur des stries profondes, et que les cellules cancéreuses sont plus sensibles aux stries peu profondes. L'analyse des noyaux révèle qu'ils suivent l'alignement des corps cellulaires plus fidèlement dans le cas des cellules cancéreuses et que les noyaux de ces dernières sont plus sensibles aux stries de faible profondeur.

Sur des micro-piliers nous démontrons que les cellules d'ostéosarcomes sont capables de se déformer et de faire adopter à leurs noyaux la forme de l'espace entre les piliers. Ceci ne se produit que durant la phase initiale d'adhésion pour les cellules saines. Les cellules immortalisées présentent un niveau intermédiaire de déformation. Quand l'espacement entre piliers est réduit, des différences de déformation sont révélées entre les lignées cancéreuses testées. La déformation est aussi liée au caractère cancéreux de kératinocytes et à l'expression de Cdx2 dans des lignées d'adénocarcinomes. Nous avons tenté d'expliquer ce mécanisme de déformation en l'attribuant au cytosquelette grâce à des analyses en microscopie confocale et avec des inhibiteurs du cytosquelette. L'imagerie de cellules vivantes a permis d'observer que les cellules sont très mobiles même quand elles sont déformées, que la mitose nécessite la perte de la déformation et que la déformation après mitose est plus rapide que la déformation pendant l'adhésion initiale des cellules.

Mots-clés: Noyau cellulaire, Déformation cellulaire, Cytosquelette, Métastase, Mécanique cellulaire, Biomateriaux, Interactions cellules-topographie

Title: The interaction of healthy and cancerous cells with nano- and microtopography

Abstract

This thesis deals with the differential response of healthy and cancerous cells to surface topography at the nanoscale and the microscale. Using a statistical method we developed we studied the interactions of cells with grooves of nanoscale depth. We demonstrate that healthy cells have a greater ability to align with deeper grooves, whereas cancerous cells are more sensitive to shallow grooves. Analysis reveals that the nucleus follows the alignment of the cell body more closely in cancerous cells, and that the nucleus of cancerous cells is more sensitive to shallow grooves.

On microscale pillars we demonstrate for the first time that osteosarcoma cells deform to adopt the surface topography and that the deformation extends to the interior of the cell and in particular to the nucleus. We show that healthy cells only deform during the initial stages of adhesion and that immortalized cells show intermediate deformation between the healthy and cancerous cells. When the spacing between the pillars is reduced, differences in the deformation of different cancerous cell lines is detected. Deformation was also found to be related to the malignancy in keratinocytes, and related to the expression of Cdx2 in adenocarcinoma. The mechanism of deformation is tentatively attributed to the cytoskeleton and attempts to identify the main actors of deformation were performed using confocal microscopy and cytoskeleton inhibitors. Live cell imaging experiments reveal that the deformed cells are very mobile on the surfaces, loss of deformation is necessary for mitosis to occur and deformation after mitosis is more rapid than initial deformation upon adhesion to surfaces.

Keywords: Cell nucleus, Cell deformation, C*ytoskeleton, Metastasis, Cell mechanics, Biomaterials, Cell-Topography interactions*

Acknowledgements

First of all I would like to acknowledge Karine Anselme and Günter Reiter, who offered me the chance to work on a project that I find fascinating and has inspired me in my research for over three years. I thank Karine for her enthusiastic contribution to my research, and especially for supporting me in each of my ideas and allowing me enough freedom to choose the directions of my research, and thus fostering my continuing interest in science. Günter has always provided encouragement and a welcome alternate view of the project with his ability to encourage me to think about the bigger picture. Both of them have made a significant impact on my approach to research.

I would also like to acknowledge all of the people who have helped me in my research, starting with the people who were at the institute when I first started and helped me in my first steps, who were there for scientific discussions and who have helped me with my experiments. This includes Lydie Ploux, Artur Ribeiro, Helena Marques, Yu Ma, Mia Mateescu, Felix Sima, Janina Möller, Nicola Cottenye, Judith Böhmler, Dorra Ben Jazia, Laurent Vonna, Doris Campos, Emilia Kulaga, Lionel Dos Ramos, Gautier Laurent, Tatiana Bourgade, and Florent Badique.

I would like to thank all of the numerous collaborators we have been working with for their support and enthusiam for this project. Vasif Hasirci provided the original samples that we worked on and I would like to thank him and his group in Ankara for welcoming me to their laboratory during my secondment. Marta Giazzon, Martha Liley and the people at the CSEM provided samples and also provided support in Neuchatel for experiments. Jean-Noël Freund and his group allowed me to conduct experiments on adenocarcinoma cells by taking care of the cell culture in Strasbourg. Gerhard Baaken and Jürgen Rühe

at IMTEK provided guidance for designing a microfabrication template and arranged to have the samples microfabricated for me. The group of Pascal Tomakidi, in particular Thorsten Steinberg, Simon Schulz and Eva Mussig, graciously provided me with support and access to their lab to conduct experiments on keratinocytes. Maxence Bigerelle contributed extensive analysis work to the microgrooves project. Olivia Fromigué, Pierre Marie and his group graciously welcomed me to Paris several times to allow me to conduct PCR experiments. They also provided numerous cell lines that are an important part of this work. I would also like to especially thank Hiraoka-san and Haraguchi-san for their generous invitation to come work in their laboratory in Japan to conduct experiments. This allowed me to gain significant experience in live cell imaging, which provided me with the background necessary to set up my own experiments in Mulhouse, and which I present in this thesis. Other experiments are ongoing through this collaboration and I am confident that significant breakthroughs will result from this. Also ongoing are mechanical experiments on cells and the cell nucleus with Clemens Franz in Karlsruhe, which I am not presenting here, but will certainly lead to exciting results.

On a more personal level I would like to thank all of my friends and family who have supported me not only during this thesis, but also before and certainly after. This includes all of the people I left behind in Montreal, and newer friends I have made at the institute. In particular, I would like to thank my parents and my brothers for always being there for me and their unwavering support for each of my undertakings. Lastly I would like to thank Jeffrey Mativetsky for his constant support, for listening to me and offering his wisdom, and for his openness and willingness to explore life (and science!) with me.

Table of Contents

Chapter 1

Introduction

The subject of this thesis is the response of human cells to surface topography. In this chapter an introduction to cells with emphasis on points which are important to this thesis will be provided as well as a description of the methods used to fabricate surface topography. The current literature on the effect of surface topography on cells will also be reviewed. In the second chapter the ability of healthy and malignant cells to sense surface structures, and in particular grooves, of nanometric depth will be discussed. In the third chapter the impact of micrometric structures on cells of varying malignancies and type will be studied. We will show that certain types of cells are able to deform themselves, and in particular their nucleus, in response to surface topography. Possible intracellular mechanisms for this deformation will be described. Finally, in the conclusions chapter, we will discuss the impact of our studies on the fields of biology, cancer and cell mechanotransduction, and present future directions for the research in this field.

1.1 Cells

Cells are a basic unit of life. All living organisms are composed of cells. There are two large families of cells: prokaryotic and eukaryotic cells. Archea and bacteria are prokaryotic cells which lack any internal membrane-bound organelles. Animal and plant cells are eukaryotic cells which contain membrane-bound organelles such as the cell nucleus and the golgi apparatus. In the studies performed in this thesis human cells were used in all experiments.

Human cells, like all animal cells, contain a nucleus, which is the information center of the cell. (See

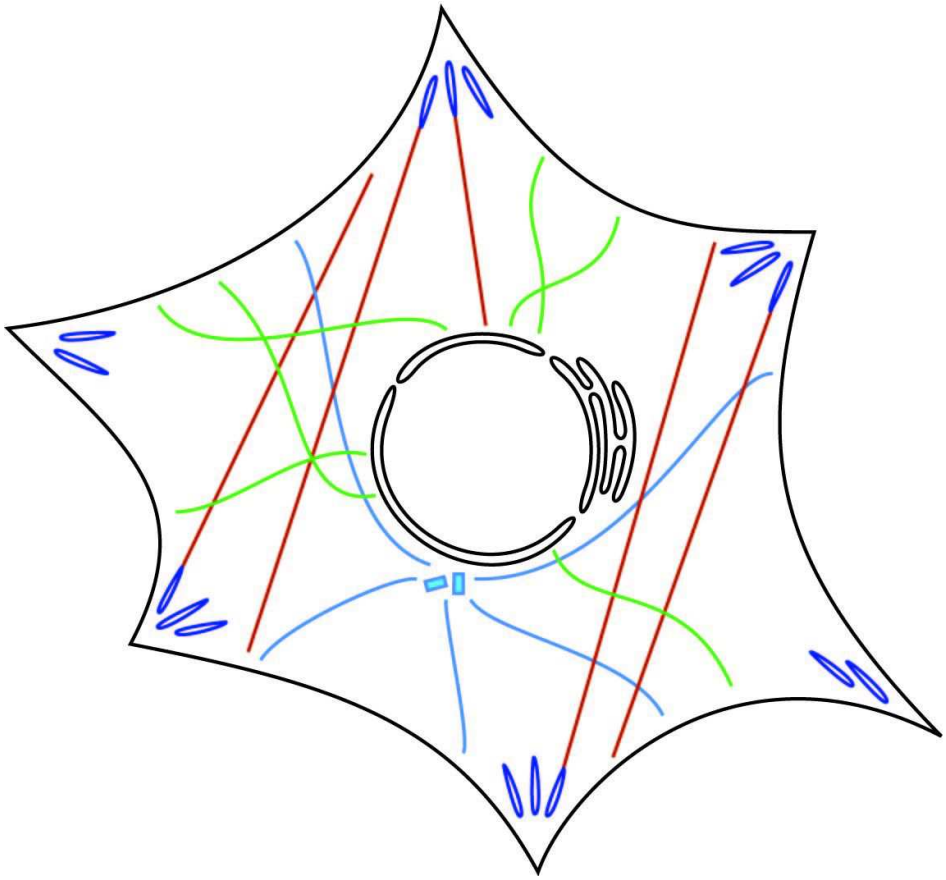

Figure 1: Schematic representation of an animal cell. The cell is delimited by the cytoplasmic membrane (black). In the cell interior are represented the nucleus (black), focal adhesions (purple) and the different components of the cytoskeleton: the actin filaments (red), intermediate filaments (green) and the microtubules (light blue), which are organized around the microtubule organization center (MTOC). Adapted from Rowat et al. [5]

figure 1 for a schematic view.) The cell itself is bound by a cytoplasmic membrane. Structural integrity is provided by the cytoskeleton. Cells are bound to surfaces through adhesion sites termed "focal contacts" or "focal adhesions". In this introduction we will pay close attention to the nucleus, focal adhesions, the cytoskeleton and their properties.

1.1.1 The Cytoskeleton

The cytoskeleton provides structural integrity to the cell. It also allows movement of the cell and movement of entities within the cell. There are three main components of the cytoskeleton: the actin

filaments (microfilaments), microtubules and the intermediate filaments.[1] Although the name "cytoskeleton" implies a solid structure the cytoskeleton is actually a very dynamic structure. Cytoskeletal filaments are constantly being built and taken apart, for example the half-life of microtubules is on the order of minutes.[1] The cell is therefore a dynamic structure that is in constant evolution.

Actin microfilaments have a diameter of 6-8 nm. Actin filaments are made of actin monomers: they are reversible assemblies of monomers (globular actin, or G-actin) into linear polymers (filamentous actin, or F-actin). These filaments can form bundles termed "stress fibres" which generally align themselves in the direction of motion of the cell. Actin filaments play an important role in mobility and structural integrity of the cell. They form an important part of the actin cortex (along the inner cytoplasmic membrane). Myosin is the motor protein responsible for actin-based mobility. Polymerized actin filaments have higher resistance to deformation than the other cytoskeletal filaments.[1]

Recent reports describe the actin network as an assembly of actin filaments with different architectures, depending on the localization of the filaments.[2] These different architectures are a result of the type of actin cross-linking and bundling proteins. Filopodia protrusions contain parallel actin bundles cross-linked with fascin, whereas in the cytoplasm orthogonal networks of filaments are cross-linked with actinin and filamin. At the basal surface of the cell actin filaments assemble into stress fibres which contain the motor protein myosin II, at the dorsal surface (above the nucleus), actin filaments organize into parallel bundles that form the perinuclear actin cap.

Intermediate filaments have a diameter of about 10 nm. They consist of a family of filaments and the type of filament expressed will depend on the type of cell: types I to IV are cytoplasmic and type V are present in the nucleus. These latter filaments form the nuclear lamina, which provides structure to the nuclear membrane. In bone cells the major type of intermediate filament present are vimentin, which

are type III filaments. Vimentin filaments provide rigidity to cells. Intermediate filaments are the least studied of the cytoskeletal filaments but are now believed to be dynamic networks that can crosstalk with the other cytoskeletal filaments.[1]

Microtubules are the thickest filaments with a diameter of approx. 25 nm, consisting of hollow rods with an inner diameter of approximately 14 nm. Microtubules are not stiff enough to impart mechanical integrity to the cytoskeleton. However, they act in concert with other filaments to stabilize the cytoskeleton. They also play a major role in mitosis. Microtubule motor proteins are Kinesin and Dynein. The microtubules are organized around the centrosome, or microtubule organization center (MTOC).[1]

1.1.2 Focal adhesions

The cell attaches to surfaces at discrete points called focal adhesions. These macromolecular assemblies are made up of a cluster of integrins and associated proteins. The focal adhesion sites are the points of attachment of the cell with the extracellular matrix and are the points of transfer of information from the outside of the cell to the interior of the cell. This transfer of information is two-fold: information is transmitted to the cytoskeleton that is anchored in the focal adhesion sites[3] and it is also transmitted through biochemical signalling that is transmitted to the cell from the focal adhesion sites.

Upon attachment of an integrin molecule on a surface other integrin molecules and cytoplasmic proteins are recruited to this attachment site to form a focal adhesion. Integrins are heterodimeric receptor proteins composed of an α and a β subunit.[3] The type of integrin and protein recruited will depend on the cell type and the chemistry present at the surface. Although focal adhesion sites are micrometric structures, the individual integrins that form the connection to the outside are nanometric structures and may thus be sensitive to nanometer scale topography.

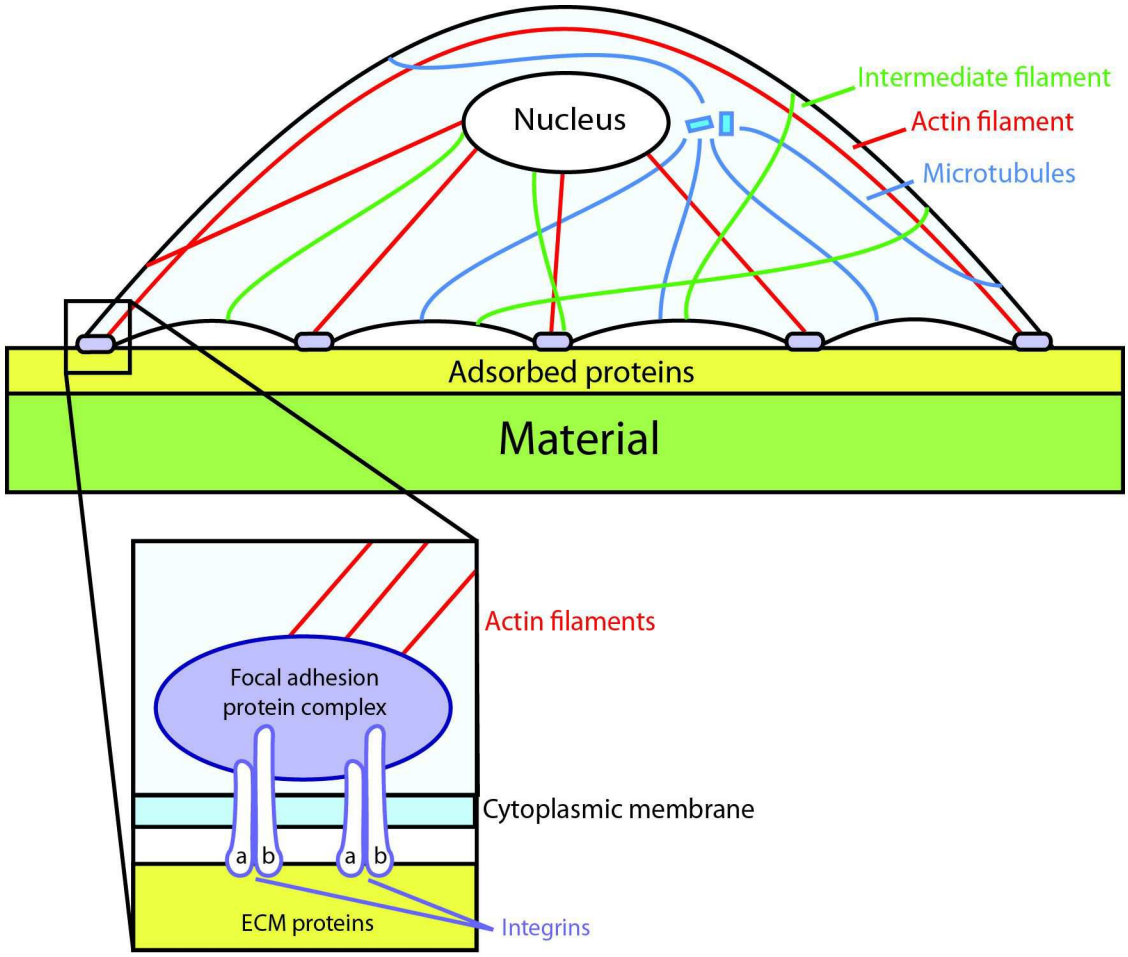

Figure 2: Schematic view of cell-surface interface. Attachment of the cell occurs through the layer of proteins that have been adsorbed at the surface of the material. The points of attachment are the focal adhesion points, which consist of a cluster of integrins attached to the extra-cellular matrix proteins contained in the adsorbed protein layer. On the cytoplasmic side of the membrane, the integrins recruit cytoplasmic proteins that form a protein complex from which signaling occurs and to which cytoskeletal filaments can attach. Actin and intermediate filaments can provide a direct link between the cytoplasmic membrane and the cell nucleus.

Focal adhesion sites differ in mobile and sessile cells. In mobile cells, the focal adhesions are smaller as they are constantly being created at the leading edge of the cell and disassembled from the back of the cell. When a cell is moving it first probes the area surrounding it using a filopodium: a thin actin projection of the cytoplasm. Once a suitable site has been found a focal adhesion is formed at the end of the actin spike.[4] Thus, the first step in cell movement is the focal adhesion formation followed by cell movement towards this new adhesion site.

1.1.3 The Nucleus

The cell nucleus is a membrane-bound organelle that contains the genetic information of the cell. It is principally composed of the nuclear membrane, proteins and DNA. The nucleus can be described as a sac of aqueous solution surrounded by a stretchable membrane that resists shear forces.[5] The nuclear membrane is a double membrane that is continuous with the endoplasmic reticulum. The inner nuclear membrane (INM) and outer nuclear membrane (ONM) are continuous with each other but have specific roles and associated proteins. The nuclear membrane system has transmembrane proteins as well as several pores that allow passage of macromolecules.

1.1.3.1 Mechanical properties of the nucleus

Studies on the nucleus have shown that it is a viscoelastic solid that is 3-4 times stiffer than and twice as viscous as its surrounding cytoplasm.[5,6] It has been suggested that the nuclear envelope is compressed or pre-stressed in its natural state and the lamina on its inner surface can stretch to act as a molecular shock absorber.[7,8] In fact, defects in nuclear lamin have been shown to be related to abnormal nucleus shape and mechanics.[9,10] The rigidity of the nucleus has been shown to be related to the presence of lamin A/C: the nuclei of stem cells which do not express lamin and cells in which lamin has been knocked down are less rigid.[11] Recently, Khatau et al. have proposed a model in which the lamin A/C determines the rigidity of the nuclear cortex, while a peri-nuclear actin cap pulls the nucleus towards the cellular basal surface, resulting in a disk shape rather than a spherical one.[12]

The malignant state of the cell is also thought to affect the rigidity of the nucleus. Atomic force microscopy measurements of the Young's modulus of pre-cancerous cells in the area above the nucleus has shown that the nuclei of healthy cells is more rigid than metaplasic cells which is more rigid than dysplastic cells.[13] This is not surprising given that cancer cells have less lamin A.[14]

1.1.4 Mechanotransduction within the cell: links between the cytoplasmic membrane, the cytoskeleton and the nucleus

As has already been discussed in section 1.1.2, interactions between focal adhesions and actin have already been shown in cell movement. In fact, staining of focal adhesion sites and actin fibres often shows actin stress fibres that are anchored at focal adhesions.[15] Intermediate filaments have recently been shown to associate with focal adhesion sites as well.[16] Specifically, the vimentin cytoskeleton has been shown to interact with β3 integrins.[17] Microtubules have also been shown to interact with focal adhesions, although it is thought that they have a role in disassembling focal adhesions.[18,19]

An area of recent extensive research is the connections between the cytoskeleton and the nucleus. Several links between the cytoskeletal elements and the nucleus have been found and it is now believed that the cytoskeleton has an active role in shaping the nucleus and transmitting information to the interior of the nucleus from the outside of the cell. Specifically, connections have been found between the cytoskeleton and the nuclear membrane. The nuclear membrane contains transmembrane proteins. Some of these proteins, such as the SUN (at the INM) and KASH (at the ONM) families of proteins, bridge the two membranes and provide a link between the cytoskeleton and the nucleus' interior.[20] This

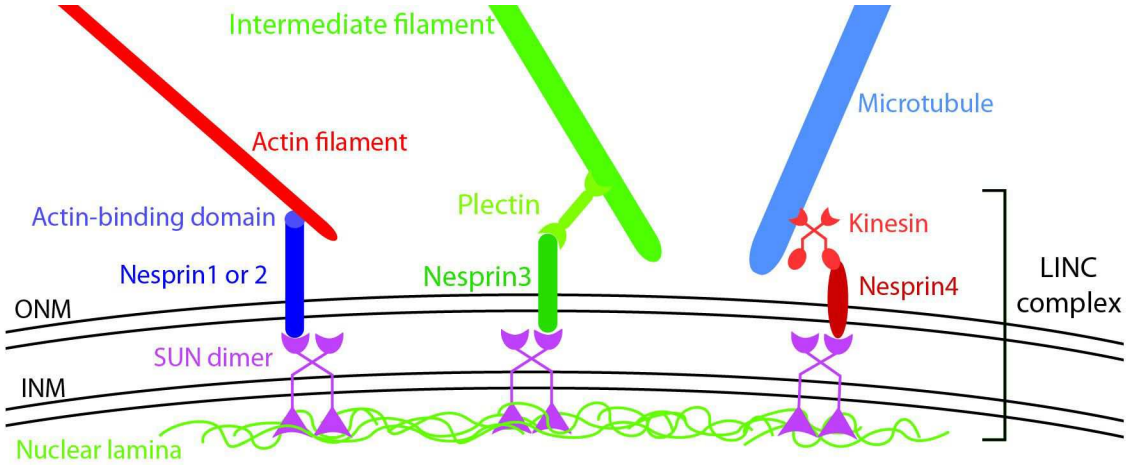

Figure 3: The interactions between the cytoskeleton and the nuclear membrane proteins. Each component of the cytoskeleton is able to connect directly to the nuclear lamina at the interior of the nucleus through the SUN and KASH proteins, which are present at the inner nuclear membrane (INM) and outer nuclear membrane (ONM), respectively. Adapted from Jaalouk et al.[24], Burke and Roux[21] and Starr[23].

complex has been termed the LINC complex, for Linker of the Nucleoskeleton and Cytoskeleton.[21,22] These allow positioning of the nuclei as well as transmission of information to the nucleus[21] and the interior of the nucleus, including displacement of chromosomes.[23] Though these complexes have been discovered only recently, nuclear membrane proteins have been described for each of the cytoskeletal fibres in the cell. In mammals, it has been shown that SUN1 and SUN2 form a dimer with binds to Nesprin 1 or Nesprin 2 (also known as SYNE1 and SYNE2) which have an actin-binding domain, Nesprin 3, which interacts with intermediate filaments through Plectin[24], and Nesprin 4, which interacts with microtubules through kinesin.[21]

The cytoskeleton may also have a more passive role in shaping the nucleus. Recently evidence has been found of a perinuclear actin cap which regulates nucleus shape.[25] The actin filaments in the perinuclear cap are more dynamic than basal stress fibres and small amounts of actin inhibitor will result in a taller nucleus. Additionally, there is evidence that the actin cap fibres are the only ones attached to the nucleus: disruption of LINC complexes disorganizes or eliminates the actin cap without affecting basal stress fibres.[12] The authors have proposed that the function of the actin cap is to pull the nucleus towards the cellular basal surface, resulting in a nucleus that is not spherical, but a disk shape.

There is also additional evidence for involvement of the other types of filaments in nuclear movement and shaping: microtubules are involved in rotation of the nucleus, which is mediated by dynein[26], and defects in vimentin (a type of cytoplasmic intermediate filament) disrupts nuclear morphology.[27]

It is thus well-established that there are direct links between the exterior of the cytoplasmic membrane and the nucleus. This system passes through the focal adhesions sites, through the cytoskeleton and to the interior of the nucleus at the LINC complexes. There are two main hypotheses that try to explain how information is transmitted: percolation and tensegrity. In the percolation hypothesis the signal is believed to percolate through the cytoskeletal system of the cell.[28] On the other hand the tensegrity

hypothesis proposes that the cell is a pre-stressed system under mechanical equilibrium and that any change in one part of the cell will immediately affect the equilibrium of the whole cell.[29]

1.1.5 Cell types

There are many types of mammalian cells. The most basic type of cell is the pluripotent stem cell. This type of cell can give rise to any cell in the body, and in particular to cells of the three germ layers: endoderm, mesoderm and ectoderm. Each of these can give rise to several types of cells through a process known as differentiation. In humans this process is irreversible: differentiated stem cells cannot give rise to pluripotent stem cells. There are several families of cells: among these are the epithelial cells, which are present at the surface of the body (skin, intestinal tract), connective tissue cells, which comprise bone cells, nervous cells and muscle cells.

Cells of the same family may also differ because of genetic mutations. This may lead cells to become cancerous. In fact, cancerous cells have several mutations compared to healthy cells. It is also common for cancerous cells to have multiple copies of chromosomes. In cell culture studies, cancerous cells are obtained from tumours in patients. They are a popular cell type to culture because they proliferate rapidly and do not change their behaviour with time. Comparatively, healthy cells are much harder to culture: they do not proliferate rapidly and their phenotype changes with time in culture. In fact, some healthy cell types cannot be cultured and cancerous counterparts have had to be used in studies. *In vitro*, healthy cells can be modified with viral oncogenes to become ‘‘immortalized’’. This process generally involves inactivation of tumour suppressor genes, which results in increased proliferation.

Generally, immortalized cells are infected with the SV40 virus which blocks the p53 and pRB tumour suppressor genes.[30] Although these cells have now acquired a modification that is specific to cancerous cells they are often not tumorigenic and are used as a substitute for healthy cells.[31] Nevertheless, studies have found several phenotypical modifications in immortalized cells compared to healthy cells and

immortalized cells have also been used as models for cancerous cells. In particular, stimulation of p53 was found to be associated with an increase in organized microfilament bundles[32], and immortalized cells have been found to have an increase in deformability and a decrease in cytoskeletal filament production when compared to healthy cells.[33,34] Care must therefore be taken when these types of cells are used for studies that aim at reproducing conditions within the body.

1.2 Surface topography fabrication

In order to conduct studies on the effect of surface topography, reliable methods to create well-controlled surface structures have been developed. A brief discussion of the available methods is provided here.

The type of structure created for biological studies will depend on the type of interaction that is studied and the available techniques. There are several factors that can be modified in studies: height, aspect ratio, periodicity, size. Additionally, the choice of substrate that is used will determine the rigidity of the structures presented to the cells. Each of these factors has to be looked at when choosing what type of surface will be used.

There are several ways to create topography: material can be etched away from the surface, material can be added to the surface, or a mould can be applied to a soft deformable substrate to alter its topography (embossing). In each case the process can be done using a fabricated mask which will result in controlled structures on the surface, or using a mask-less method, resulting in irregular features.

1.2.1 Controlled surface etching and deposition

Fabricated masks can be used so that the surface can be etched or deposited through these. Several types of mask fabrication techniques are discussed here.

In photolithographic etching a mask is used to create protected areas on a surface. These will result in features upon etching of the surface. The shape and sizes are dictated by the features of the mask, but the limiting factor is usually the light used for mask exposure: resolutions that can be obtained are on the order of half the wavelength of light. Higher resolution features have been obtained by using deep ultraviolet light of extreme ultraviolet light.[35] Unfortunately this requires the use of synchrotron radiation facilities and the lowest resolutions are only possible on very small surface areas. More typical resolutions in standard microfabrication facilities are on the order of a few hundred nanometers. The grooved surfaces used in Chapter 2 were fabricated using conventional photolithography.

In a similar technique a layer of colloids can be used as an etching mask. Using a monolayer will result in regularly-spaced pillars or holes of the same size, although the only packing that can be obtained is hexagonal and the shape is roughly triangular. Smaller structures with larger spacings can be produced by using two monolayers of colloids on top of each other.[35] There are some excellent recent reviews to be consulted on this subject.[36,37]

In order to circumvent the limitation of light in photolithography masks with smaller feature sizes have been created through self-assembly. A technique has been demonstrated in which block copolymer micelles made using an LB trough are transferred to a gold or silicon surface and used to make 50 nm wide disks 5 nm high with hexagonal packing.[38] The sizes of the micelles and the distances between them are tuneable via the size of the polymer blocks and the solvents used.[39,40]

Micelles can also be created on a surface by spin-coating a polymer solution.[41] This technique has been used to make structures with higher aspect ratios. This is done by loading the micellar cores with metal salts which are then reduced to obtain metallic nanoparticles which affect the etching speed.[42] The nanoparticles created can subsequently be removed to obtain uniform chemistry over the entire substrate.

Higher resolution structures can be obtained via sequential techniques. These are usually slow and costly as each structure has to be made individually. The technique that is most widely known is e-beam lithography in which an electron beam is used to create a mask similarly to photolithography. The advantage of using an electron beam is that the resolution is limited to the wavelength of electrons which is much lower than the light used in conventional lithography. Resolutions that can be achieved are as low as 15 nm.[35]

1.2.2 Embossing techniques

Microfabricated substrates can be used as stamps to emboss soft substrates. This technique is often termed "soft lithography". In nanoimprint lithography (NIL, also called hot embossing) a mould containing the negative of the features desired is pressed into a polymer film heated above its glass transition temperature. This is the technique used in the experiments conducted in Chapter 3. In step and flash imprint lithography (S-FIL) a monomer solution is used and exposed to UV light. This technique permits higher aspect ratio features as the solution is of lower viscosity and a rigid mould can be used. Other techniques that can be used on non-planar surfaces using elastomeric stamps are solvent-assisted micromolding (SAMIM), in which a solvent is deposited on top of the polymer film before applying the mold, and microtransfer molding (μTM) in which the mold is filled with curable monomer and subsequently pressed onto the desired surface and cured. More information on these techniques can be found in a recent review by Truskett and Watts.[43]

1.2.3 Mask-less fabrication techniques

Other techniques can be used in which material is etched or deposited without having a controlled mask. These techniques result in even topography that is not easily controllable, but nonetheless results in surfaces of biological relevance.

Nanometer-scale structures are obtainable by polymer demixing. As the process is pushed by the

incompatibility of the two polymers and not by directed self-assembly there is less control over the shapes obtained. Typically worm-like structures can be easily obtained and the average sizes and distances can be controlled.[44] The main disadvantage of this technique is that it may be difficult to separate chemistry from topography as it is the inherent chemical difference between the two polymers that creates the pattern. However, annealing of certain polymers that have the right chemistry can result in uniform surface chemistry.[45]

Fibres can be deposited on a surface by electrospinning, in which a polymer solution is pushed out of a nozzle towards a surface under an applied voltage. This technique produces a fibrous surface which has uniform features, roughness and chemistry. Additionally it is also possible to control the direction of the fibres on the surface.[46] An advantage in biological applications is that these types of surfaces mimic the structure of the extracellular matrix.[47]

1.3 The effect of surface features on cells

Surface topography is a useful tool to understand cellular mechanisms. Studying how cells behave on surfaces of different topographies should provide insight in the way cells relate to their environment. When all of the possible factors are taken into account (width, height, shape, separation between features) there is an infinite number of surface topographies that can be tested. Yet, the limiting factor is the type of structures that can be fabricated with our current technologies, especially at the nanoscale. Hence, the topographies that have been tested are often a result of availability rather than biological relevance. Nevertheless some significant findings have come out of the research performed. In this introduction I will present an overview of the field and highlight some particularly significant results.

There are two main types of surface topography to be distinguished: structural topography, which can affect the shape of the cell, and chemical topography which can confine or govern the type of

interactions the cell can have with the surface.

For a more extensive discussion on the subject of cell interactions with nanotopography, please see the recent review by Anselme et al.[48]

1.3.1 How cells sense surface structures

From a physical perspective, cells should be able to sense the surface topography via their attachment points. Cells attach to a surface through focal adhesions, which have been discussed earlier (section 1.1.2). These adhesion sites are often formed at the leading edge of a cell, and at the end of surface-probing filopodia. Hence, it is likely that these are the features responsible for surface sensing by the cell.

Cells adhered to surfaces typically have diameters of approximately 50-200 microns. Surface topography at this scale can direct the growth of cells. Features in the tens of microns may limit the size or shape of the cell's footprint on the surface, resulting in an altered appearance and architecture when compared to cells grown on flat substrates. Topography that is on the order of 10 microns or less will match the size of sub-cellular components. Structural topography at this scale may direct the placement of filopodia on surfaces. At sub-micron scales, the placement of filopodia may be influenced by the ability of cells to form focal adhesions: small (immature) focal adhesions measure less than 2 μm^2, whereas super-mature adhesions measure more than 6 μm^2.[49] Hence topography at this scale or smaller may result in disruption of normal focal adhesion formation. Examples of this will be shown in the following sections.

Changes in cell behaviour in response to surface topography may be due to several factors. Firstly, the disruption or modification of normal focal adhesion formation may result in cell signalling transmission to the interior of the cell and the nucleus. This may be performed via differences in mechanical transduction to the nucleus or through changes in biochemical pathways. Secondly, the

change in shape that the cell undergoes will result in a strain on the cell when compared to its shape on flat surfaces. This will result in alterations of the balance of forces within the cell, which may be sensed by the nucleus.

1.3.2 Structural topography

Structural topography can act as a barrier to cell movement or as a template to which the cell is forced to conform in order to spread. These result in differences in the cell shape which will be reflected in cell behaviour and differentiation.

1.3.2.1 Micron scale topography

One of the most extensively studied effects of surface topography on cell behaviour is the phenomenon of contact guidance. When cells are grown on a substrate presenting grooves, these will often grow in the direction of the grooves. Alignment in the direction perpendicular to the grooves has also been shown in neurites.[50] A further description of the current knowledge on contact guidance will be provided in Chapter 2.

Structural topography at the micron scale can be combined with chemical confinement. Recently experiments have been undertaken in which cells were seeded on surfaces to which they could only adhere in wells. These wells were meant to mimic the *in vivo* conditions of cells. Cells in the body do not grow on surfaces but within a tissue: they are surrounded by other cells and do not adopt a flattened shape, but rather a more cubic shape. By confining attachment to the interior of a cubic well, the authors were able to study cells in an environment that resembled *in vivo* conditions more closely.[51] They found that the arrangement of the actin cytoskeleton changed significantly with the shape of the cell: on flat surfaces the actin filaments were concentrated at the cell-surface interface whereas in microwells actin was present above and below the nucleus, which occupied the space at the center of the well.[52] It was also found that the assembly of the actin cytoskeleton differed greatly: stress

fibre formation was impeded in the microwells. This is particularly interesting as stress fibre formation does not occur *in vivo* and is thought to be a consequence of surface properties. Additionally, the effect of the stiffness of the substrate was studied and it was found that an actin network was only formed on soft flat substrates and not in cells grown in the soft microwells. Cell metabolism, as measured by mitochondrial activity, was found to be increased in cells in 3D microwells compared to cells confined to the same size on 2D substrates.

Experiments with micron-scale pillars have also been conducted within this thesis. These experiments will be discussed further in Chapter 3.

1.3.2.2 Nanoscale topography

Numerous studies have been conducted at scales around 10 nm. One such study showed that cells were able to respond to islands 13 nm tall, resulting in cells that were more spread, proliferated at a higher rate and had increased actin and tubulin cytoskeleton.[53] Analysis of gene expression revealed that cells grown on these surfaces showed up-regulation of genes related to spreading and growth.[54] On islands 10 nm tall, cells showed increased filopodia production and decreased focal adhesion sizes.[55] In another study a reduction in proliferation was observed for cells grown on rough surfaces with feature sizes on the order of 5 nm.[56] These results suggest that the smallest feature a cell can sense is below 10 nm. At this size scale the effect is certainly due to alterations in the formation of focal adhesions on a molecular scale.

An attempt was made by Dalby et al. to synthesize the information on cells' responses to island surface nanotopography. They proposed that smaller islands result in increased initial adhesion (24 nm or smaller), increased long-term adhesion (13 nm or smaller) and increased cytoskeleton (13 nm or smaller). For larger features the opposite effect was witnessed: reduced adhesion (above 95 nm) and decreased cytoskeleton (above 35 nm).

Experiments have been conducted on TiO_2 nanotube surfaces, in which the cells are exposed to the cross-section of the nanotubes stacked side-by-side. One group has shown increased spreading and differentiation on the nanotubes with larger diameters.[57,58] However, another group showed increased adhesion, proliferation and differentiation on the smaller nanotubes.[59,60] This difference may be due to the type of cell used, in the first case immortalized osteoblast mouse cell line, whereas in the second study mesenchymal stem cells were used.

The organisation of nanostructures may also influence cells. One very important result was the discovery that pitted surfaces can induce differentiation of mesenchymal stem cells into bone cells.[61] This discovery is important in areas such as bone implants, where acceptance of the foreign material may be governed by the ability of cells to behave on the implants as they would on their native substrate. One striking aspect of this discovery was that it is the organization of the surface features that was the determining factor: the surfaces that produced the best results were those in which the structures had the correct amount of disorganization (a mean square displacement of 50 nm). Cells cultured on the organized and random samples did not show the same type of differentiation.

1.3.3 Chemical topography

Chemical topography, as opposed to structural topography, refers to the chemical patterning of the surface. This is different from structural topography because the barriers are not physical structures but differences in chemistry. Hence, geometrically flat surfaces can present patterns to which cells can react to. Chemical topography can be used to confine or restrict the attachment of cells to surfaces.

1.3.3.1 Micrometric patches

Micrometric patches can have an effect on cells when they confine the spreading or movement of the cell. This is the case when the size of the patch is smaller than the size of the spread cell. Using patches of fibronectin of sizes 5 to 40 microns it was found that the number of apoptotic (dying) cells increased

with decreasing patch size.[62] In a similar study they compared the growth and apoptosis rates of cells grown on patches of 20 microns in diameter spaced 40 microns apart, 5 microns in diameters spaced 10 microns apart and 3 microns spaced 6 microns apart. They showed that the rates scaled with geometric spreading of the cell rather than total attachment area with the surface, which stayed more or less constant.[62] In a later study it was shown that patch size can be used to decide stem cell differentiation: mesenchymal stem cells plated on patches 1 or 2 μm^2 differentiated preferentially into adipocytes (fat cells), whereas when they were plated on larger (10 μm^2) patches they differentiated preferentially into osteoblasts (bone cells).[63]

Cell-surface interactions in which the cell shape is constrained have also been shown to modulate organization at the interior of the cell. In a series of experiments Théry et al. have shown that the shape of the adhesions to the surface will determine the orientation of the mitotic spindle during division: square shapes will result in mitotic spindles orienting predominantly along the diagonals of the square, on an L-shaped patch the mitotic spindle will orient along the hypothenuse.[64] Surface adhesion patches can also decide the orientation of the nucleus, centrosome and golgi apparatus of the cell, as well as the arrangement of the cytoskeleton.[65]

1.3.3.2 Nanometric patches

Substrates on which the attachment of cells is restricted on the nanometer scale disrupt the formation of focal adhesion sites. These are structures at the cell surface that have sizes from a few hundred nanometer to several microns; they are composed of clustered integrin receptors that have diameters that are on the order of 10 nm. It has been shown that cells grown on substrates with adhesive patches smaller than the control focal adhesion size have smaller focal adhesions that correspond to the patch size. These also have a different distribution within the cell: focal adhesions are found throughout the cell rather than at the periphery.[66] It has been shown that when the size of the adhesion is limited by the

adhesion patch size, an actin fibre can link several focal adhesions to provide a more stable adhesion complex.[67] In a ground-breaking study, single RGD motifs (to which integrins can attach) were adsorbed onto gold nanoparticles that were positioned with different nanometer-scale spacings. Using this system the authors were able to show that there is a threshold value of the spacing of integrins (around 60-70 nm) during clustering above which attachment is not successful.[3] Thus there is a minimum integrin clustering distance that is necessary for signalling to the cell that attachment has been achieved.

There is also a minimum patch size for stable focal adhesion formation. This is supported by experiments in which cells were unable to spread on adhesive patches 120 nm wide and 250 nm apart.[68]At this size scale, only 4 or 5 integrin moieties would be able to cluster together. Hence, there may be a minimum number of integrin moieties to form a stable moiety.

1.4 Conclusions

The experiments conducted in this thesis compare the behaviour of cells of different malignancies with surface structures. In this introductory chapter we have presented how cells interact with surfaces at the nano and the micron scale. This is an area of research in which there are many points still left to study. In particular, how does the state of the cell (differentiation, malignancy) affect its interactions with the surface? This is an important question that we have attempted to clarify in this thesis. In particular, in the second chapter we are studying the differences between contact guidance of healthy and cancerous cells. This question is of fundamental importance as numerous studies are conducted nowadays in which cancerous cells are used as a substitute for healthy cells. However, do healthy and malignant cells react to surface structures in the same way? The multiple transformations that cancerous cells undergo when compared to healthy cells result in higher proliferation and greater deformability. It is

unreasonable to assume that this does not translate to a difference in cell-surface interactions as well. In this second chapter we will thus study the contact guidance of these two cell types in a quantifiable manner to obtain comparable data.

Studies performed at the micron scale are often at scales that are much larger or much smaller than the cell. Few studies have been performed at the sub-cellular scale. At this scale, the surface topography matches the size of the components at the interior of the cell, the organelles. Based on results shown in the literature, we would not expect deformation of the cells. However, if the cell adhesion to the surface was high enough and the cell was deformable enough, could we see deformation of the cell in response to the surface structures? Would we also see deformation of components at the interior of the cell and reorganisation of the cell's interior? Once again, the question of the state of the cell arises: mechanical properties have been reported to depend strongly on the differentiation and malignant state of the cell. Could these have an effect on the interactions of the cells with the surface?

Some of the results described in this thesis have already been published. This includes an article on a statistical method to quantify cell orientation, which is covered in chapter 2,[69] and two articles on the effect of micrometric topography on cells, which is covered in chapter 3.[70,71]

Chapter 2
The interactions of cells with structures at the nano-scale

2.1 Introduction

The interest in topography has stemmed from observations that many cell types move along well defined topographical features and change their morphology in response to physical cues.[72] Cells are known to be able to align with and elongate in the direction of grooves. This behaviour was first described in 1911 and termed "contact guidance" by Weiss in 1964.[73] This phenomenon has been of particular interest because *in vivo* cells reside on an extracellular matrix composed of fibres, which may play a role in directing cell motility and tissue organisation. Contact guidance has been shown in micro- and nanogrooves and on fibrous textures. Several studies have tried to address and quantify this behaviour, including studies as a function of groove depth and for different cell types. Studies have been performed on several cell types, including fibroblasts,[74-77] epithelial cells,[77,78] and osteoblasts[79] and a few studies have attempted to compare the contact guidance of different types of cells,[80] including a paper comparing healthy and cancerous cells,[81] which hinted that cancerous cells showed less alignment with surface grooves. A study by Sutherland et al. has also pointed out the effect of cell confluence in aiding contact guidance.[74]

Contact guidance, through its effects on cell shape, regulates cell survival,[82] proliferation,[62,83,84] and differentiation[85] but also has a profound effect on matrix organisation.[86,87] Some review papers have summarized the studies that have documented the effects of synthetic micro- and nano-grooved surfaces on cell behaviour.[88]

Contact guidance is often quantified in articles by determining the percentage of cells that are within 10,[73,74,77,89] 15,[76,90] or 45 [81] degrees of the structures, or by building histograms of the distribution of

angles.[79,91,92] One study has reported the values of the standard deviation of the distribution,[4] which we have also evaluated to be a meaningful description of the spread of angle values, and therefore the degree of alignment of the cells. However very few of them have developed statistical comparisons of the contact guidance of cells as a function of groove width or depth.[93,94] Yet, it is known that the cell response to grooves depends on their depth. A parameter that quantifies the influence of the grooves on the cells, as a function of depth, would allow the comparison of experiments in which grooves of different dimensions were used.

Cancerous cells are used extensively in cell culture as models for the interactions of cells with biomaterials. However, little thought is put into the fact that cancerous cells may have different responses to surfaces than healthy cells. It is therefore important to compare the behaviours of these two cell types on surfaces. In this first experimental chapter we will look at how cells of different malignant phenotypes can respond to grooves to a different extent. We will develop a statistical method to quantitatively analyze the data, which will allow us to compare different conditions more accurately, something that is currently missing in the field. We will then compare the contact guidance of a cancerous and a healthy cell line and we will also look at the effect of contact guidance of the cell on the nucleus.

2.2 Statistical analysis methods used

The aim of the statistical analysis developed was to have a simple method of comparing the contact guidance behaviour across different experiments. As discussed above, currently contact guidance is compared across samples by calculating the fraction of cells aligned within a set angle of the structures.

Our approach is based on the standard deviation of the data. This value is a measure of the spread of the angle measurements. It can thus be used as a measure of how disperse the angles between the cell and

the grooves are. If the cells are well aligned, they will have small values of the angle, therefore the standard deviation will be small. To reflect the importance of this parameter, we have named it the cell orientation parameter. We have decided to retain the notation "σ" for simplicity.

In our analysis, we first determined that the data can be modelled on a truncated Gaussian distribution, the shape of which can be obtained from the cell orientation parameter following a simple equation. Secondly, we developed a test to determine whether the data is aligned within a 95% confidence interval, based on the cell orientation parameter and the number of data points. Thirdly we used the cell orientation parameters of the samples at each time point and plotted them against the groove depth. From this figure we could fit the data to a function that we proposed and obtain sensitivity parameters that are independent of the groove depth. We can thus compare different experiments independently from the type of groove that is used.

2.2.1 Finding a model for the data

The alignment data is a random distribution that is constrained within the interval -90 to +90 degrees. We can therefore consider that it has a Gaussian distribution that is constrained to that interval. There are two ways we can consider that the Gaussian distribution is constrained: firstly that it is truncated at those values, or secondly that it is a wrapped distribution, i.e. that it is a continuous distribution that repeatedly folds over on itself at -90 and +90 degrees. Wrapped distributions have been studied by mathematicians and mathematical equations have been established to model these. However, in our case it is difficult to understand how a wrapped distribution could model the behaviour of a cell on a surface, as cells will react to the direction of the grooves within an interval of [-90, +90] degrees, and not greater. Based on this consideration we have developed a truncated model and tested both models with data obtained in the experiments to test whether both can be used.

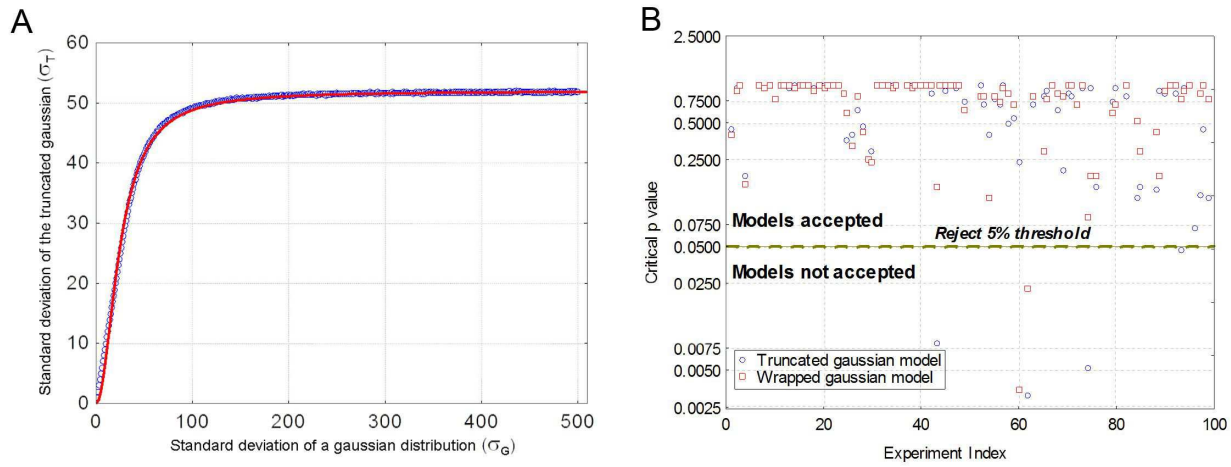

Figure 4: A) Comparison of the Standard deviation of a Gaussian and its standard deviation when it is truncated between -90 and +90 degrees. B) Comparison of the Truncated Gaussian model and the Wrapped Gaussian model, showing that our truncated model is rejected in 3 cases, and the wrapped gaussian is rejected in 2 cases, both of which are within the 95% confidence interval.

2.2.1.1 Modelling the truncated Gaussian distribution

A few considerations are necessary before we can try to model our truncated Gaussian distribution. If the cells are not aligned with the surface structures, we should obtain a square function that has a value of zero except within the [-90, +90] interval, where the value is constant. Such a distribution is called a uniform distribution and its standard deviation is calculated using the following formula:

$$\sqrt{\frac{((max-min)^2)}{12}}=\sqrt{\frac{((90-(-90))^2)}{12}}=\sqrt{\frac{180^2}{12}}=52$$

To model our truncated Gaussian distribution we simulated distributions by generating Monte Carlo simulations of Gaussian distributions and rejecting values that were outside the [-90, +90] interval. For each value of a standard deviation of a normal Gaussian distribution (σ_G) we obtained a set of 100000 data points that were not rejected (within the [-90, +90] interval) and calculated the resulting truncated standard deviation (σ_t). We repeated this for different values of σ_G and then plotted these against the σ_t obtained. (Figure 4A.) We fitted the data and obtained the following relationship:

$$\sigma_t = \frac{52}{1 + 534\,\sigma_G^{-1.96}} \quad (1)$$

Thus, for any value of the cell orientation parameter (i.e. the standard deviation of the alignment angles) we can obtain the corresponding normal Gaussian distribution to be truncated to model the data. Using this simple relationship we can model any truncated distribution using simply the cell orientation parameter of the sample.

2.2.1.2 Comparing to the Wrapped normal distribution.

Modelling using the wrapped normal distribution was performed on our data (99 samples). The wrapped normal distribution uses parameters that are not intuitive and are much more difficult to process for a non-mathematician. To validate our model we performed a chi-squared test on both the analysis performed using the truncated Gaussian model and the wrapped normal distribution. The results are shown graphically in figure 4B. Three tests fail for the truncated Gaussian distribution, whereas only 2 tests fail for the wrapped normal distribution. However we can say that both models are valid for our distribution at a 95% confidence interval. As the results are comparable we maintain that the truncated Gaussian distribution is a reasonable approximation. Its ease of use makes it an attractive solution for this type of modelling.

2.2.2 Confidence on the cell orientation parameter

As we have explained above, the cell orientation parameter of a randomly oriented sample would have a value of 52 degrees. Thus, samples that have cell orientation parameters below this value can be considered to be aligned. However, there is a confidence interval on the cell orientation parameter that depends on the number of data points used to calculate it. Therefore, a sample can be considered to be aligned with the grooves within a 95% confidence interval if the value is smaller than:

$$\sigma_{H0}(n)=52-\sigma_n \quad (2)$$

Where n is the number of data points. The 95% confidence interval of σ_{H0} (n) was determined for several values of n using a Monte Carlo simulation. These were plotted against n and equation 3 was derived to fit this plot. Thus, the threshold value can be calculated using the following model:

$$\sigma_{H0}(n)=\frac{52}{1+0.94\mathrm{n}^{-0.51}} \quad (3)$$

Figure 5 represents this relationship, the line corresponding to the equation 3 and points representing the values of σ_{H0} obtained by Monte-Carlo simulation. Thus, for any sample containing n alignment data points, we can obtain the corresponding value of σ_{H0} using this relationship. This value will be the upper limit of the cell orientation parameter below which the cell can be considered to be significantly aligned with the surface groove at a 95% confidence interval.

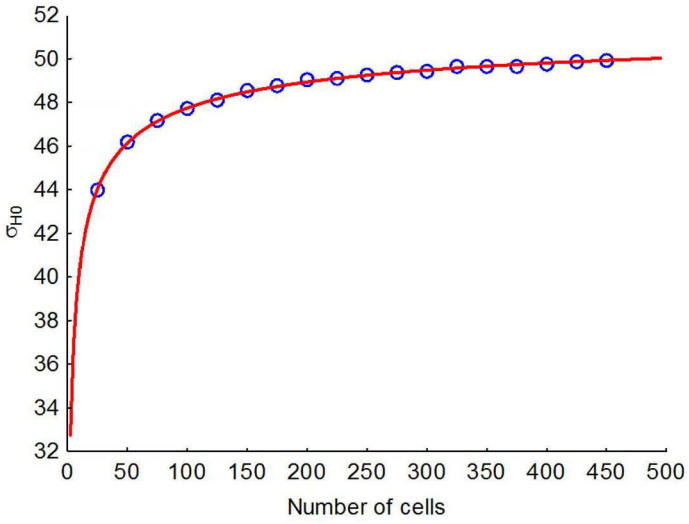

Figure 5: Relationship between the number of cells and the threshold value of the standard deviation

2.2.3 Determination of parameters that describe contact guidance and are independent of experimental conditions

Based on the results we obtained, for any given time in culture, the value of the cell orientation

parameter decreases with increasing groove depth. After plotting the cell orientation parameters versus the depth we have proposed the following relationship:

$$\sigma = b + \frac{\sigma_0 - b}{1 + aR} \tag{4}$$

Where σ_0 is a constant that corresponds to the value of the cell orientation parameter for a randomly aligned sample (52 degrees), and R is the groove depth. We can validate this model by considering the values obtained for the cell orientation parameters under extreme conditions, i.e. zero depth, and infinite depth. For zero depth, the value of the cell orientation parameter becomes σ_0, which is correct as it is the value of the cell orientation parameter of a randomly oriented sample. At infinite depth we obtain $\sigma = b$, therefore we have renamed this term the cell orientation at infinite depth, $\alpha_{inf:}$

$$\sigma = \alpha_{inf} + \frac{\sigma_0 - \alpha_{inf}}{1 + aR} \tag{5}$$

The value of "a" is related to the slope of the asymptote of the curve at zero groove depth, a measure of the sensitivity of the cells to shallow grooves. This slope, termed the groove depth effect coefficient (C_{GDE}) can be derived from the equation and was determined to be equal to:

$$C_{GDE} = (52 - \alpha_{inf}) * a \tag{6}$$

The values obtained for the variables α_{inf} and C_{GDE}, which are independent of the groove dimensions, provide us with quantifiable parameters which we can use to compare the behaviors of different cell lines. In particular, the value of α_{inf} is only dependent on cell type, whereas the value of C_{GDE} is also

dependent on time in culture, as we will see later.

2.3 Experimental methods

2.3.1 Quartz surfaces

Micropatterned quartz surfaces were fabricated by photolithography and plasma etching at the CSEM in Neuchatel. These consisted of surfaces presenting nine circular areas on which grooves 2 microns apart and 5.9 microns wide with depths of 30, 100, 200 or 500 nm had been etched. Glass slides were also used as a flat control. Before cell seeding these were cleaned in a piranha solution (3:1 H_2SO_4:H_2O_2), resulting in a hydrophilic surface, followed by a basic piranha (3:1 NH_4OH:H_2O_2). The samples were then sterilized by incubating them in ethanol overnight.

2.3.2 Cell culture

Human Osteoprogenitor (HOP) cells were prepared from the bone marrow of normal patients as previously described[95] and SaOs-2 cells were obtained from the ECACC. HOP cells were cultured in complete modified DMEM (Iscove) medium and SaOs-2 cells were cultured in complete McCoy medium, both containing 10% fetal bovine serum, 100 U ml^{-1} penicillin and 0.1 mg ml^{-1} streptomycin. Prior to cell seeding the samples were rinsed with sterile PBS twice and the cells were inoculated on the samples in 24-well plates at a seeding density of 7000 (HOP) or 10000 cells/cm^2 (HOP and SaOs-2). The samples were then kept in an incubator at 37 degrees and 5% CO_2 until they were ready to be fixed. Incubation times were 4, 24, 48, 72 and 120 hours for HOP cells and 24, 48, 72, 120 and 168 hours for the SaOs-2 cells which took longer to create stable attachments to the surfaces. The medium was changed after 3 days of incubation (after the 72 hour time point). When the desired amount of incubation time had passed the samples were rinsed twice with warm PBS and then incubated in 2%

paraformaldehyde in Na_2HPO_4 buffer for at least 20 minutes.

2.3.3 Fluorescent labelling and image acquisition

The cells were prepared for immunofluorescence staining by permeabilising the membranes with 0.2% Triton 100-X and blocking with 1% BSA. The samples were then incubated in 0.4 μg ml^{-1} Phalloidin-FITC (Sigma, L'Isle d'Abeau, France) solution for one hour at room temperature, followed by incubation in 100 ng ml^{-1} DAPI (Sigma, L'Isle d'Abeau, France) for 15 minutes at room temperature. Each step was followed by three rinses with PBS. Following staining, each sample was mounted in between glass slides using a PBS:glycerin 50:50 mixture. The samples were then imaged on an epifluorescence microscope (Olympus BX-51). Nine images were obtained per sample. Images using a direct interference contrast (DIC) filter were also obtained to determine the direction of the grooves.

2.3.4 Alignment and aspect ratio measurements

Following image acquisition the fluorescence images were used for alignment measurements using ImageJ software. In the case of the cells, the alignment was determined by drawing a line on the cell along its main axis in a contrasting colour. The direction of each line was then collected by ImageJ. Briefly, a threshold was applied to convert the images to black and white images where only the lines drawn on top of the cells remained. Each line was then fitted to an ellipse and the major axis of the ellipse was used as the direction of the main axis of the cell. Similarly, the orientation and aspect ratio of each nucleus were determined by fitting the shape of the nucleus to an ellipse and obtaining the orientation of its major axis and the lengths of its major and minor axes. The direction of the grooves was also determined from the DIC images. This was used to obtain the orientation of the cells relative to the grooves.

2.3.5 Cell coverage

The area fraction of the image taken up by the cells on each sample was determined by analyzing the images using ImageJ. Briefly, the threshold function was used to convert actin-labelled micrographs to black and white images indicating the presence of the cells. The software was then able to calculate the area fraction of the two zones. The number of cells per image was determined from the number of nuclei in each of the DAPI-stained images. The area fraction per cell was determined from the area fraction of the image and the number of the cells in that image.

2.4 Results

2.4.1 Morphology of the cells

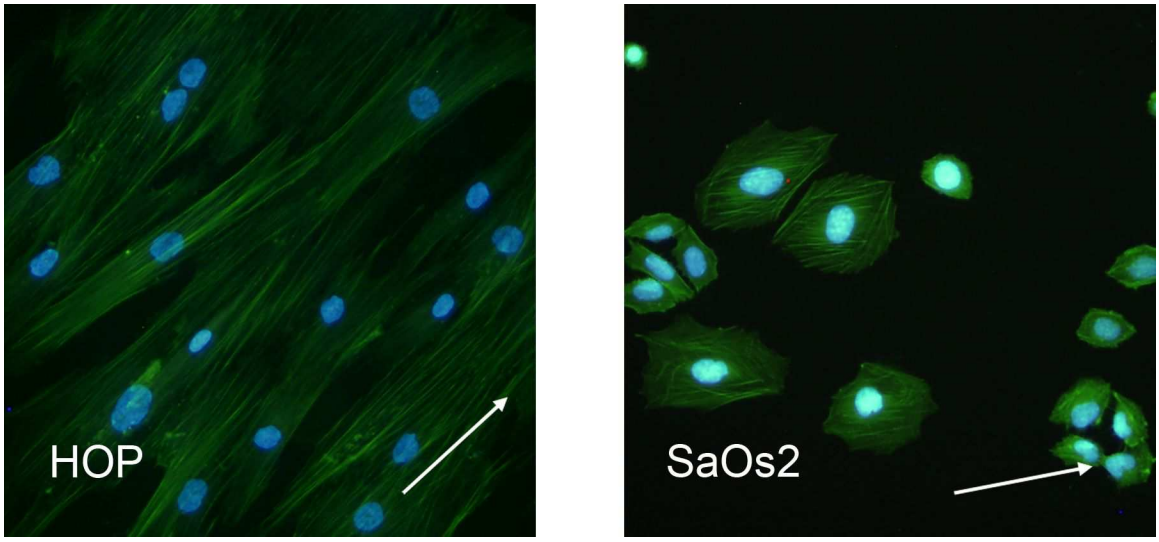

Figure 6: Fluorescence images of HOP and SaOs2 cells grown on grooves 200 nm deep for 72 hours. The arrows indicate the direction of the grooves.

Experiments were conducted on two types of human bone cells. One of them is an established cell line that originates from an osteosarcoma (SaOs-2) and the other was obtained from the bone marrow of healthy patients (HOP). The cells showed classical morphologies for their cell types when grown on the substrates. (Figure 6.) Both were more rounded at short incubation times and spread more with time.

HOP cells showed an organized cytoskeleton, which occasionally seemed to match the orientation of the deeper grooves even at short incubation times and the cells were increasingly elongated in the direction of the grooves at longer incubation times. SaOs-2 cells took up a smaller surface area on substrates. At long incubation times more of the SaOs-2 cells were elongated and well-spread with a well-defined organized cytoskeleton, but a significant population of cells was small and rounded with a more diffuse cytoskeleton, compared to HOP cells which were all well-spread. The nuclei of both cell types had a normal appearance, and were of similar area, despite the size difference visible in the cell bodies.

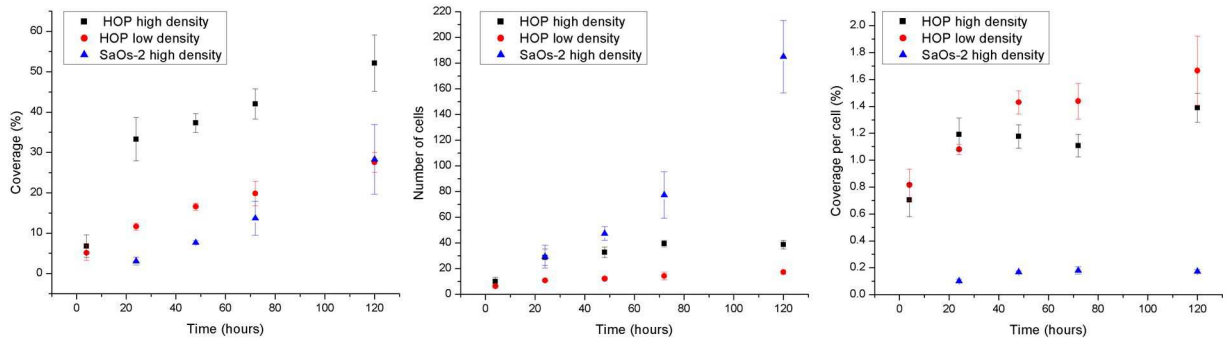

Figure 7: Area coverage, number of cells per sample and area coverage per cell for each of the conditions studied.

2.4.2. Cell coverage

The surface coverage of the cells was determined to study the cooperative effect that may occur when cells are close enough to sense each other. The area fraction covered by the cells was determined by examining the micrographs for one batch of experiments for each condition. The values were not found to depend on the groove depth, and thus the values obtained for each time point were averaged. The coverage values were found to increase steadily with time for each cell type. (Figure 7.) Initial values of the coverage of SaOs-2 cells at the same density are much smaller than for the HOP cells. In fact, the coverage density of the SaOs-2 cells is much closer to the lower density HOP cells. Therefore, when comparing the SaOs-2 cells and the HOP cells for evidence of confluence effects, the SaOs-2 cells

should be compared to the low density HOP cells. The coverage rate and the cell number of the SaOs-2 cells increases more quickly than the HOP cells. This reflects the higher proliferation rates of the cancerous SaOs-2 cells. The coverage difference between the low density and the high density HOP cells is higher than expected given that the initial seeding difference is only 30%. (Figure 7.)

2.4.3. Alignment measurements

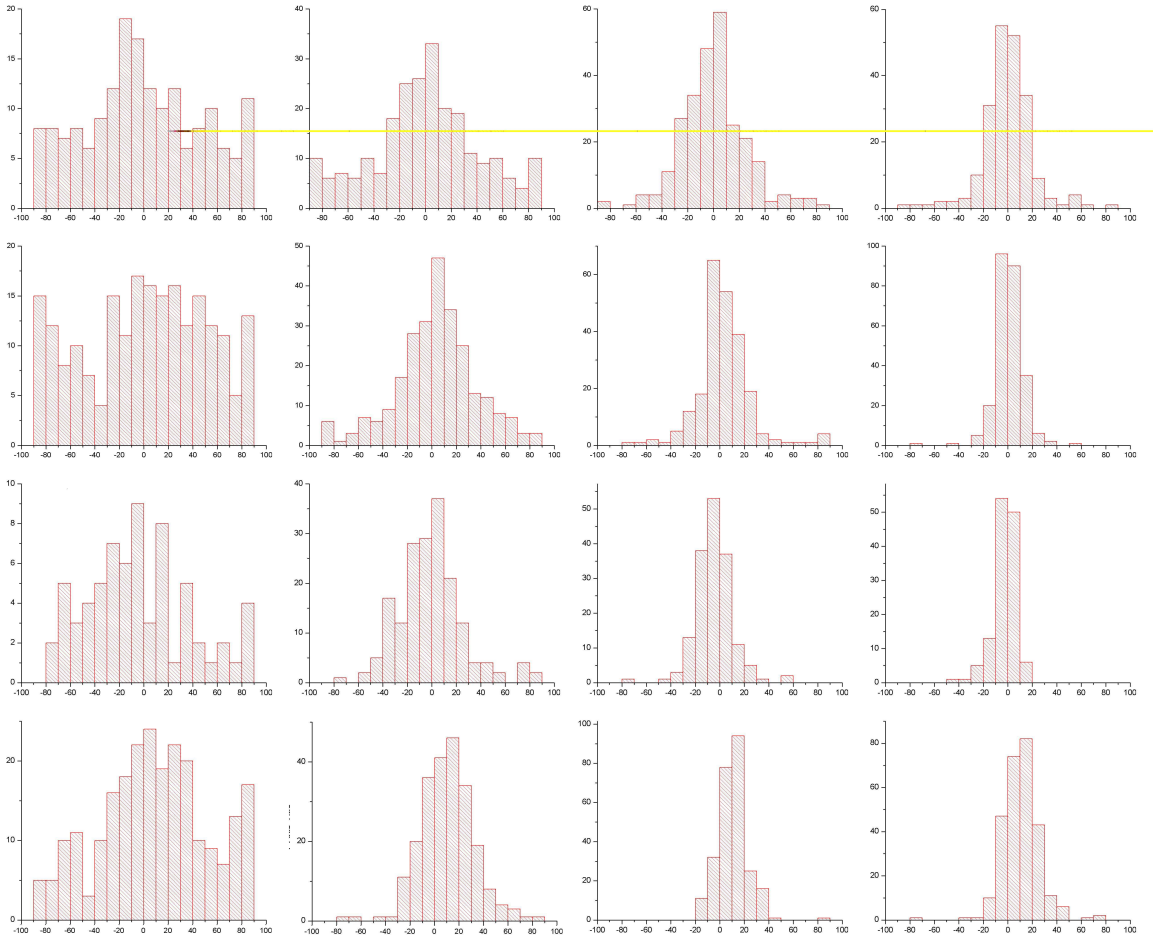

Figure 8: Histograms for one of the batches of high density HOP cells

The alignment data consists of the angle difference between the cell's major axis and the groove. This data was reported as a histogram for each time and groove depth. In figures 8 and 9 we show a histogram that was compiled with all of the data for one run. From these histograms, we can tell that the spread of angles becomes smaller for deeper grooves, but also for increasing times in culture.

Visually, it is difficult to compare the two sets of histograms. However, the HOP cells seem to have a smaller spread of the angle measurements for the 500 nm samples.

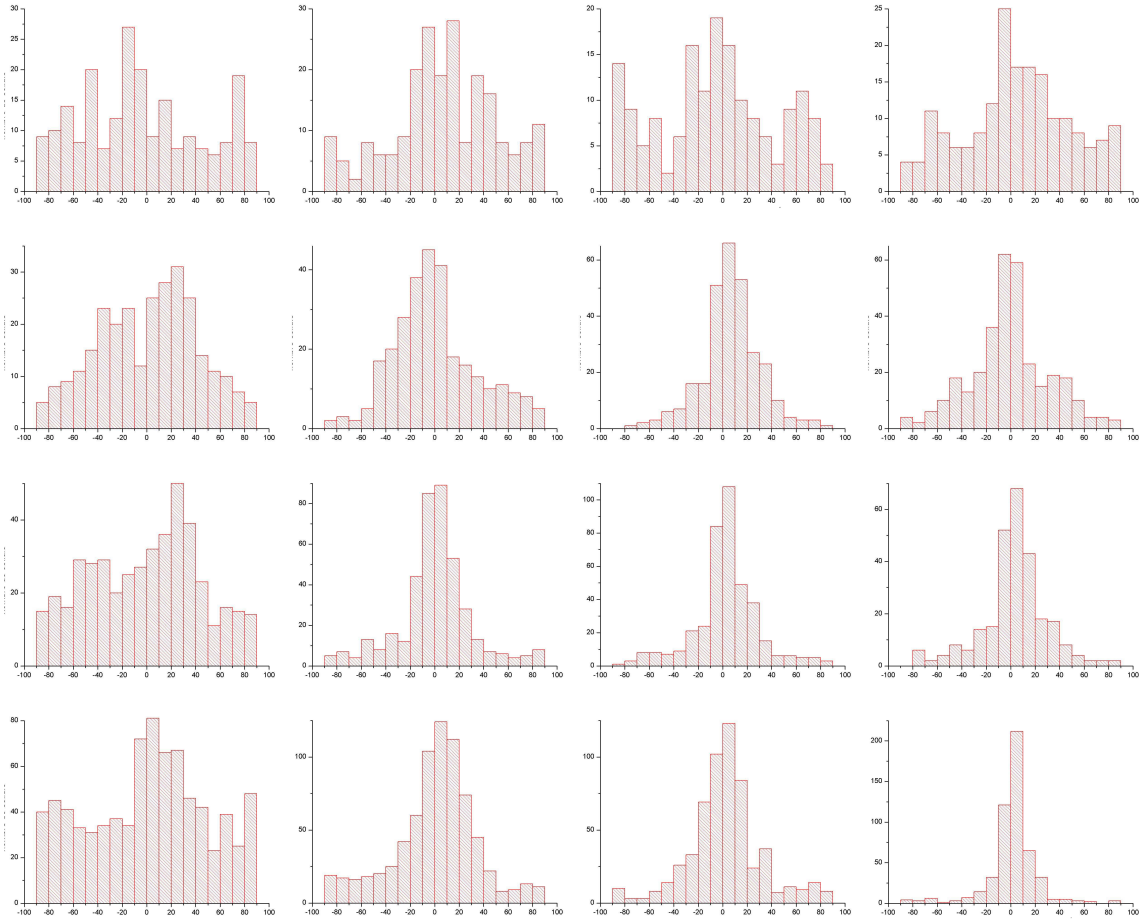

Figure 9: Histograms for one of the batches of SaOs-2 cells

2.4.4 Orientation parameters: Orientation at infinite depth

The cell orientation parameter at infinite groove depth (α_{inf}) is assumed to be a property of the cell and is thus independent of experimental conditions. This value was determined for each cell type by finding the minimum value of the residuals when fitting all the data for each of the conditions tested (time in culture, groove depth) and each batch. This analysis was performed on the cell bodies and the cell nuclei of the SaOs-2 and HOP cells and the results are summarized in table 1.

	Cell body	Nucleus
HOP	0	21
SaOs-2	23	29

Table 1: Orientation at infinite depth for the cell bodies and the nuclei of the SaOs-2 and HOP cells.

2.4.5 Sensitivity to the grooves, cell and nucleus

The cell orientation parameters of each of these data sets were obtained from the standard deviations of the data. These were then plotted against the groove depths as shown in figure 10.

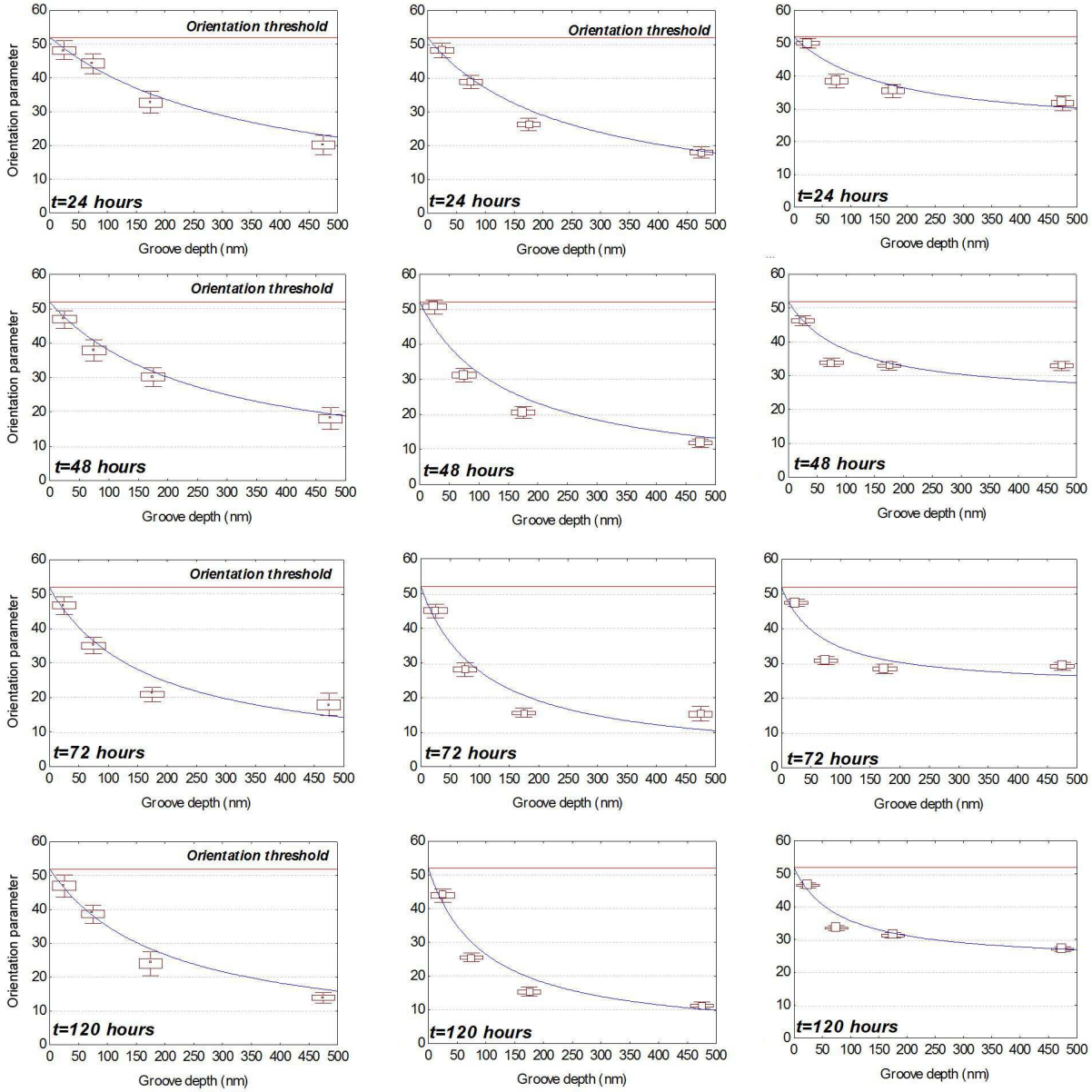

Figure 10: Comparison of the orientation parameters of the cell bodies of the HOP low density (left), HOP high density (middle) and SaOs2 (right).

The threshold value for a randomly oriented sample is shown as a solid red line. We can see that the cell orientation parameters decrease with increasing groove depths. When the two plots for the HOP cells at different densities are compared we can see that the high density cells have smaller values of the cell orientation parameters at smaller grooves depths, resulting in plots that appear more curved. When we compare these two to the SaOs-2 plots we can see that the HOP plots level off at a lower value at high groove depths. This is reflected by the higher value for the cell orientation parameter at infinite depth that we found for SaOs-2 (23 compared to 0 for HOP). Fitting these plots to equation 5, we can obtain the cell groove depth effect (C_{GDE}), a measure of the sensitivity of the cells to shallow grooves. This analysis was performed for the cell body and the cell nucleus. (Figure 11.)

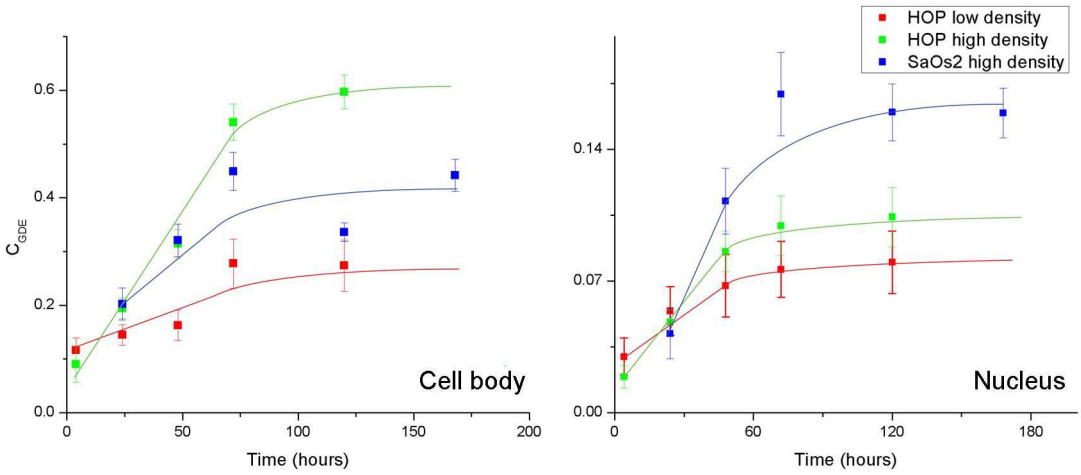

Figure 11: Values of the Groove depth effect (C_{GDE}) for the cell body and the nucleus, in each of the conditions studied. The solid lines were drawn as a guide to the eye.

The initial density of cells has a large effect on the sensitivity of the HOP cells to shallow grooves, as evidenced by the 2-fold difference in figure 11. This difference can be attributed to a cooperativity effect of the cells as they are closer to each other at higher densities. The SaOs-2 cells have sensitivities that are intermediate between the two HOP cell densities. The initial density of the SaOs-2 cells was the same as the high density HOP cells, but as we have shown above, the SaOs-2 cells have a surface coverage that is similar to the low density HOP cells. Therefore, for the same surface coverage, the

SaOs-2 cells are more sensitive to the shallow grooves than the HOP cells. In the case of the contact guidance of the nucleus, the SaOs-2 cells are clearly more sensitive than either of the HOP cells, at long incubation times. The values of the sensitivity of the nuclei of both HOP cell experiments overlap at all time points, therefore the density of the cells does not have a significant effect on the sensitivity of the nuclei to shallow grooves.

2.4.6 Comparison of the alignment values of the cell and its nucleus in single cells

Analysis of a subset of the data was performed to be able to compare values of the alignment of the cell body with its nucleus in individual cells.

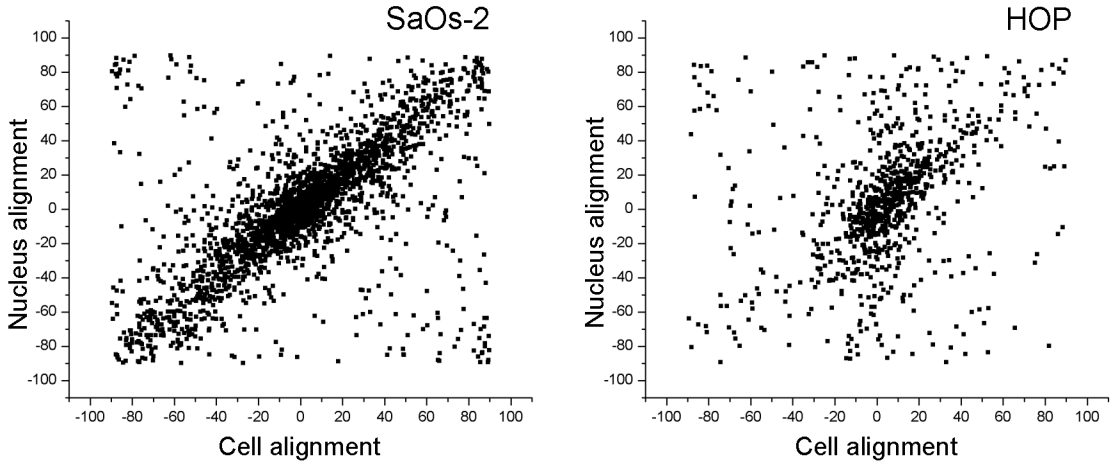

Figure 12: Correlation between the alignment of the cell and the nucleus in individual cells

When comparing the values of the alignment of the nucleus and the cell for the SaOs-2 cells in Figure 12 we can clearly see a correlation appearing between the alignment of the nucleus and the alignment of the cell: the values seem to confine themselves mostly to a x=y line. This indicates that the alignment of the cell nucleus follows the alignment of the cell body quite well. And this is true even for cells that are not well aligned: the correlation is visible for values of the angle that are not close to zero. When the alignment of the nucleus and the cell are compared for HOP cells, there is still a correlation between the two values, but it is not as obvious as for the SaOs-2 cells. In fact, for high values of the

angle (above 45 degrees) there is no clear correlation. Additionally, many of the data points with low deviations from alignment for the cell body do not have low values for the nucleus: this is visible as a "column" of data around the cell alignment value of zero. This shows that there are many cells that have an aligned cell body, but not an aligned nucleus. Conversely, we do not see the opposite effect: there are very few values around the nucleus alignment value of zero. Therefore, the alignment of the nucleus for the HOP cells is more likely to be more disperse than for the cell body. This data indicates that the determination of the alignment of the nucleus is a reasonable measure of the contact guidance of the cell body for SaOs-2 cells, but not for HOP cells.

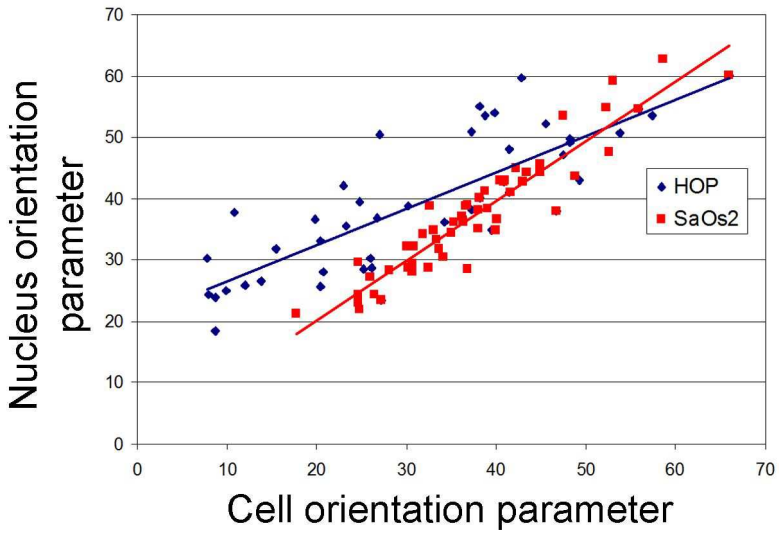

Figure 13: Comparison of the orientation parameters of the nucleus and the cell for each sample

When the values of the orientation parameters are plotted for each sample, these observations are confirmed. (Figure 13.) We can fit the points to a line to obtain information about the trends of each of these sets of data. The slope of the orientation parameter comparison for the SaOs-2 cells is 0.97, which is very close to 1, indicating that the spread of the orientation of the cell body and the nucleus are very close. In the case of the HOP cells we obtain a slope of 0.59, which is far from the value of 1, indicating that the cell body tends to be more aligned than the nucleus. From the intercept of this graph

we can also tell what the alignment of the cell nuclei would be for perfectly aligned cell bodies, i.e. The value of the orientation parameter of the nucleus when the orientation parameter of the cell body is zero. For the SaOs-2 cells, because of the close relationship between the cell and the nucleus, the value of the orientation parameter of the nucleus becomes 0.9, a very small value. For the HOP cells, because the cell body does not influence the nucleus as much, the value of the dispersion of the nuclei for completely aligned cells is 20.5. This is a large deviation from alignment, as randomly oriented cells would have an alignment of 52 degrees.

2.4.7 Effect of the alignment of the cell on the elongation of the nucleus

During the analysis of the direction of the nucleus we also determined the aspect ratio of the ellipses fitted to the nuclei. We can thus determine the relationship between the aspect ratio of the nucleus and the alignment of the cell. Dunn et al. had previously hypothesized that the orientation of the cell is purely due to the elongation in the direction of the grooves.[96] When they modified the images by contracting them in the direction of the grooves to obtain similar aspect ratios to the ones found on flat substrates the cells no longer appeared aligned with the grooves. It is difficult to determine the aspect ratio of the cell as it is not generally a well-defined shape. In our case we are not looking at the elongation of the cell, but of the nucleus.

2.4.7.1 Elongation of the nucleus as a function of groove depth

The aspect ratios measured are shown in table 2. From this data we can see that the aspect ratios of the HOP cells do not greatly differ across the different conditions. There seems to be a slight increase in the aspect ratio with increasing groove depth, which could be correlated with the increased alignment of the cells. The SaOs-2 cells show a very clear increase in the aspect ratio of the nuclei with increasing time in culture. This is also visible on the control flat surfaces. There is a trend visible with increasing depth of the grooves, but it is weaker.

	HOP			SaOs-2		
	24h	48h	120h	24h	48h	120h
Flat	*1.4*	*1.41*	*1.39*	*1.46*	*1.59*	*1.75*
30 nm	1.41	1.4	1.38	1.39	1.57	1.6
100 nm	1.4	1.45	1.41	1.45	1.64	1.66
200 nm	1.42	1.47	1.45	1.5	1.64	1.69
500 nm	1.44	1.44	1.43	1.39	1.69	1.75

Table 2: Aspect ratios of the nuclei of HOP and SaOs-2 cells under the experimental conditions used.

2.4.7.2 Elongation of the nucleus compared to the alignment of the cell and its nucleus

The relationship between the aspect ratio of the nucleus and the alignment of the cell was studied to determine whether elongation alone could explain the contact guidance phenomenon, as described by Dunn et al., and whether this elongation is translated to the nucleus.[96] Analysis of the relationship in single cells shows there is some correlation between cells of high aspect ratios and alignment in SaOs-2 cells, but this effect is less pronounced in HOP cells. (Figure 14.) When the orientation parameters across samples are compared to the average aspect ratios (Figure 14, right), we can see that there is a small correlation for the HOP cells, but it is not as significant as the correlation that is visible for the SaOs-2 cells, where a decrease in the orientation parameter (cells are more aligned) results in an increase in the aspect ratio.

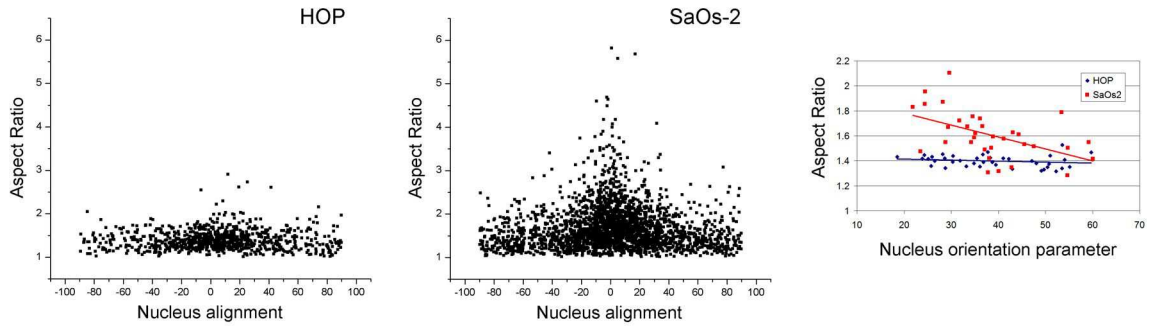

Figure 14: Comparison of the aspect ratios and the alignment in individual cells for HOP (left) and SaOs-2 (middle) cells and comparison of the average aspect ratio and the nucleus orientation parameter for individual samples (right).

2.5 Discussion

2.5.1 The effect of cell density on the contact guidance

The healthy osteoprogenitor cells (HOP) were seeded at two different densities: 7000 and 10000 cells/cm^2. The lower density was chosen to obtain sub-confluent images.

2.5.1.1 Cell coverage

When these two samples are compared, the difference in area coverage is similar at 4 hours (25%), but much bigger after 24 hours (65%), indicating a great difference in the ability of the cells to spread on the surfaces or proliferate that may be related to the proximity of cells with each other. This behavior is already known in cell culture where it is thought that a minimum number of cells need to be seeded in a flask for proper cell growth. The difference in area coverage decreases with time, which is likely due to a decrease in the proliferation rate of the high initial seeding density cells as they reach confluence.

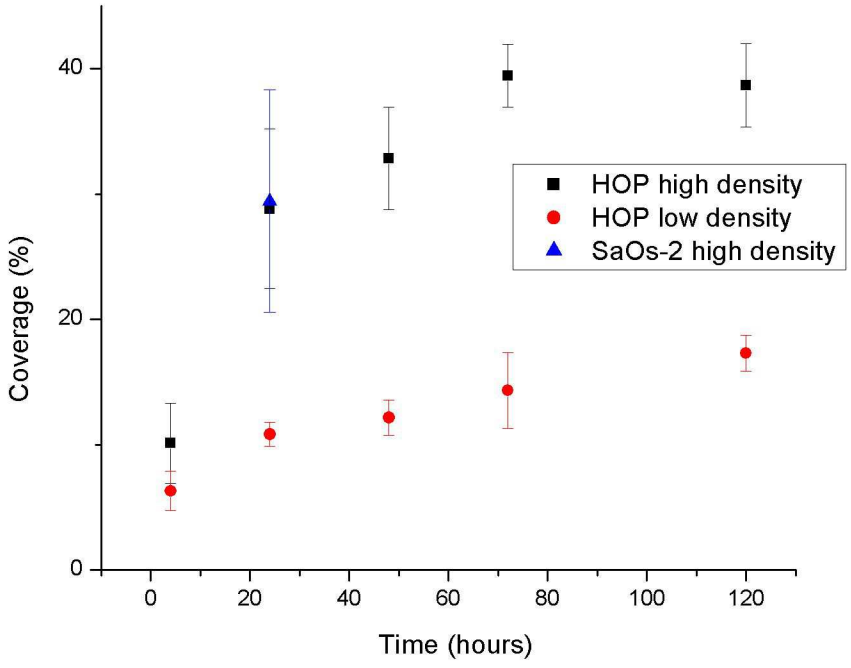

Figure 15: Area coverage of the HOP cells as a function of the time the cells were grown on the surfaces, a close-up of figure 7.

Concomitantly the number of cells for the high density cells reaches a plateau, as seen in figure 15, a close-up of the region of the plot for the two HOP samples. The difference in the surface density of the two samples is also visible in the area coverage per cell: the lower density cells, having more space to spread out, have higher area per individual cell. (Figure 7.)

2.5.1.2 Orientation parameters

The sensitivity of the cells to shallow grooves is greatly affected by the cell density on the surface: the cells seeded at a higher initial cell density had higher sensitivities than the cells seeded at a lower density. Therefore, cells grown on surfaces with a higher density of cells are more likely to become aligned with the grooves. An increase in cell density on a surface results in an increase in cell proximity and cell-to-cell contact. This has been shown to result in a decrease in cytoskeletal elements, such as a decrease in the production of actin, alpha-actinin, vimentin, beta-tubulin as well as a decrease in the polymerized actin content of the cell.[97] Yet, it seems unlikely that a decrease in cytoskeleton production and organization could result in an increased alignment of cells on a surface. Rather, we have attributed this increase in sensitivity to a cooperative effect of the cells on the surface. This behaviour has also been discussed by Sutherland et al. who have previously shown an increase in alignment in confluent cells when compared to low density cells.[74] Cells need to compete for space and thus the presence of aligned cells on the surface will increase the likelihood of a cell becoming aligned. This effect will be increased by the ability of cells to elongate: cells that have a higher aspect ratio will be more likely to affect the cells around them. Thus, this effect will be even more pronounced in healthy cells, as these are able to elongate more than the cancerous cells (Figure 6).

In a different system, Clark et al. had previously reported seeing a loss of alignment for epithelial cells with increasing surface density.[98] This effect, which is in contradiction to our results and those of Sutherland et al.,[74] can be attributed to the epithelial nature of the cells which form strong cell-to-cell

contacts and favour 3D organization and confluent film formation over cell-to-surface interactions. These cell types are more likely to form polarized cells of a cubical shape, form cell-to-cell contacts and lose their surface adhesions than the cells used in our study, that spread on the surface and retain strong attachment to the surface, even in the presence of other cells.

2.5.2 Comparison of healthy and cancerous contact guidance behaviour

SaOs-2 cells are an extensively used model for bone cells. These are particularly popular for they are easy to culture, produce an extracellular matrix, are well-differentiated and have a phenotypical expression pattern that is similar to normal bone cells. Here we will compare their behaviour on surface grooves to that of healthy human osteoprogenitor cells (HOP).

2.5.2.1 Cell coverage

The morphology of the two cell lines used in this study differ in some aspects. The healthy (HOP) cells are large and well-spread with an organized cytoskeleton in which it is easy to distinguish the actin fibres. The cancerous (SaOs-2) cells also show cytoskeleton organization at long incubation times in well-spread cells, but they have a smaller surface area and a significant population of these cells is not well-spread, and takes up a smaller surface area. This difference could be due to the differences in phenotypes of the cells. The cancerous cells are more proliferative than the healthy cells (Figure 7). To undergo division, cells become round and compact before undergoing several processes resulting in replication of the DNA and division into two daughter cells. An increased proliferation rate will mean that a higher proportion of cells is undergoing division at any point in time, but also that there is a shorter interphase period for attachment, and as a consequence the cells will have less time to spread out and will appear smaller.

The differences in the phenotypes of the cells are also reflected in the area coverages obtained for each cell type. The number of cells increases steadily with time for each cell type, indicating that they are

both proliferating. The area coverage per cell of the cancerous cells is much lower than the healthy cells: the area that each cancerous cell takes up is much smaller than the healthy cells. This could be due to several factors: the cancerous cells may be smaller, or they may spread less, or more slowly, than the healthy cells. The difference in total area coverage decreases with time, from a ten-fold difference at 24 hours to less than a 2-fold difference at 120 hours. This is due to the high proliferation rate of the cancerous cells and to the decrease in proliferation rate of the healthy cells as they reach confluence at late incubation times.

2.5.2.2 Orientation at infinite groove depth

The value of the orientation at infinite depth is an indication of the limit of alignment of the cells, or of their natural dispersion, at extreme alignment conditions (i.e. infinite depth). Hence, cells that have a strong tendency to explore their surroundings and move in random directions will not be strongly aligned with the grooves even at large groove depths. They may have a high sensitivity to the grooves, meaning that the cell population shows significant alignment even for very shallow structures, but does not show strong alignment on very deep grooves. We assume that the alignment at infinite groove depth is a property of the cell and is independent of experimental conditions.

In the case of the healthy cells, the value of the orientation parameter at infinite depth is very small, with a value of 0 (±1) degrees. This low value indicates that the cells are very well aligned; in fact, at extreme groove depth the cells are able to align completely with the grooves. The cancerous cells have a much higher orientation parameter value at infinite depth than the healthy cells. The alignment at infinite depth obtained was 23 (±1) degrees. This indicates that the cancerous cells do not respond to deep grooves the same way that healthy cells do. With increasing groove depth the cancerous cells will not increase their alignment infinitely but will retain some disorder. These results are consistent with the findings of McCartney et al.[81] who found a decrease in the alignment of cancerous fibroblastic and

epithelial cells when compared to their healthy counterparts. In that study they found a 6-7% decrease in the number of cells that were aligned within 10 degrees of the surface grooves.

This behaviour may be attributed to the differences in phenotypes of the cells. As discussed above, there are large differences in the surface area occupied by each cell type, and in their proliferation rates. Higher proliferation rates may result in loss of alignment during the division process in which the cell reorganizes itself and becomes more compact. However, examination of the micrographs (figure 6) reveals that there is a large variation in the cell area for the cancerous cells. This may arise from an increase of proliferation rate, as described above, or may also be due to subpopulations of the cell line, which could also result in changes in the alignment of the cells due to the behaviour of the different subpopulations.[99,100]

Cancerous cells are also known to be more deformable and produce less cytoskeletal filaments than healthy cells.[33] There are several proposed hypotheses to explain contact guidance.[98] It has been suggested that cells elongate in the direction of the grooves because the grooves are a topographical barrier to the filopodia of nanometer-scale width that the cell uses to explore its surroundings and create attachment points in the direction of movement. Another hypothesis is that focal adhesion points, which are oval shaped contact points of the cell with the surface, can only be created parallel to the grooves, and that filopodia that attempt to attach perpendicular to the groove cannot form a stable attachment point.[4] Both these mechanisms involve the cytoskeleton (filopodia are thin extensions of actin) and modification of the cytoskeleton of the cell and its movement mechanisms could certainly have an effect on the contact guidance ability of the cells. A reduction in the organization of the cytoskeleton and in the filamentous components of the actin network may result in a reduction of the long-range order within the cell and thus cancerous cells may have more randomly oriented protrusions than healthy cells. This could result in more random orientation of the cells on grooves than well-

organized cells that have protrusions that are aligned with each other. Hence cancerous cells would not be as well aligned.

2.5.2.3 Sensitivity to shallow grooves

The sensitivity (C_{GDE}) parameter is an indication of the sensitivity of the cells to the grooves, i.e. the value of the orientation parameter per unit depth of the grooves. The larger this value is, the more easily cells can react to even very shallow grooves.

The sensitivity of the cancerous cells was comparable to the sensitivity of the high density healthy cells at short incubation times (Figure 11). Although the values for the two cell types are very similar and the initial density of the two samples was the same, the values cannot be easily compared as the two samples did not have the same surface area coverage (Figure 7). In the case of the healthy cells we have shown that cell cooperativity is a very important factor in contact guidance. In fact, although the initial seeding density is the same the surface coverage of the cancerous cells is very small (3.1%) when compared to the healthy cells (33.3%). Even though the cancerous cells have a higher proliferation rate, their surface coverage does not reach the value of the high density healthy cells at the incubation times studied. The surface coverage values of the cancerous cells are much closer to the low density healthy cells and the values are very similar at 120 hours (Figure 7). If the surface coverage is taken into account instead of the initial seeding density, then the sensitivity of the cancerous cells is higher than the sensitivity of the healthy cells to shallow grooves. This behaviour could be due to the differences in attachment area of the two cells or their phenotypical differences (proliferation rate, cytoskeletal organization).

As discussed above, contact guidance has been suggested to be a consequence of the inability of cells to overcome the physical barrier of the grooves with their filopodia, or the higher stability of focal adhesions when formed in the direction of the groove. At very shallow groove depths both these factors

become less important: it is easier to overcome the groove when it is shallow, and focal adhesions could be formed across grooves if they are shallow enough. However, the distance between integrin receptors within a focal adhesion have been demonstrated by the Spatz group to be on the order of 58 nm, which means that a 30 nm height difference (our shallowest grooves) is relatively large. In fact, cells have been shown to be able to respond to surfaces with height differences of 10 nm.[48] Cancer cells are known to be more motile than healthy cells and this will have an impact on the maturity of the focal adhesions and possibly their size and content. This could result in difficulties to form focal adhesions across the edge of a groove, and possibly in focal adhesion placement parallel to the groove edge when the cell encounters it. Additionally, because of their increased motility, the cancer cells have a higher turnover of the focal adhesions, meaning they produce more focal adhesions and are more likely to encounter groove edges than the healthy cells.

We thus propose that alignment of the cells with the grooves occurs through both proposed mechanisms. When cells are grown on deep grooves their contact guidance is dominated by the physical barrier of the grooves to movement of their exploratory filopodia, whereas on very shallow grooves, the main factor is the stability of the focal adhesions points. It has been suggested by McCartney et al.[81] that metastatic migration may not be directed by contact guidance as cancerous cells are less sensitive to grooves than healthy cells, but our findings suggest otherwise. In fact, we have found that cancer cells are just as sensitive or more to shallow grooves, and thus their migration may be directed by fibres found in the extracellular matrix, which have sizes that are intermediate between the two shallowest grooves in our study (collagen fibres have a diameter of 50 nm with a 67 nm band).

In each cell type we can see that the sensitivity reaches a plateau around 72 hours, which indicates that the cells have reached a steady-state of alignment: the alignment of the cell population no longer continues to increase with time, the number of aligned and non-aligned cells remain the same. This is

likely due to the increase in surface coverage of the cells: as the surface density of the cells increases it becomes more difficult for the cells to move and they can no longer alter their alignment with the surface. However, these experiments are performed after fixation of cells and it is not possible to say whether or not the cells are still moving and have retained their degree of alignment or they have stopped moving.

2.5.3 Comparison of the effect of contact guidance on the nucleus of healthy and cancerous cells

In the experiments conducted in this study there is evidence that the nucleus of the cancerous SaOs-2 cells follows the direction of the cell body much better than the healthy HOP cells. This is most clearly shown in the alignment measurements performed on individual cells. This is not an effect that is due to contact guidance: even SaOs-2 cells that are not well aligned have values of the alignment of the cell body and the nucleus that are well correlated. (Figure 12.) The low values of the aspect ratios for the HOP cells at long incubation times are additional evidence that the nucleus is not affected by the shape of the cell. Even though the HOP cells are elongated at high incubation times (figure 6), much more than the SaOs-2 cells, this does not result in a significant change in the aspect ratio of the nucleus. Interestingly this may be related to the experiments in chapter 3, where the SaOs-2 cells demonstrate a great degree of control over the positioning of the nucleus. Similarly, in the experiments demonstrated in this chapter, the cancerous cells seem to have more control over the nucleus than the healthy cells do. There are two possible reasons that we see such a difference in behaviour of the two cells lines: either the cell nuclei are less deformable, or the cell has less control over the nucleus.

There is some evidence that the mechanics of the nucleus change with the level of differentiation of the cell. Pajerowski et al. demonstrated that adult stem cells have an intermediate plasticity due to the lack of Lamin A/C, a component of the inner nuclear membrane that provides rigidity.[11] Differentiated cells, which express this protein, have a higher rigidity. The healthy cells used in this study are indeed stem

cells, as they are human osteoprogenitor cells. They are weakly differentiated. The SaOs-2 cancerous cells, on the other hand, have a differentiated phenotype. The HOP cells should therefore have a more rigid cell nucleus. However, there is also evidence that certain cancerous cells have lowered expression of lamins A and C, which would result in a lowered rigidity of the nucleus.[101] This behaviour could be due to the metastatic ability of cancer cells and the need for them to be able to deform extensively when traveling throughout the body. In a study where the elasticity of the cell was measured by AFM in the region over the nucleus, the elasticity of mesenchymal stem cells, osteoblasts and MG63 osteosarcoma cells where not significantly different on polystyrene or glass surfaces, but the MG63 cells were found to have a lower young's modulus (i.e. more elastic) when grown on collagen fibres.[102] Unfortunately, there is little evidence in the literature on the rigidity of the nuclei of SaOs-2 cells, therefore it is difficult to determine whether the HOP cells have more rigid nuclei and further study on these two cell types is necessary to elucidate this point.

The position of the nucleus within the cell is determined by the cytoskeleton, namely the microtubules[103] and the actin network.[20] Movement of the nucleus within the cell is controlled by these filaments and their motor proteins, through their connections to the cell exterior, via the integrins, and their connections to the nucleus membrane, via the LINC complexes. Differences in the nucleus trafficking abilities of cancerous and healthy cells could be due to variations in the intra-celllular architecture, the type of filament available or the way the cell interacts with the surface. The malignant transformation of cancer cells has been associated with overexpression of Rho GTPases, which regulate the microtubule and actin cytoskeleton.[104] Cancerous cells are known to have decreased filamentous actin content.[105,106] There are therefore large differences in the intracellular architecture of healthy and cancerous cells, and this may give rise to the differences in the type of forces applied to the nucleus and the cell-nucleus connections.

Another important factor in the ability of cells to affect the shape of the nucleus is the spreading capabilities of the cells. Cancerous cells do not spread as much as healthy cells, they take up smaller areas on surfaces. This implies that the cell periphery is not as far away from the nucleus in cancerous cells than in healthy cells that can send protrusions to greater distances. Therefore, changes in the elongation of healthy cells may not have as much impact on the nucleus as in cancerous cells. However, experiments performed in the Ingber lab have shown that changes at the periphery of the cell result in noticeable changes in the shape of the nucleus.[22] Hence, even processes occurring at the cell edge can result in force exerted on the nucleus, and thus deformation. It is unclear whether processes occurring at a greater distance from the nucleus will have a lesser effect. Therefore we cannot tell whether the greater spreading capacity of the HOP cells has a role in the efficiency of transduction of forces from the cell periphery to the nucleus.

2.6 Conclusions

Using the interactions of cells with the surface, we have shown that cell density is an important factor for the contact guidance of healthy cells. We have also shown that cancerous SaOs-2 cells are less sensitive to deep grooves, but more sensitive to shallow grooves, than healthy osteoprogenitor cells. We have interpreted these findings in terms of the possible cellular mechanisms at these scales. At larger scales the leading phenomenon is most likely the physical barrier presented to the cell's filopodia. The cytoskeleton of SaOs-2 cells may be less well-organised than in HOP cells and have shorter filopodia, which would result in less of an effect on the cell. On shallower grooves the prevailing effect is proposed to be the disruption of focal contact formation at the groove edge. The cancerous cells would be more sensitive to this disruption because of their higher turnover of focal contacts.

We also studied the interaction between the cell body and the nucleus. We showed that the nucleus of SaOs-2 cells follows the body of the cells more than the the HOP cells. This is also reflected in the

ability of the cells to elongate the nucleus, which was measured by determining the aspect ratio of the nuclei. The SaOs-2 cells were found to translate the contact guidance information of the cell body to the nucleus effectively and the alignment of the nucleus was found to be a good measure of the contact guidance of the cell body. However, in the case of HOP cells, this was not found to be the case: the cell nuclei did not always follow the body and the alignment of the nuclei was much more disperse. We interpreted these results in terms of possible differences in the rigidity of the nucleus and difference in the intracellular cytoskeleton architecture.

These results pointed out the differences in the cells' intra-cellular architecture and management of the nucleus. This could help us understand how cells manage their organelles, how this differs in cancerous cells and provide clues to understand how cells migrate and move their inner structures. Nucleus positioning is a fundamental process in several cellular processes including cell polarization for epithelial cells, and tissue growth and development.[107] Understanding how malignancy affects the cell's ability to move and position its inner organelles will provide clues to the metastatic movement of malignant cells and ways to disrupt it, possibly providing new strategies for therapies for cancer treatment.

Chapter 3
The interactions of cells with structures at the micron scale

3.1 Introduction

Studies have shown that surface cues can significantly alter the viability and differentiation responses of cells. (See Chapter 1.) Similarly, the surfaces encountered by cells in the body have varying shapes, sizes and rigidities, which may dictate their behaviour. One important aspect in tissue engineering is being able to grow cells so that they will form the specific type of tissue that is sought, with the same properties as that type of tissue in the body. Hence, it is important to understand how the various physical cues that cells encounter in the body can lead to physiological response in the cell. For this reason it is necessary to study the cell's responses to each of these types of physical cues independently. In this chapter we have chosen to study the effect of topography on the micron scale on human cells.

When a cell adheres to a substrate, the surface properties of this substrate will have a large impact on the fate of the cell. If the surface is favorable to cell attachment, it will respond by undergoing several processes. First the cell will form attachment points and the cytoskeleton will initiate spreading on the surface. On a flat surface the cell will go from a spherical shape to a flattened one. On surfaces with very large features the cell will follow the contours of the surface topography. At the micron scale, surface features are on the scale of sub-cellular components such as the nucleus. At this size scale several studies have shown that cells span the surface structures. In one paper, pillars of 1 micron in diameter resulted in very elongated cells.[108] On pillars of a slightly larger sizes (3 or 5 microns diameter, 5 microns tall) Matschegewski et al have shown reduced initial cell adhesion and spreading, as well as lower levels of differentiation in an osteosarcoma line (MG63).[109] They also described the lack of actin stress fibres in these cells and the concentration of actin on the top and around the pillars'

edges. In one paper by Steinberg et al., deformation of the nucleus of immortalized keratinocytes on micropillars can be seen but has not been discussed.[110] Interestingly, the actin pattern they saw is the opposite to that seen in the previous study: labelling of the actin was predominantly in the areas between the pillars and not on the top.[111] In experiments conducted on larger pillars (25 microns diameter, 5 or 15 microns high), Thakar et al. showed that proliferation was reduced in cells in contact with a micropillar.[5] Flexible micropillars have also been used in articles aimed at studying the forces generated by the cytoskeleton.[113]

Chemical patterning on the micron scale has been useful for revealing important characteristics of cells. In particular, pivotal studies have shown that the size of the patch a cell can adhere to will determine whether it survives and what its differentiation state will be.[62,63] Studies on the effect of microtopography on the cytoskeleton have concentrated on chemical patterning on the micron scale.[65] In these the topography behaved as “pinning points” to which the cell attached and were used to study the arrangement of the cytoskeleton in confined cells.[114] Preferential directionality of actin fibres has also been seen in cells grown on grooved surfaces.[115] In one of these studies the nucleus was also found to elongate in the direction of the grooves.[116]

In this chapter we will examine the behaviour of cells on square micropillars. Guided by preliminary results, we have focused on the differences between healthy and cancerous bone cells. We will first describe the relevant experimental procedures and cell types used. We will then present the behaviour of cancerous bone cells, which we will compare to healthy bone cells to establish the link between deformation and malignancy. We will extend this comparison to other types of cells. Finally, a tentative interpretation for the origin of the deformation will be proposed based on various types of imaging. The importance of the surface chemistry and rigidity will be briefly discussed.

3.2 Experimental methods

3.2.1 Substrate preparation

The substrates used in the experiments in this chapter were first microfabricated to obtain microstructures in silicon templates, then replicas of these were obtained in PDMS and finally hot embossing of the PDMS substrates was performed on PLLA films to obtain microstructured PLLA substrates.

3.2.1.1 Silicon Templates

Microfabrication was used to obtain the microtopography of the substrates discussed in this chapter. Two sets of samples were produced. The first was designed by V. Hasirci (Middle East Technical University, Ankara, Turkey) and kindly realized by A. Aydinli (Bilkent University, Ankara, Turkey). From this set we have used a sample denoted “C2”, which has square features that are approximately 7 microns in diameter and 4 microns tall, measured by AFM, SEM and confocal microscopy. The second set was designed by myself and fabricated at the IMTEK in Freiburg in the group of Dr. Jürgen Rühe. This set consists of an array of sizes of square pillars, ranging from 2 microns to 20 microns. Both the spacing and the size of the pillars were varied. The height of these structures was determined to be around 6 microns by confocal microscopy.

3.2.1.2 PDMS replicas

In order to obtain PDMS (polydimethyl siloxane) replicas of the silicon substrates that are easy to unmould, the silicon surfaces were coated with a fluorinated silane. The surfaces were cleaned with acetone, isopropanol and water to remove the protective polymer layer resulting from the fabrication process and allowed to air dry. These were then introduced in a vacuum chamber above a vial containing 1H,1H,2H,2H-perfluorodecytrichlorosilane in paraffin oil. The chamber was closed and put under vacuum for one hour to allow evaporation of the silane onto the surface.

The PDMS replicas were produced using an elastomer kit produced by Dow Corning (Sylgard 194). The Silicon substrates were placed in an aluminium cup and the elastomer mixed with its curing agent were poured on top of the substrates. This solution was allowed to sit for 30 minutes to allow the bubbles to float to the surface and be removed. The solution was then heated on a hot plate to 150 degrees for at least one hour. Following this curing step, the silicon surfaces were easily unmoulded, and observation under an optical microscope showed that the surface of the PDMS structures closely resembled the Silicon surface, indicating that the PDMS had penetrated into the microstructures and that the resulting surface was a replica of the initial surface.

In one experiment a PDMS replica of a PDMS mould was obtained. This was performed similarly to the PDMS moulding of the Silicon substrates. However, silanisation was not performed and the two PDMS surfaces had to be pried apart. Hence, the surfaces obtained were not uniformly patterned, but the areas obtained were sufficient for the experiments performed.

3.2.1.3 Hot Embossing

Hot embossing was performed by pressing a PDMS stamp into a film of polymer above its glass transition temperature. A silicon wafer coated with a layer of PDMS was used as backing. This was produced by spin-coating a solution of PDMS onto a flat piece of silicon wafer which was then cured on a hot plate at 150 ^{o}C.

Thin films of poly(L-lactic acid) (PLLA) (Resomer L 210, Boehringer Ingelheim) were made by solvent casting a dichloromethane solution of PLLA in a Petri dish. The concentration and volume of the solution were chosen so that the final PLLA amount per unit area would be the same (2 mg/cm^{2}). The PLLA film was then peeled off the Petri dish and cut into square pieces. The hot plate was heated to a temperature above the melting temperature of PLLA (180^{o}C). A piece of PLLA film was

sandwiched between the PDMS mold and the PDMS-coated silicon wafer. This was then placed on the hot stage where the assembly was manually pressed down onto the silicon wafer. Pressure was exerted for approximately 5 seconds, after which the entire system (Si wafer + PLLA film + PDMS mold) was plunged in cold water to vitrify the PLLA before demoulding. The PLLA film was peeled off the PDMS. In cases where flat PLLA films were needed as controls, films were "hot embossed" using a flat piece of PDMS stamp to reproduce the same processing conditions as for the micropatterned PLLA films.

3.2.2 Cell culture

3.2.2.1 Bone cells

Several cell lines were used in this study. HOP cells were obtained as described previously by Anselme et al.[95] F/STRO1^{+}A and FHSO6 cells were provided by P. Marie (Inserm and Hopital Lariboisiere, Paris, France) and prepared as described in previous studies.[117,118] SaOs-2 cells were purchased from the ECACC, U2OS from the ATCC and OHS4 were provided by G. Rodan.[119] MG63 cells were provided by J. Amedee (Inserm, Bordeaux, France). All cells were cultured in Iscove complete medium except for SaOs-2 cells, which were cultured in McCoy complete medium, containing, in all cases, fetal bovine serum (10%), glutamine (2 mM), penicillin (100 units/ml) and streptomycin (0.1 mg/ml).

3.2.2.2 Adenocarcinoma cells

The Adenocarcinoma cells were cultured in Dulbecco's Modified Eagle's medium (DMEM) with 4.5 g/l of glucose, to which 20% (v/v) of fetal bovine serum, 1% v/v of non-essential amino acids and 1% v/v penicillin/streptomycin and gentamicin were added. All cell cultures were performed in the laboratory of Jean-Noël Freund at the INSERM U682 in Strasbourg, France.

3.2.2.3 Keratinocytes

The keratinocytes used in this study were cultured in Dulbecco's Modified Eagle's medium (DMEM) (PAA, Pasching, Austria) containing 10% fetal calf serum (Seromed, Biochrom, Berlin, Germany). All cell culture experiments were conducted in Pascal Tomakidi's laboratory at the Zahnklinik in Freiburg, Germany.

3.2.2.4 Transformed epithelial cells

The transformed epithelial cells were obtained from Prof. William Hahn's group as frozen pellets of suspended cells and amplified at the IS2M. The medium used was composed of 374 ml of Knockout DMEM, 93 ml of Medium 199 containing L-Glutamine, 82 ml of fetal bovine serum, 5 ml of Penicillin/Streptomycin 100x, and 10 ml of 200 mM Glutamine.

3.2.2.5 Sample preparation for cell seeding

The microstructured PLLA surfaces were briefly sterilized in ethanol before cell seeding, followed by rinsing in sterile water. The PLLA surfaces, which are able to float in water, were placed in 24-well plates and fixed in place by melting two corners of the film with a soldering iron, which had been covered with aluminium foil. The wells containing the PLLA films were then rinsed and covered with sterile PBS and kept in the incubator at 37 degrees until cell seeding.

3.2.3 Biochemical tests

Several biochemical techniques can be used to test the biological response of the cells to the substrates. In our experiments we tested the viability and differentiation using colorimetric assays, the proliferation rate using antibody staining and the RNA production using real-time PCR.

3.2.3.1 Viability test

An MTT assay was carried out according to standard procedure, using a plate reader to obtain the

values of the absorbance. Thiazolyl blue formazan was purchased from Sigma. The cells were seeded at 10^4 cells/ml and 1 ml was seeded on each sample in a 24-well plate. Three types of substrates were used: a micropillared PLLA surface, a flat PLLA surface, and tissue culture plastic (the bottom of the 24-well plate). Prior to assay addition, the PLLA surfaces were removed from the 24-well plates and placed in clean wells to avoid contamination from cells around the sample. Three samples were used for each experiment and for each sample measurements of the optical density were obtained on three aliquots. The results obtained were normalized to the area of each sample and reported as a percentage of the value of the absorbance of the cells grown on the tissue culture plastic.

3.2.3.2 Cell proliferation tests

The ability of the cells to replicate their DNA was tested via BrdU incorporation. The procedure provided with the anti-BrdU-fluorescein was followed. Briefly, the cells were cultured on the substrates under normal condition and at a set time point the medium was exchanged for a solution containing BrdU for 2 hours. Following this, the cells were fixed and treated to label the BrdU with fluorescein-conjugated anti-BrdU antibody. The samples were subsequently labelled with DAPI or anti-lamin antibody to stain the nuclei and obtain information about the total number of cells. Analysis of the samples was performed by taking fluorescence images of the samples. The total number of cells and the number of BrdU-labelled cells were manually counted and tabulated.

3.2.3.3 Differentiation tests

Two types of tests were carried out to understand how the deformation of the cell affected its differentiation.

3.2.3.3.1 Alkaline Phosphatase assay

The cells were seeded at 10^4 cells/ml and 1 ml was seeded on each sample in a 24-well plate. Three

types of substrates were used: a micropillared PLLA surface, a flat PLLA surface, and tissue culture plastic (the bottom of the 24-well plate). Briefly, the cells were cultured for 10 days in an incubator, in parallel with the MTT experiment for normalization of the number of cells. The cells on PLLA surfaces were then transferred to a new 24-well plate and all of the surfaces were carefully rinsed with warm PBS. Following this, 150 microliters of Triton X-100 were added to the cells, followed by 150 microliters of the substrate solution. The substrate solution is composed of 20 mM p-nitrophenyl phosphate, 10 mM diethanolamine and 10 mM $MgCl_2$ adjusted to a pH of 9.5. After 30 minutes of incubation 150 microliters of stop solution (0.1M EDTA in 1M NaOH) were added and the optical density at 405 nm was determined on a plate reader. Three samples were used for each experiment and three aliquots were used to measure the optical density of each sample. The results obtained were normalized to the area of each sample and then normalized to the value of the viability obtained in the MTT tests which were run in parallel. The results were reported as a percentage of the value of the absorbance of the cells grown on the tissue culture plastic.

3.2.3.3.2 PCR measurements

PCR measurements were carried out to obtain information about the RNA production of the cells and whether deformation of the cell could alter it. Cells were seeded at a high density ($3 * 10^5$ cells/ml) to obtain confluent films of the cells after adhesion, to promote the expression of genes related to differentiation rather than proliferation. Cells were seeded on microstructured substrates and flat PLLA substrates were the control surfaces. In each case 6 samples had to be pooled together to obtain sufficient RNA for a proper reading. The experiment was repeated 3 times, the first time 12 samples were used (2 replicas) and the two other times 18 samples were used (3 replicas).

After 24 hours of culture the medium of the samples was changed and replaced with either fresh medium or medium containing BMP2, a growth factor for bone cells. The cells were then cultured for

an additional 24 hours, at which point the RNA was harvested using Trizol. The area around the sample was cut with a sterile scalpel to avoid cells from around the sample to attach to it, and the sample was taken out and placed in Trizol. Three samples were placed in each ml of Trizol and were left in the Trizol for 10 minutes before recuperating the Trizol/RNA solution and storing it at -80 degrees until ready for extraction. The RNA purification procedure that was followed was the one given with the Trizol solution (Invitrogen, France). Briefly, phase separation is induced by the addition of chloroform and the RNA is recuperated from the clear upper aqueous phase. Isopropanol is added to the aqueous phase to induce RNA precipitation, the supernatant is removed and the precipitate is rinsed with 75% ethanol. The RNA is then redissolved in RNase-free water.

Reverse-transcriptase was performed on 3 micrograms of RNA: the RNA was denaturated for 10 min at 70°C then reversed-transcribed at 37°C for 90 min using 300 U MMLV reverse transcriptase, 15 µg oligodT primers, 1 mM dNTP in 30 µl total volume and finally inactivated at 85°C for 5 min. Quantitative PCR on the resulting cDNA solution was performed on a LightCycler 480 Instrument (Roche Applied Science, Indianapolis, OH, USA) using a SYBR Green Master kit (ABGen, Courtabœuf, France) supplemented with 0.5 µM of specific primers. The signal was normalized to 18S as an internal control using sense 5'-TCAAGAACGAAAGTCGGAGG-3', antisense 5'-GGACATCTAAGGGCATCACA-3'. The primers were as follows: sense 5'-TCTGGCCTTCCACTCTCAGT-3', antisense 5'-GACTGGCGGGGTGTAAGTAA-3' for Runx2; sense 5'-GGACATGCAGTACGAGCTGA-3', antisense 5'-CCACCAAATGTGAAGACGTG-3' for ALP; sense 5'-AGCCAGCAGATCGAGAACAT-3', antisense 5'-CGCCATACTCGAACTGGAAT-3' for Col1A1. The PCR conditions were 45 cycles of: 95 degrees for denaturation, 58 degrees for annealing and 72 degrees for amplification. The detection of the DNA strand produced by PCR was done using a Sybr Green dye, which preferentially binds to double-stranded DNA, emitting fluorescence when in a

DNA-dye complex. The threshold at which the fluorescence is detected is determined by the software and the number of cycles needed to attain this threshold are reported by the software after fitting the curve. This value is used to obtain relative values of the amount of cDNA present in the sample, which is used to compare the number of copies of RNA between samples. The quality of the cDNA used in the PCR experiment is then verified by doing a "melting curve" experiment, in which the dissociation of DNA strands (loss of fluorescence) is measured against temperature. This allows detection of more than one type of DNA, indicating whether the measurement was selective. The values are reported here as the relative amount of RNA between samples. The relative amount of RNA was calculated by the 2^(-ΔCt) method.

We have studied the effect of the surface topography by comparing relative values on flat or topographied surfaces and the effect of the growth factor (BMP2) by comparing the relative values for the same conditions with or without BMP2.

3.2.4 Immunohistochemical staining and imaging

The DNA of the cells (i.e. the nucleus) was labelled using DAPI, the nuclear membrane was labelled using anti-lamin A, the actin cytoskeleton was labelled with phalloidin-TRITC the microtubules were labelled with anti-beta tubulin and the intermediate filaments were labelled with anti-vimentin. After reaching the appropriate time point samples destined for labelling were rinsed twice with warm phosphate buffered saline (PBS) and then covered with a solution of 2% para-formaldehyde for 20 minutes. The cells were permeated with Triton in PBS (0.2 %) for 15 minutes and blocked with bovine serum albumin (1%) in PBS for 20 minutes. Each step was followed by three rinses in PBS. For actin labelling, phalloidin-TRITC (0.4 ug/ml) was added for one hour at room temperature. In the case of lamin, microtubule and vimentin labelling the primary antibody was added to the samples for 1h at room temperature, followed by rinsing with buffer, and the addition of the secondary antibody for 1h at

room temperature. The primary antibodies were rabbit anti-lamin A IgG (1:300), mouse anti-beta-tubulin IgG (1:200) and mouse anti-vimentin IgG (1:20). The secondary antibodies were anti-rabbit IgG-FITC (1:300) or anti-Mouse IgG-FITC (1:32). All antibodies were obtained from Sigma. Samples labelled with DAPI were incubated in a solution prepared in PBS (100 ng/mL) for 20 minutes, followed by rinsing with PBS and observed with an epifluorescence microscope.

3.2.5 Live cell imaging

3.2.5.1 Cell transfection

SaOs-2 cells were transfected using the Effectene transfection reagent kit (Qiagen). The procedure provided with the kit was followed. Two types of DNA were used for transfection: DNA for actin and for lamin transfection (Clontech). The cells were found to have maximum fluorescence 3-5 days after transfection.

3.2.5.2 Live cell imaging

Transfected cells were seeded on the appropriate surfaces in 3 cm plastic petri dishes. Two hours before imaging the medium on the cells was replaced by medium containing HEPES buffer and without phenol red. The petri dish was then placed in the incubator for two hours to allow the medium to stabilize in temperature and gas composition. The microscope (Zeiss LSM 700) was prepared by turning on the temperature control (Okolab) several hours before the experiment. At the start of the experiment the sample was transferred to the temperature controlled chamber around the microscope and placed on the microscope stage. A water-immersion objective was used to obtain high-resolution images without being affected by the evaporation of the medium, which could change the focal plane when imaging from above the medium. A cover through which the objective could fit was used to limit evaporation of the medium during the experiment.

3.2.6 Cytoskeleton inhibitor experiments

Six cytoskeleton inhibitors were tested on SaOs-2 cells grown on flat surfaces. The aim was to obtain a concentration at which the aspect of the cell as a whole appeared relatively unaffected by the addition of the disruptor, but the aspect of the filaments, when imaged using antibody staining, had visibly been disrupted. These include 2 disruptor for each type of cytoskeleton (actin, tubulin and vimentin). Staining of the actin and tubulin cytoskeleton was performed for the actin and tubulin samples, which was replaced by staining of the actin and vimentin cytoskeleton for vimentin disruptors. Concentrations tested are summarized in table 5. The concentrations were chosen based on the range of concentrations reported in the literature for nocodazole[120,121,122], colchicine[122,123,124], latrunculin A[123,9,125], cytochalasin D[125,120], acrylamide[124,13,129] and imminodiproprionitrile[127,128].

Disruptor	**Function**	**Concentrations (µM)**				
Nocodazole	Microtubule depolymerization	0.5	2	5		
Colchicine	Tubulin binding	0.25	1	5		
Latrunculin A	Actin monomer binding	0.1	0.5	1		
Cytochalasin D	F-Actin depolymerization	0.05	0.2	0.5	2	5
Acrylamide	Vimentin dissolution	2000	5000	10000	25000	
IDPN	Vimentin inhibitor	0.2 v%	1 v%	4 v%		

Table 3: Concentrations of cytoskeleton disruptors tested

3.2.6.1 Microtubule inhibitors

Nocodazole solution preparation: 10 mg were dissolved in 2.5 ml DMSO for several hours in a hot water bath (37^0C). A dilution of this stock solution was performed in complete medium to obtain a solution of high concentration of Nocodazole with little DMSO (which may be toxic to cells). Solutions were then prepared by diluting the appropriate amount of stock solution in warm medium. An additional control sample with the highest concentration of DMSO was prepared to verify that the effect on the cells was not due to DMSO toxicity.

Colchicine: a stock solution of 50 μM colchicine was prepared in distilled water. The experiment was performed by adding the appropriate amount of medium followed by an aliquot of colchicine secondary stock to obtain a total volume of 1 ml. The control sample was prepared by adding the same amount of distilled water to warm medium as the highest concentration sample.

3.2.6.2 Actin inhibitors

Latrunculin A was dissolved in ethanol to obtain a stock solution of a concentration of 0.5 mM. This was followed by a further dilution in complete medium to obtain a 1 μM stock solution. Individual solutions were made for each well by adding the appropriate amount of stock solution to a well and completing with medium. The control sample was cultured in pure complete medium.

A solution of Cytochalasin D was prepared by dissolving it in ethanol. A secondary stock solution in complete medium of concentration 5 μM was prepared. Individual solutions were made for each well by adding stock to a well containing the appropriate amount of medium for a final volume of 1 ml. Control samples were in pure complete medium.

3.2.6.3 Vimentin inhibitors

A stock solution of Acrylamide was made by dissolving it in water to obtain a solution of 100 mM. This solution was used to add directly to the wells containing medium in volumes sufficient to obtain the appropriate concentrations. The control sample contained water at the same concentration as the highest concentration test sample.

Iminodiproprionitrile (IDPN) was added directly to the medium (0.2, 1 or 4 %). A control sample was prepared that contained only complete medium.

3.2.6.4 Experiments on flat substrates and micropillars

Control experiments on flat surfaces were performed by seeding the cells on cleaned glass surfaces for

24 hours and replacing the medium with fresh medium followed by the appropriate volume of inhibitor stock solution. Experiments on micropillared surfaces were conducted similarly, only the cells were grown for 24 hours or 48 hours before addition of the inhibitors. After addition of the inhibitors, the cells were placed back in the incubator for 2 hours, then rinsed with warm PBS, fixed with 2% formaldehyde, labelled and imaged. The results obtained on flat samples determined the concentrations to use on the micropillars.

3.3 The interactions of cancerous bone cells

Although one would expect that growing cells on topographically structured surfaces would not affect the interior of the cell, the actual outcome of growing cells on surfaces with topographies on the length-scale of the cell nucleus is not obvious and has not yet been investigated. In figure 16 we schematically indicate several possibilities. On a flat surface the cell simply spreads and extends laterally. Similarly, on a micro-structured surface the cell will spread, it may have little interaction with the surface (Figure 16b,i) or it may deform to adopt the topography of the surface (Figure 16b,ii), potentially resulting also in a deformation of the cell nuclei (Figures 16b,iii and iv). As of yet, no strong deformation of the nucleus has been reported, which is in accordance with its measured stiffness: studies on the mechanical properties of the nucleus have shown that it is a viscoelastic solid that is 3-4 times stiffer than and twice as viscous as its surrounding cytoplasm.[5,6] It is also not clear whether such a severe

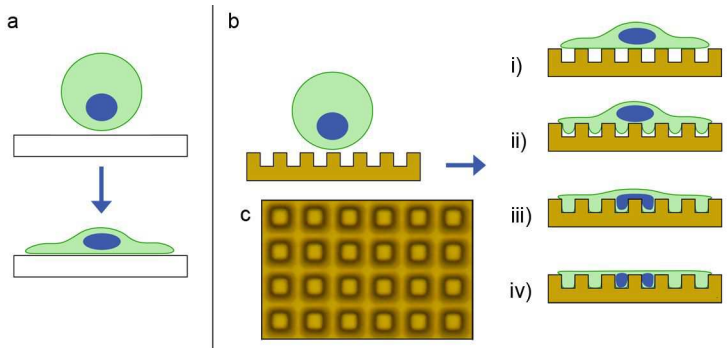

Figure 16: The behaviour of a cell upon deposition on a flat surface (left) and the possible behaviours upon deposition on a surface with micron-scale topography

deformation of the nucleus would result in a modification or hampering of the functioning of the organelle or even cause cell death.

3.3.1 The behaviour of SaOs-2 cells on micropatterned surfaces

Human osteosarcoma-derived cells (SaOs-2) were grown on poly(L-lactic acid) (PLLA) surfaces presenting micro-pillars obtained via hot embossing of polydimethylsiloxane (PDMS) templates. Their nuclei showed a deformed shape with features that matched the underlying surface topography, as evidenced by fluorescent labelling (Figure 17). This altered appearance is probably due to a mechanical deformation which caused the bulk of the mass of the nucleus to be hanging in between the pillars. This

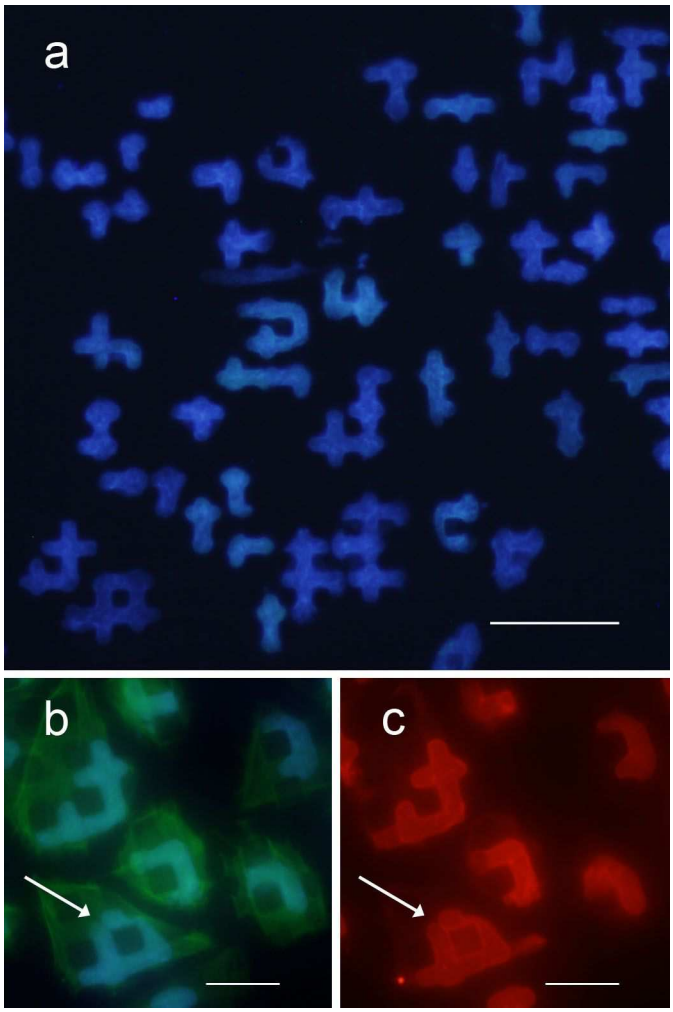

Figure 17: SaOs-2 cells grown on micrpillared surfaces. a: DAPI-labelling to evidence the cell nucleus, b and c: labelling of the nucleus (blue), actin (green) and nuclear membrane (red) to show that the blue DAPI label corresponds well to the nuclear membrane label.

deformation can be interpreted as the nucleus being stretched across the pillars (the small volume across the top of the pillar would not be visible), or, alternatively, by the nucleus being inserted in the spaces between the pillars. The possibility that the observed effect is due to the former configuration was discarded by labelling of the membrane of the nucleus (Figure 17). This labelling confirmed that the majority of the nuclei were located between the pillars, as the membrane was clearly seen conforming to the shape of the pillars. In some cases, it was seen that the nucleus could stretch over the top of the pillar, which is visible as red fluorescence across the top of the pillar (Figure 17b and c, arrows).

The deformation of the nucleus increased with time in the first 24 hours of adhesion (Figure 18). During the early stages of adhesion it was found that the deformation was proportional to the contact area of the cell, which increased as the cell spread on the surface. The cells which were barely attached to the substrate showed little deformation (after 6 hours), whereas when they were well-spread (after being in contact for 24 hours) they had the most visible deformation. The observation of deformed nuclei after such short incubation times suggests that the deformation occurs early, indicating rapid attachment of the plasma membrane to the sides of the pillars. Additionally, it is clear that even at 24 hours the nucleus still spanned the top of the pillars (blue colour present at the top of the pillars), whereas at later times (Figure 18) the majority of the nuclei were found to be exclusively inserted in between the pillars. Consequently, the nuclei continued to deform and rearrange at times longer than 24 hours. The rate of deformation was observed to depend on the rate of the spreading.

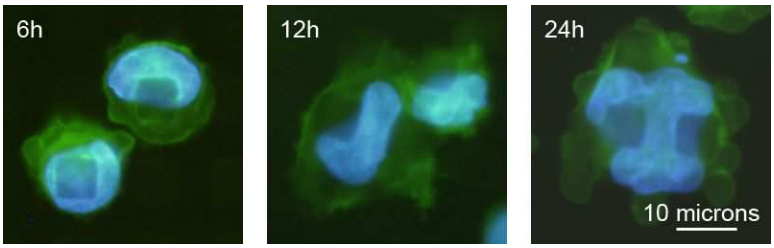

Figure 18: Early deformation of SaOs-2 cells on micropillared surfaces

3.3.2 Viability and Proliferation

The viability of SaOs-2 and MG63 cells at 10 days of incubation was verified using an MTT assay. Cells grown on micropillared surfaces showed the same level of viability as cells grown on flat surfaces without topographical features (Figure 19). The results obtained on the viability of the cells are in agreement with the aspect and number of cells present on the sample after 7 days of incubation (Figure 17): adherent cells need to be attached to a surface to survive and if the surface structures were detrimental to the cells they would not adhere (or not as strongly) and this would result in few to no cells on the sample after several days. Additionally, the number of cells on the two PLLA samples is similar (as determined by the MTT test), indicating that they have similar proliferation rates. If the proliferation rate was higher on one of the samples, the MTT measurement would result in a higher value because of the greater number of cells after 10 days of incubation.

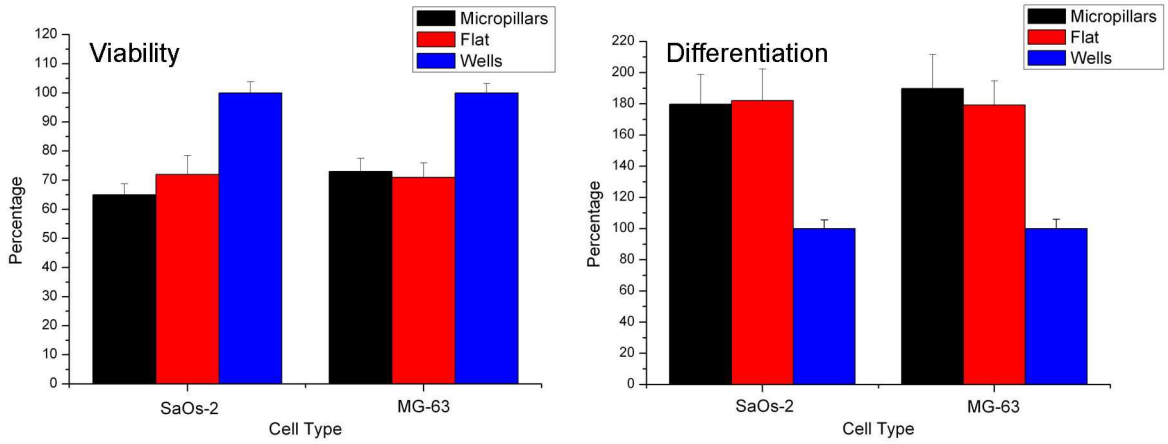

Figure 19: Measurement of the viability and differentiation of SaOs-2 and MG63 cells on PLLA micropillars, PLLA flat surfaces and tissue culture plastic ("Wells").

The replication rate was monitored using a BrdU assay. Such an extensive deformation of the cell nucleus could result in hampering of the proliferation, as mitosis is a highly organised and complex process that requires precise rearrangements within the entire cell. The ability of the studied cells to proliferate on micropillared surfaces was tested with a fluorescence marker for cells which have entered the S-phase of mitosis (Figure 20).[129] This label showed that even when cell nuclei were

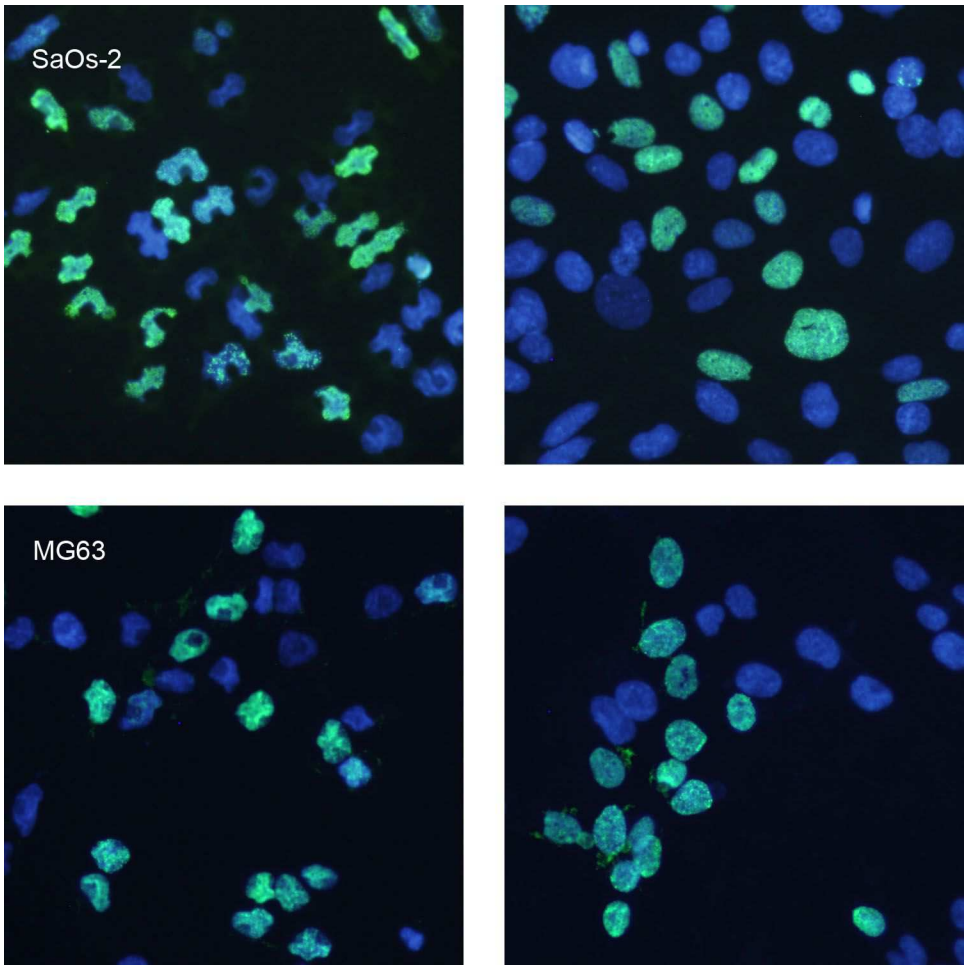

Figure 20: SaOs-2 and MG63 cells grown on micropatterned and flat surfaces for 96 hours, stained for the nucleus (blue) and replicating cells (green). The larger size of the nuclei of cells grown on unpatterned surfaces is due to the volume of the nucleus being restricted to the surface, whereas cells on the patterned surfaces can take up volume in between the pillars.

severely deformed, they were still able to enter the proliferation cycle. No difference was found in the number of replicating cells for SaOs-2 and MG63 cells compared to cells grown on unpatterned polymer surfaces, even after extending the incubation time over several days. (See Figure 20 and Table 4.) This indicates that the deformation of the nuclei did not impede proliferation of these cells. Cells can undergo mitosis several times, i.e., undergo rearrangements of the internal structure of the cell, while exhibiting a strong deformation of their nucleus during interphase.

The absence of any detectable effect on viability and proliferation is very surprising given the extensive deformation of the cells. This may be an indication of the ability of cancer cells to sustain their

phenotype even under stress, probably an essential requirement for metastatic cells that need to deform severely when travelling through the body.[1] The possibility to survive even when the nucleus is deformed indicates an important feature in the biology of cancerous cells.

	Sample	24h	48h	96h	148h
SaOs-2	Pillars	34% (492)	29% (457)	36% (1647)	27% (1606)
	Flat	28% (357)	28% (897)	36% (1537)	27% (1167)
MG63	Pillars	49% (707)	47% (195)	36% (1537)	9% (580)
	Flat	45% (1104)	51% (229)	38% (979)	11% (1138)

Table 4: Percentage of replicating cells on each sample. The numbers are reported as the percentage of BrdU-stained nuclei. The numbers in parentheses are the number of cells used in the measurement. Note the higher initial proliferation rate of MG63 cells compared to SaOs-2 cells (higher number of replicating cells at shorter times).

3.3.3 Differentiation and gene expression

Deformation of the cell, and in particular the nucleus, should have a profound impact on the functioning of the cell: it has been shown that gene expression is affected by the position of chromosomes in the nucleus and deformation would lead to unusual nucleus architecture.[130] In fact, positioning of genes near the nuclear membrane has been linked to the switching off of gene expression.[131] Extensive deformation of the nucleus increases the surface-to-volume ratio and should therefore result in a higher proportion of genes at the surface, which should result in modifications in gene expression. This was monitored by measuring the production of an enzyme that is commonly found in bone cells and the RNA expression of bone differentiation genes.

3.3.3.1 Alkaline Phosphatase activity

The differentiation of the investigated cells was studied by measuring the alkaline phosphatase activity, which is a typical indicator of differentiated bone cells.[132] The differentiation of SaOs-2 and MG63 cells was lower on the tissue culture plastic, but there was no significant difference between the differentiation on the two types of PLLA surfaces, patterned or flat. (See figure 19.) This difference is

thus due to the surface chemistry of the substrates and not the topography. SaOs-2 and MG63 cells grown on pillared surfaces showed an activity that was comparable to those grown on an unpatterned surface, indicating that deformation of the nucleus did not have a significant effect on the behaviour and functioning of the cell.

3.3.3.2 RNA expression

The expression of three bone differentiation genes was monitored by PCR. The expression on patterned surfaces was compared to that on flat PLLA surfaces. The three genes monitored were Alkaline Phosphatase, Collagen and Runx2. These are early markers of differentiation for bone cells.[133] A growth factor for bone cells, BMP-2, was added to samples to determine its effect on differentiation behaviour.

It is apparent from the results obtained in the RNA expression measurement that there may be a decrease in the differentiation of SaOs-2 cells when grown on the micropillars. (Figure 21.) However, the RNA expression of the cells grown on the micropillars was not found to be significantly different from the RNA expression of these cells on flat surfaces, due to the high errors associated with the measurements. Similarly, there is no significant difference between the differentiation of cells grown on flat or pillared surfaces in the presence of growth factor.

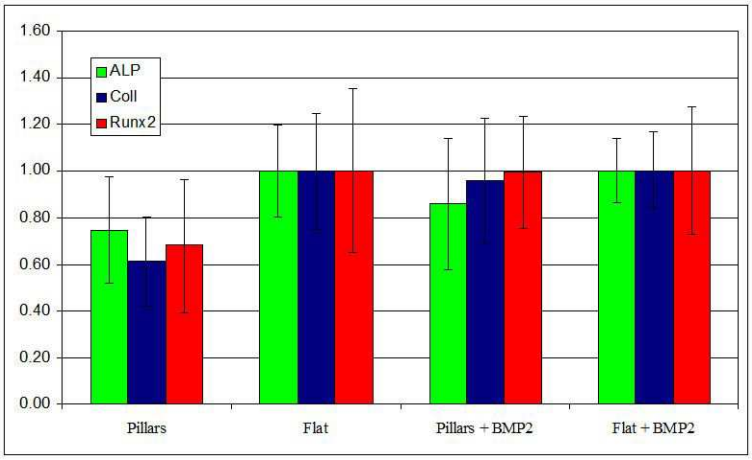

Figure 21: RNA expression levels of three early osteoblastic markers of differentiation in SaOs-2 cells grown on patterned surfaces, with or without growth factor induction, normalized to the expression on their respective flat substrates.

These results are in agreement with the alkaline phosphatase activity measurements performed above. However there is a (non-significant) trend that shows that cells that were not treated with growth factor may have decreased levels of RNA production of bone cell differentiation genes. The difference between the two types of measurements can be explained by the differences in the two techniques. Firstly the alkaline phosphatase activity measurements were performed after 10 days of culture, whereas the RNA expression measurements were performed after 2 days of culture. Secondly, the RNA expression measurements are more sensitive to changes in expression and detect differences upstream from the alkaline phosphatase activity measurements.

The (non-significant) difference between the RNA production of early bone differentiation genes on flat or microtopographied surfaces disappears on the samples to which growth factor was added. These samples show values which are much closer together. (Figure 21.) Addition of growth factor should lead to an increase in RNA production of bone differentiation genes. Hence, this difference in behaviour in the presence of growth factor may be explained by the purpose of the cell. In the presence of microtopography, the cell becomes deformed and may reduce its expression of differentiation genes to focus on other phenomena related to the surface topography. But in the presence of growth factors, the focus of the cell may be redirected back to differentiation, explaining that there is a decrease in the difference between cells grown on flat and micropillared surfaces.

The cell differentiation was significantly increased in the presence of growth factor for one of the conditions studied (Runx-2 on pillars, see asterisk in figure 22). In the other cases the difference is not significant, although once again trends are visible. (Figure 22.) It appears that the presence of growth factor increased the RNA expression of bone differentiation factors.

A similar study was conducted by Matschegewski et al., who looked at the behaviour of MG-63 cells grown on titanium cubic pillars of widths and spacings of 3 or 5 microns and heights of 5

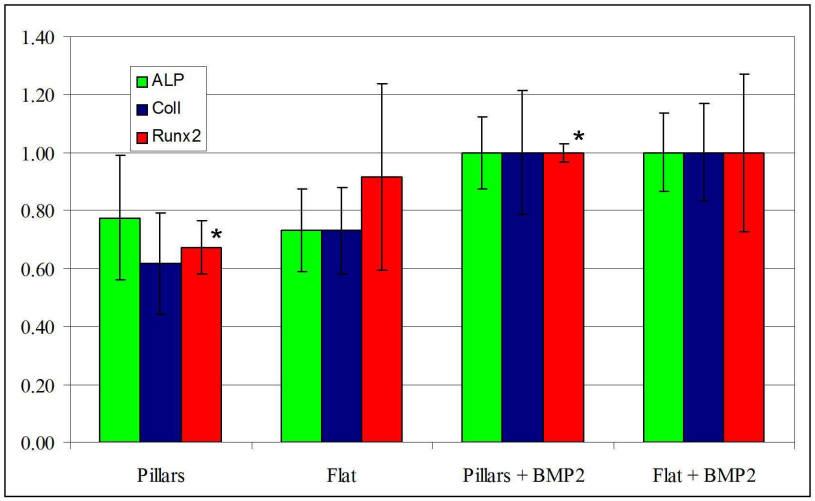

Figure 22: The effect of micropillars on the differentiation of SaOs-2 cells, normalized to cells grown in the presence of growth factor. The asterisk denotes significantly different samples.

microns.[109] Unfortunately they did not perform labelling of the nucleus to detect whether a similar deformation to the one we encountered is present on the titanium surfaces. However, they found reduced levels of Collagen-1 and Bone Sialo protein (BSP-2). This also resulted in a reduced expression of beta-3 integrins, although not in alpha-2, alpha-3 or beta-1 integrin receptors. These results are similar to ours, in which we found a slight (non-significant) decrease in the expression levels of bone differentiation genes. However it is difficult to compare these results with ours given that the cell lines and surfaces studied were different and we cannot know whether the cells were deformed to the same extent as ours.

Unfortunately lack of time and available primers prevented us from doing more extensive studies on additional RNA expression patterns that could have been informative, such as degradation enzymes used by cancerous cells (matrix metalloproteinases, MMPs), integrin receptors, cytoskeleton and nuclear membrane proteins. These could have provided us with clues regarding the type of protein expressed by the cell in response to the surface microtopography. However, in the case of cytoskeletal proteins, a large quantity is produced by the cell and the effect of the deformation may not be easy to distinguish. A proteomic measurement of the ratio of assembled cytoskeleton monomers to single

monomers may thus be a useful piece of information, giving us information on how the cell is managing its cytoskeleton network.

Additionally, future experiments should be carried out in a time-dependent manner to monitor the adaptation of the cells to the surface. Indeed, it has been observed that even though the cells initially deform slowly over a period of 24 hours, the cells deform rapidly after mitosis (there are no cells of intermediate deformation observed at longer time points). It could be thought that the cells facilitate deformation by adapting their composition, i.e. the type and quantity of nuclear membrane proteins and cytoskeletal proteins. In fact, it has been shown that cells can respond to shear stress by upregulating nuclear lamins and moving lamins from the nuclear interior to its periphery.[134] The authors suggest that the modification in lamin expression and location results in changes in the mechanical properties of the nucleus, allowing it to protect itself from exterior forces. It is therefore likely that similar changes are occurring in the SaOs-2 cells during their deformation. Hence, the RNA expression of the cells should be monitored before, during and after the early stages of deformation, as well as on flat surfaces.

3.3.4 Other cancerous bone cells

Four cell lines derived from osteosarcoma were used in our studies to examine the reproducibility of the deformation on these cell types. The cell lines used were SaOs-2, MG63, OHS4 and U2OS. These are well-established cell lines that are available commercially (except for OHS4). Despite their common origin, these cell lines have varying properties, such as their levels of differentiation and expression of known oncogenes such as p53 and pRB: SaOs-2 expresses neither, MG-63 only expresses pRB and U2OS expresses both.[135] However, these cell lines have similar aspects when grown on flat surfaces. They also showed similar behaviour when grown on micropatterned surfaces. (See figures 20 and 23.)

Cancerous cell lines come from cells that have been harvested from tumours. The cells used in this

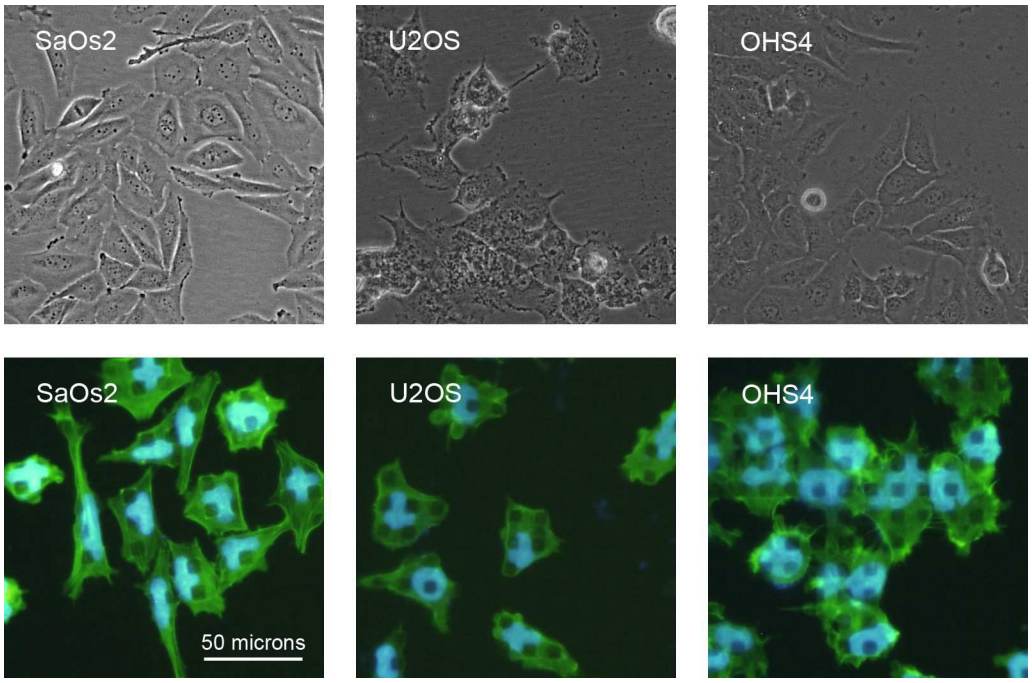

Figure 23: Phase contrast image of three osteosarcoma in cell culture (top) and these three same cell lines grown on micropatterned surfaces for 96 hours (bottom) and stained for their nucleus (blue) and their actin cytoskeleton (green).

study all came from osteosarcoma. Cancerous cells have a modified cytoskeleton which allows them to be motile and replicate quickly. They are also known to be more deformable than healthy cells.[33] Moreover, this has been related to their metastatic potential: cells that are more likely to form tumours *in vivo* are more deformable.[136,34] However, we did not see a clear relationship between the metastatic potential of cells and their ability to deform on surfaces. MG-63 cells have a higher metastatic potential than SaOs-2 cells *in vivo*.[137] In addition, MG-63 cells have a higher proliferation rate (shorter cell cycle time).[138] (See also Table 4: the initial number of replicating cells is higher.) When grown on microstructured surfaces, both MG-63 and SaOs-2 showed a deformation of their nuclei and their cytoskeleton, but there was a visible difference in the level of deformation: the MG-63 cell nuclei did not deform as extensively as SaOs-2. (Figure 20.) Therefore, a higher metastatic potential does not translate to a greater deformation on micropillared surfaces. Additionally, force measurements performed with an AFM have reported that SaOs-2 cells are more rigid than MG63 cells.[102] The difference in the extent of deformation is most probably linked to the viscoelastic

properties of the nuclei and much less to the deformability of the cytoskeleton of both cell types. The deformation is most likely the result of a balance between the rigidity of the nucleus and the force that the cytoskeleton is able to exert on it.

3.3.5 The behaviour of osteosarcoma on patterns of varying sizes

Many studies have been published recently in which the shape of biological objects has been related to the forces exerted upon them.[139] In the same manner, the shape of the nucleus should procure clues about the forces that are exerted upon it and hence, the architecture of the cell that contains it. In order to obtain information about the mechanical properties of the cells, substrates with pillars of different spacings were microfabricated. The smallest spacing achieved was 2 microns.

3.3.5.1 SaOs-2 cells

SaOs-2 cells were seeded on surfaces of varying spacings. Upon observation of these samples deformation was visible in every sample. In the sample with the smallest spacing (2 microns) most

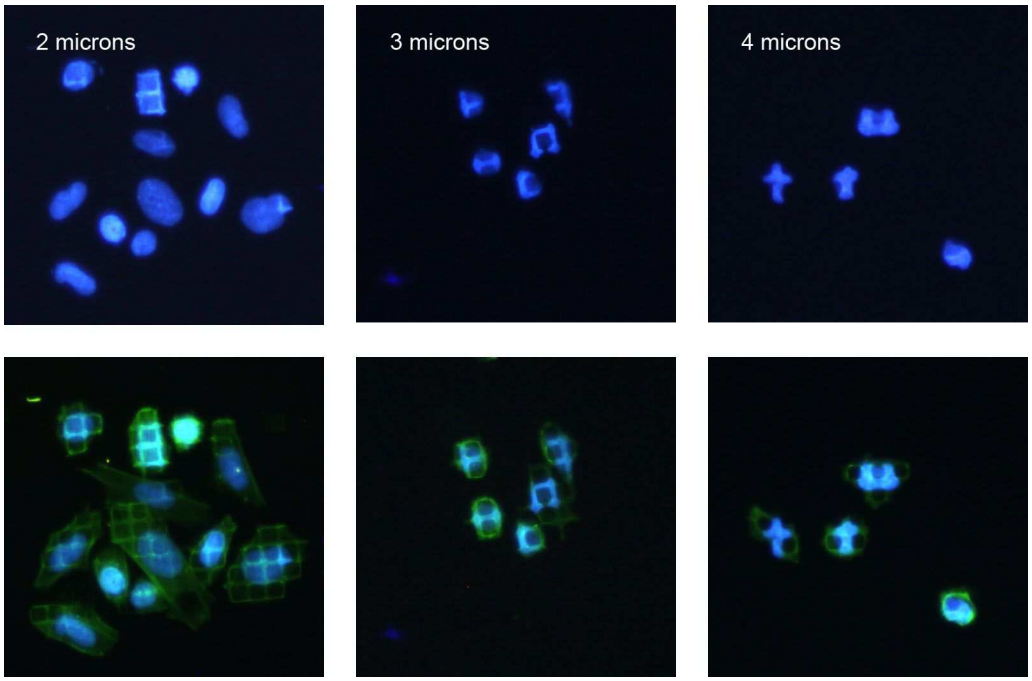

Figure 24: SaOs-2 cells grown on micropillars 7 microns wide and 2, 3 or 4 microns apart. The cells were incubated on the surfaces for 96 hours. The cell nucleus was labelled (blue) and is shown in the top images, the actin cytoskeleton was also labelled and shown in green in the bottom image, superimposed on the nucleus image.

cells show deformation of the actin cytoskeleton (about 80%), with some cells showing deformation in only certain regions of the cell. (See figure 24.) Several cells showed deformation of the nucleus as well (30-50%). However, we did not find any nuclei that had inserted themselves completely in between the pillars. With increasing time in culture we see a slight increase in the number of cells that have deformed nuclei, from around 30% at 24 hours to about 50% at 96 hours. In the sample with slightly larger spacing (3 microns) we found that all the cells showed uniform deformation of their actin cytoskeleton. Additionally, all the cells had deformed nuclei, and some even had their nucleus completely inserted in between the pillars. At a spacing of 4 microns most of the cells have nuclei that are inserted in between the pillars. Hence, the SaOs-2 cells have a threshold for deformation of the nucleus that is around 2 microns, and a threshold for complete deformation around 4 microns. However, it should be noted that the threshold may depend on the depth of the structures. The cell may be able to insert its nucleus completely in between the pillars at a spacing of 3 microns, but if the cell is unable to fit the nucleus in that space it won't be able to insert it completely. Experiments with deeper structures would have to be conducted to verify the thresholds.

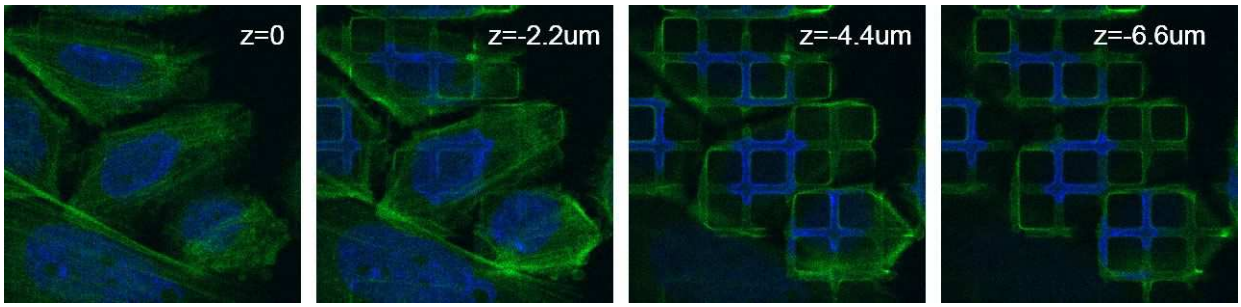

Figure 25: Images obtained on the confocal microscope of SaOs-2 cells grown on PLLA substrates with 2 micron spacing for 24 hours. Each image is in a plane approx. 2.2 microns above the next. Note that in the bottom left of the image the cell and its nucleus are not deformed and no fluorescence is visible in the lowest image.

The partial insertion of the nucleus in between the pillars in SaOs-2 cells was studied by confocal microscopy. Using this microscope we are able to take images at different focal planes and obtain information about the cells in the dimension that is perpendicular to the microscope. We were thus able

to confirm that the nuclei that show some deformation are not deformed on the top of the pillars, and deformed in the area below the top of the pillars. (Figure 25.) In images obtained above the pillars, the cells appear as if they were growing on a flat substrate. In images below the top of the pillars, the cells adopt the shape of the pillars and only the cells that are deformed remain visible. (Figure 25.)

The confocal microscope can also provide us with information about how the cell functions on the surfaces. For example, in figure 26 we can see a cell that has condensed its chromosomes and has entered the prophase of mitosis. In this figure we can see that the mitotic cell is present above the top of the pillars, an indication that cells most likely come out of their deformed state to undergo division.

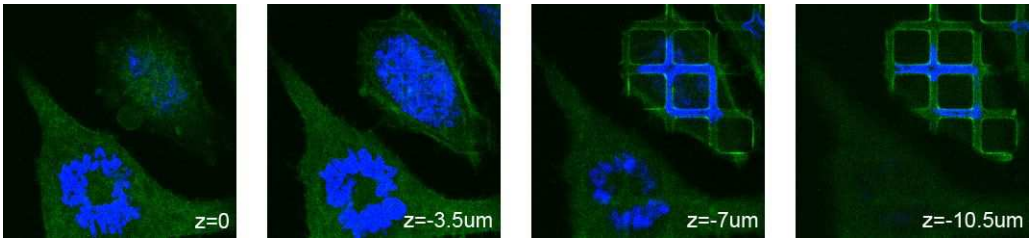

Figure 26: Two cells grown on pillars spaced 7 microns wide and 2 microns apart for 24 hours. Each image is in a plane 3.5 microns above the next. One of the cells has begun undergoing mitosis and is in a plane above the other one, which is deformed on the pillars and is thus visible in the last image.

3.3.5.2 Other cancerous cell types

Two other cancerous cell lines from bone were tested for deformation on pillars with narrow spacings. These were MG63 and OHS4 cell lines, both of which come from osteosarcoma. The cytoskeleton of the OHS4 cells showed extensive deformation of all cells at spacings of 2 microns without deformation of the cell nucleus. Deformation of the cell nucleus could only be seen at spacings of 4 microns and above and it was rare to find nuclei that were completely inserted in between the pillars. (Figure 27.)

MG63 cells had long cytoskeletal protrusions that ran along the trough between pillars on the surface for all sizes of the spacings. However, the cells were not uniformly deformed across the cell body and about half the cells showed no deformation. MG63 cell nuclei begin showing some deformation at spacings of 4 microns and nuclei that are inserted completely at spacings of 6 microns, although they

remain rare. (Figure 27.)

As reported above, most SaOs-2 cells are deformed at a spacing of 2 microns and there are some nuclei that are also deformed on these samples. We begin to see nuclei completely inserted in between the pillars at a spacing of 3 microns and at 4 microns most of the nuclei are completely deformed. (Figures 24 and 27.)

These results show that, despite initial observations that did not show any significant discrepancy between the behaviours of the different osteosarcoma-derived cell lines on the 7 micron spacing substrates, cells from similar origins and with similar malignancy do interact with surfaces differently. In particular, there is a large difference between the amount of deformation shown by the OHS4 and SaOs-2 cells on the surfaces: the SaOs-2 cells show deformation of their nucleus at very narrow spacings, whereas OHS4 cells show deformation only at larger spacing, despite the fact that their cytoskeleton is very much influenced by the microstructures, even at 2 microns. These results indicate that OHS4 cells are not able to exert forces on the nucleus the same way that SaOs-2 cells do. This may be due to differences in the mechanical properties of the nuclei or the force that the cells are able to exert on them.

Differences in mechanical properties of the nuclei of cancerous cells are most likely related to the changes in composition of the nuclear membranes of the cells with malignant transformation. It has been reported that specific nuclear membrane proteins (NMPs) are associated with specific types of cancer and that highly metastatic cells have radically different NMP profiles.[140,14] This could lead to important differences in mechanical properties of the cells as NMPs, such as nuclear lamins, play an important role in the structural rigidity of the nucleus.[11] These modifications in mechanical properties could explain the differences in the ability of cells to insert their nucleus in the space between the pillars, even though they show strong interactions with the surface through their cytoskeleton.

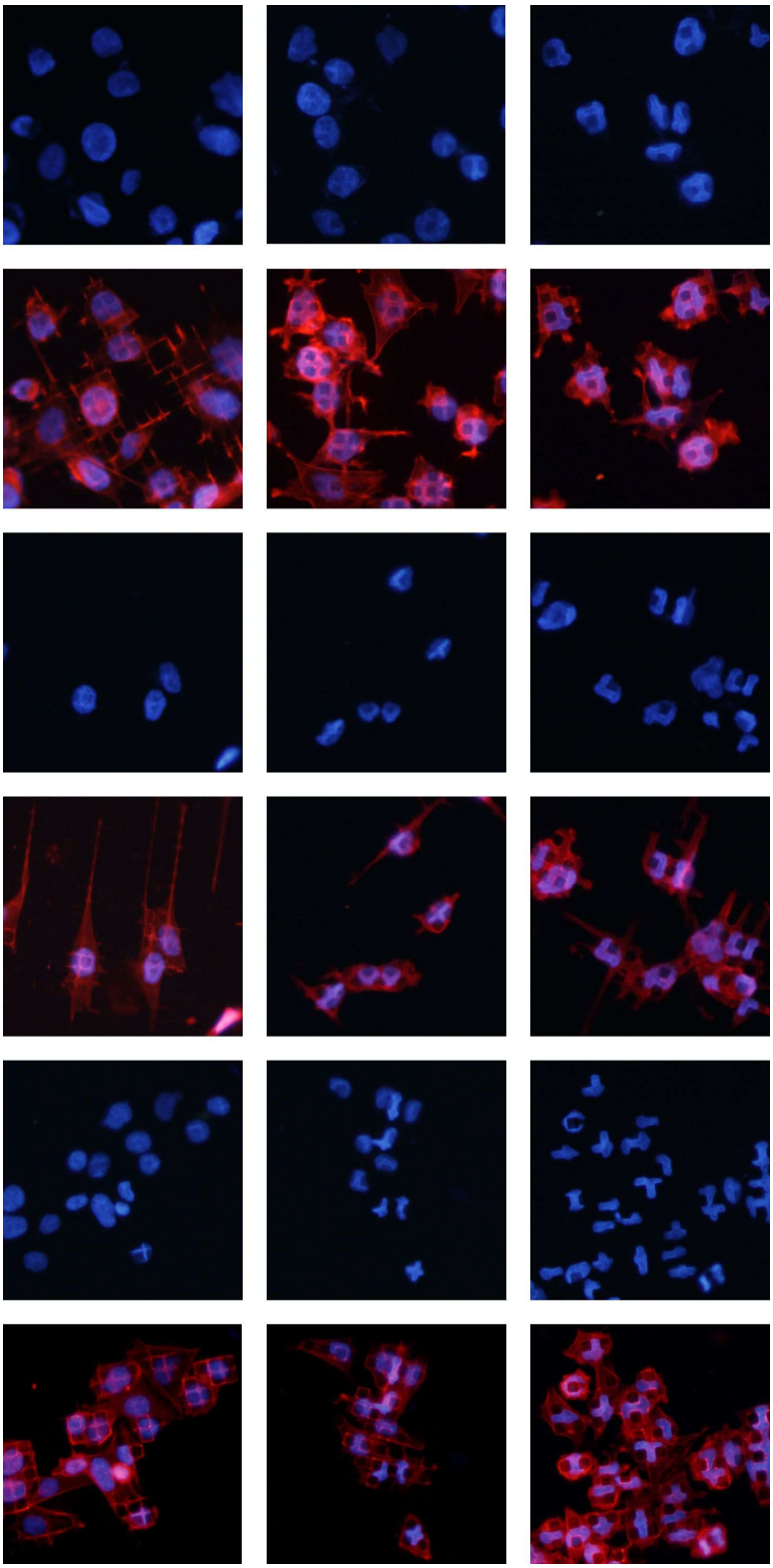

Figure 27: Fluorescence images of OHS4, MG63 and SaOs-2 cells grown on micropillars with spacings of 2 microns (left), 4 microns (center) and 6 microns (right). For each cell line, the top image shows the nucleus labelling alone (blue) and the bottom image also shows that actin labelling (red).

In addition to providing us with information about the management of the nucleus by cells, the surfaces we are using could be useful as diagnostic tools for cells. Cells with more rigid nuclei may show strong interactions with the surface without being able to deform their nucleus strongly. These surfaces could allow the identification of nuclear mechanic properties without any manipulation of the cell. We had previously discussed the possibility that the deformation may be related to the metastatic potential of the cells, however this does not seem to be the case. The ability of cells to deform their nucleus is most likely related to the mechanical properties of the nucleus and the cells' ability to exert sufficient force on the nucleus. It is also possible that the metastatic or differentiation state of cells determines whether they are "programmed" to deform on the pillars, in this case the cells would be capable of deforming but do not do so. We cannot exclude that cells have mechanisms that prevent insertion of their nucleus in the available space beneath them, however the fact that they do deform their nucleus at higher spacing sizes would indicate otherwise.

In order to understand whether the difference in deformation is due to the properties of the nucleus or the properties of the cell, these must be studied separately. The viscoelastic properties of the cell nucleus can be studied using different methods, including AFM measurements and micropipette aspiration.[5,6,11] In this manner we could compare the extent of deformation to the mechanical properties. If the cells that have stiffer nuclei are able to deform their nuclei more than cells with softer nuclei we could then take a step towards understanding the forces that cell exert on their nuclei. This study is the subject of ongoing work with a collaborator at the Karlsruhe Institute of Technology.

3.4 The deformation of bone cells as a function of their malignancy

Cancerous cells are known to be more deformable than normal cells: metastatic cancer cells are much more flexible which is in accordance with their need to move through tissues to invade other organs

and tissues.[33] AFM measurements have also shown significant differences in the mechanical properties of the nucleus region of pre-cancerous cells: normal cells were found to be more rigid than dysplastic or metaplastic cells.[13] For this reason, tests were also performed on bone cells of different malignancies: healthy cells and immortalized cells.

3.4.1 Healthy cells

When grown on micropillared surfaces the healthy human osteoprogenitor (HOP) cells showed very little deformation. In fact, almost all of the nuclei were unaffected by the presence of the micropillars (Figure 28). Very few cells presented deformation of their cytoskeleton. This result suggests that non-cancerous cells interact with structured surfaces differently from cancerous cells. The plasma membranes of the non-cancerous cells do not deform as readily to adopt the shape of the surface and allow for an increase of the contact area between cell and surface. One may speculate that the cytoskeleton of non-cancerous cells can prevent such a deformation in order to maintain the integrity of

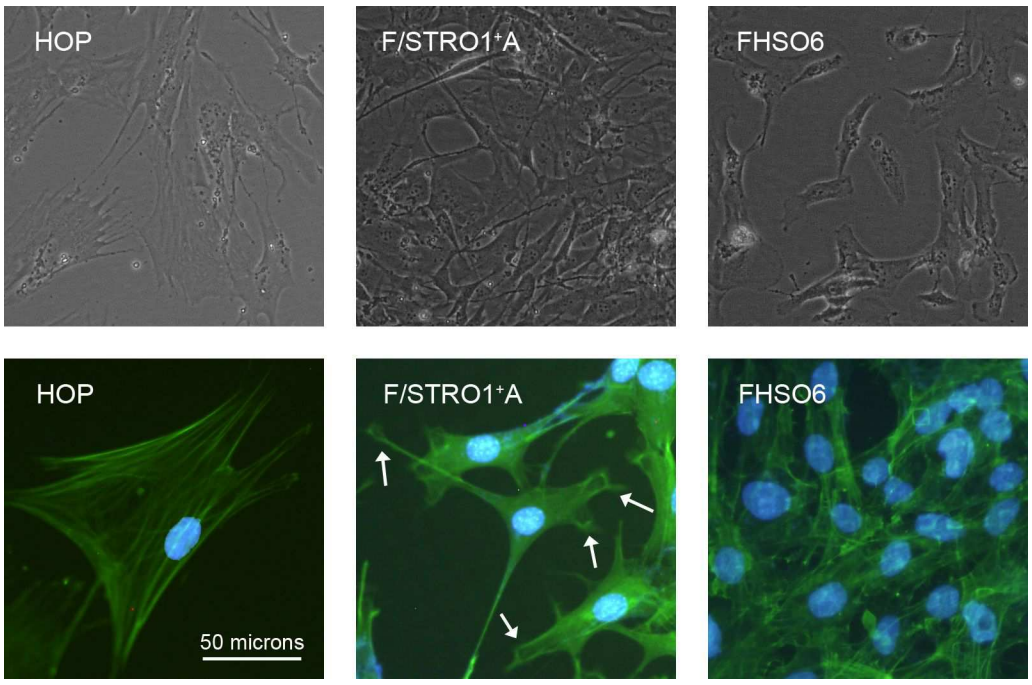

Figure 28: Healthy (left) and immortalized (center and right) cells. In the top images is shown their aspect when grown on a flat surface (phase contrast image) and in the bottom images are these same cells grown on micropillared surfaces for 96 hours. The arrows show areas in which the F/STRO-1^{+}A cells are deformed by the pillars.

the inner structure and organisation of the cell. However, we are cautious as a size effect cannot be discredited: the difference in size of the studied cells may also contribute to the observed difference in deformation behaviour.

3.4.2 Immortalized cells

Immortalized cells are healthy cells that have been infected with an oncovirus, enabling increased proliferation rates and ease of culture. These cells are not cancerous because they did not come from a tumour and, in general, would not produce a tumour in a body, yet they have some properties of cancerous cells. Studies that compare the deformability of cells often use transformed cells to establish trends, in which they show that immortalized cells are also more deformable than their healthy counterparts.[34]

The immortalized bone-derived cell lines showed interaction with the surfaces, but not in the same manner as the cancerous cell lines. The F/STRO1^{+}A cells did not show any deformation of the nucleus at all. (Figure 28.) In each cell the nucleus was perfectly rounded and undisturbed. The cytoskeleton was unaffected in the areas around the nucleus, but the extremities of the cytoskeleton were often deformed, as if micropillars had been used by the cell as anchor points. The cells also presented long protrusions (filopodia) that were often terminated by “lasso” shapes. (Figure 28, arrows.) The second immortalized cell line, the FHSO6 cells, were deformed on the pillars, although not as extensively as the cancerous cells. The entire cell appeared to be lightly imprinted with the shape of the pillars. The nucleus of the cells were rounded and lightly affected by the pillars, except in a few cases where the nucleus was deformed and a lower intensity of the labelling was visible on the top of the pillars.

The healthy and immortalized cells deform to a much lesser extent than the cancerous cells. The major difference appears to be the arrangement of the cell on the pillars: the healthy and cancerous cells do not deform their cytoplasm to adopt the topography of the pillars. Instead, they seem to span the top of

the pillars. This points to an important difference in the architecture of the cells and the response to cell topography. Upon contact with surfaces, the cells spread across the top of the pillars rather than deform to increase contact area with the surface. Hence, this difference may not be related to the mechanical properties of the cells, but rather to their mechanisms of adhesion to surfaces. This is governed by their cytoskeleton. HOP and F/STRO-1^{+}A cells have similar features when placed on flat surfaces (Figure 28): they are elongated and have a lot of filopodia-like protrusions, indicating that they have very active cytoskeletal networks. In the immunohistochemistry images, HOP, F/STRO1^{+}A and FHSO6 show distinct actin fibres whereas the cytoskeleton of the cancerous cells is more uniform across the whole cell, indicating less organization into fibre bundles. These observations are in accordance with reports that the cytoskeleton of cancerous cells is less organized than healthy cells.[33] The organization present in the non-malignant cells seems to be able to prevent severe deformation of the cell and its nucleus. The cytoskeletal filaments may be able to surround the nucleus and shield it from external topography. In this way, healthy cells may have less flexibility in their shape, whereas cancerous cells adapt to the surface on which they grow, enabling them to survive on surfaces other than their native tissue. Hence, cancerous cells may be able to survive in other parts of the body and under higher stress than healthy cells, a necessary trait for metastatic migration.

Interestingly, the responses of the different healthy and pre-cancerous cell lines to the surfaces differ greatly. The immortalized cells were chosen for their osseous phenotype, which should make them phenotypically similar to HOP cells: F/STRO1^{+}A cells display features of immature osteoprogenitor cells [117] and FHSO6 cells appear to express characteristics of immediate precursors of mature osteoblast-like cells.[118] Nevertheless, important differences have been found in the cytoskeleton of immortalized cells compared to their healthy counterparts. These cells were immortalized with the SV40 oncovirus which blocks the p53 and pRB tumour suppressor genes.[30] These genes help regulate

the cell cycle, and, in particular, stimulation of p53 was found to be associated with an increase in organized microfilament bundles.[32] Cells immortalized with SV40, have been reported to produce less actin and tubulin than normal cells,[33] and to have a less ordered cytoskeleton.[34] AFM measurements performed on normal, metaplastic (p16 deletion) and dysplastic (p53 deletion) cell lines showed important differences in the rigidities of these cell lines. It was found that the normal cells were the most rigid, with a Young's modulus of 4.7 kPa, followed by the metaplastic cells (3.1 kPa) and the dysplatic cells (2.6 kPa).[13] Similar differences where found in the stretchability of normal and cells immortalized with SV40 using an optical stretcher.[34] These changes in cytoskeleton architecture and mechanical properties are almost certainly at the root of the difference in response of the healthy and cancerous cells to the surfaces.

3.4.3 Kinetics of the deformation

SaOs-2 cells have been shown to deform at delays as short as 6 hours. (Figures 18 and 29.) At this time point, the cells are not yet well-spread, each cell only takes up one or two pillars. In spite of this the deformation is already clearly visible. With increasing time the cells spread and the deformation increases. On the other hand, at the 6 hour timepoint the HOP cells are already spread on the surface and most of the cells showed some deformation (about 70%). This was visible in the nuclei as a diminution of the fluorescence across the top of the pillars, though most still had a roughly round shape. The cytoskeleton also showed some deformation. Some cells had filopodia that ended on micropillars (Figure 29) and some had filopodia that ran along the top of a row of micropillars, or along the trough in between a row of micropillars. The cells whose filopodia ran along the bottom of the interspaces were the most deformed.

At 12 hours the HOP cells have a less rounded, more polarized shape and have spread more on the surface of the pillars to take up a larger area. The number of cells showing deformation has decreased

(about 50%) and the deformation of the nucleus is less obvious: the nuclei of the cells are still partially deformed, but less so and appear more rounded. On the other hand, all of the SaOs-2 cells show deformation of the cell body and the nucleus. This trend continues in the samples at the later time points and at 48 hours only about 10-20% of HOP cells have deformed nuclei whereas all of the SaOs-2 cells are deformed and the extent of nucleus deformation has increased. The deformation in the HOP cells is not extensive: the nuclei have rounded shapes and the deformation is only visible as a slight loss of fluorescence over the top of the pillars. The cytoskeleton of the HOP cells at later time points have distinct actin fibre bundles. In the SaOs-2 cells the cytoskeleton staining is diffuse and indicates a disorganized arrangement of thin fibres, rather than the thick fibre bundles present in the case of the

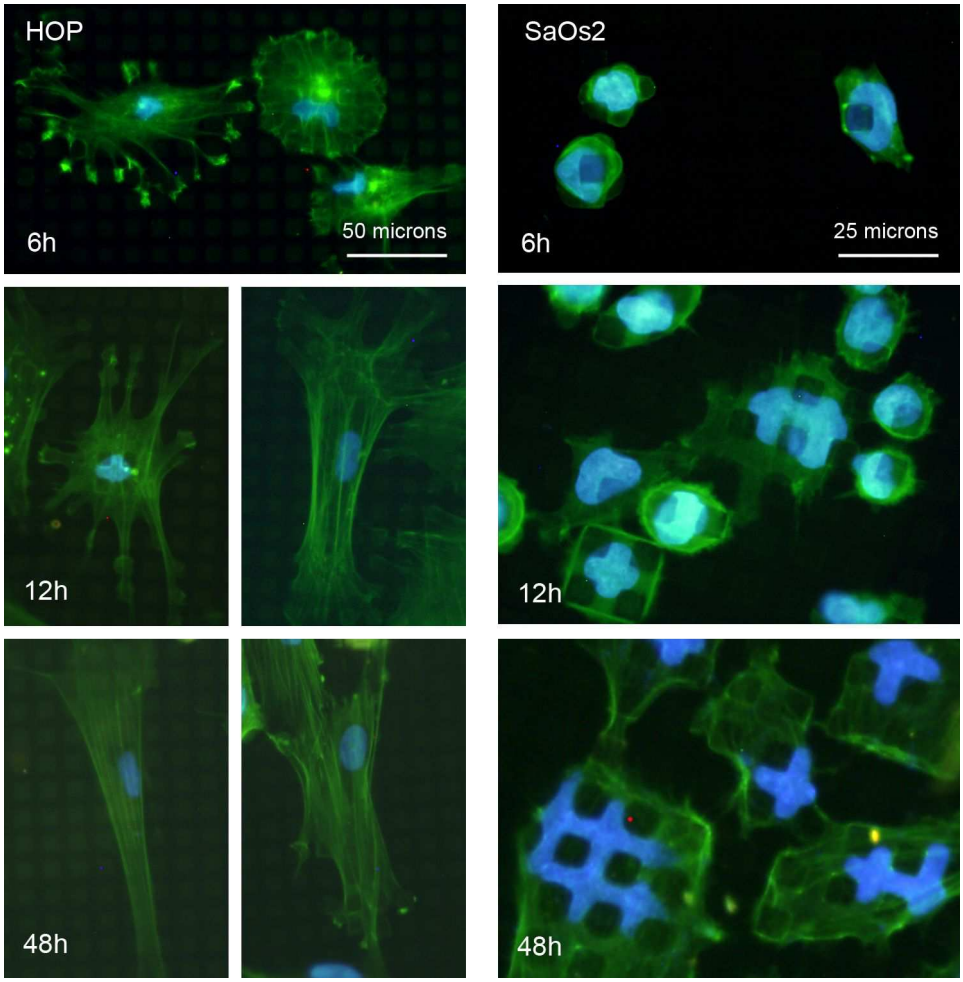

Figure 29: The kinetics of healthy (left) and cancerous (right) bone cells grown on micropillared surfaces.

HOP cells. This suggests a different cytoskeleton architecture or that the cytoskeleton of the HOP cells is more organized than the cytoskeleton of the SaOs-2 cells.

The behaviour of the cells at short times may also provide clues regarding the early organization of the cytoskeleton. Upon adhesion to a substrate, cells initially form attachment points within a matter of minutes. This is followed by a phase of cytoskeleton filament formation that occurs within hours of attachment. At longer timescales (hours to days) the cell begins to exert forces on its surroundings and migrate on the surface. In cancerous cells, deformation is visible as soon as the cells adhere to the surface and is maintained with time. This indicates that the cytoskeleton acts on the nucleus very early on. In the case of the HOP cells, deformation is also visible at short time points, during the initial stages of spreading, but is gradually lost with time as the cell continues to spread (Figure 29). By contrast, the cancerous cells show increased deformation with time. This indicates a disparity in behaviour: with time in culture, the healthy cells oppose deformation whereas the cancerous cells promote it. The entire cell, including the nucleus, is under continuous pressure to deform.

3.5 The deformation for other cell types

To understand the deformation of the cells on the microstructured surface, the behaviour of other types of cells were studied. These were all epithelial cells of different origins: Keratinocytes and dermal fibroblasts, transformed dermal cells and intestinal cells.

3.5.1 Keratinocytes and Dermal fibroblasts

The first type of healthy cells used were primary dermal fibroblasts. They did not seem to adhere to the surfaces very strongly: few cells were present on the surfaces. Deformation of the cytoskeleton of the cells could be seen: in some cells actin filaments followed the direction of the trenches in between the pillars, and the shape of the pillars could be seen in the cytoskeleton. The nucleus was rarely affected

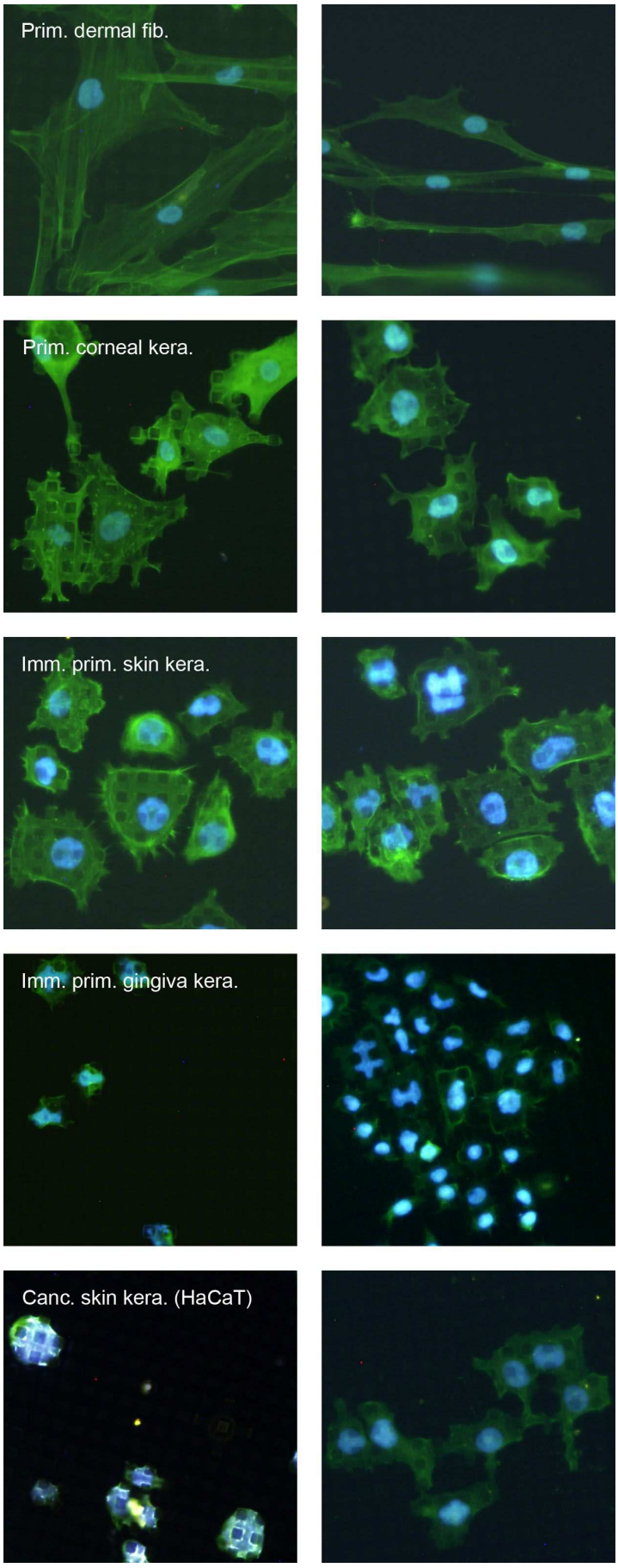

Figure 30: Keratinocytes grown on micropillars for 24h (left) and 96h (right). The cells were labelled for their nucleus (blue) and actin cytoskeleton (green).

by the structures.

Primary corneal keratinocytes were obtained from explant cultures of corneas. These cells showed deformation of their cytoskeleton at all time delays and minimal deformation of their nuclei. Nucleus deformation was visible, although the nucleus usually retained a circular shape and was not inserted in between the pillars. The cytoskeleton of the cells did not present long actin filaments similar to those present in the dermal fibroblasts.

Two immortalized cells lines were used. The first is derived from human primary keratinocytes (HPK) and originates from human foreskin. These cells showed deformation of their cytoskeleton and nucleus at all times in culture. At the shorter time delays, cytoskeleton filaments are visible at the periphery of the cell (filopodia), but the cytoskeleton within the cell body is always uniform and there are no visible filaments.

The second was obtained from human gingiva and immortalized using the HPV virus genes E6 and E7. The cells grown on micropillars showed extensive deformation of the cytoskeleton and nucleus. In particular the cell was able to insert its nucleus in between the pillar and have it adopt a deformed shape so that it was no longer spherical. This behaviour indicates that the cell is able to exert greater force on the nucleus, or alternatively that the nucleus is more deformable in immortalized primary gingival cells.

This third immortalized cell line is a non-tumorigenic keratinocyte population derived from the distant periphery of a melanoma. These are denoted “HaCaT” (Human adult skin keratinocytes propagated under low Ca^{2+} conditions and high temperature). These immortalized cells presented deformation of the cytoskeleton and nucleus at all time delays studied. The pillars were clearly visible in the cytoskeleton and the nucleus, although the nucleus retained its circular shape. The type of deformation observed is similar in nature to the immortalized primary skin keratinocytes.

The healthy cell lines used in this study presented deformation of the cytoskeleton when grown on the micropillared surfaces. The epidermal fibroblasts only showed occasional deformation of the cytoskeleton: actin filaments followed the direction of the grooves. The cytoskeleton of the corneal keratinocytes was very deformed and did not present filament bundles (stress fibres). There was a difference in the effect of the microstructures on the nuclei of the two cell types: in the case of the dermal fibroblasts the nuclei were not affected, whereas the nuclei of the corneal keratinocytes were partially deformed. The cytoskeleton of each of the immortalized cell lines were strongly deformed and each of these cell lines showed deformation of their nuclei. Whereas the healthy corneal keratinocytes showed some deformation of their nuclei, this was more prominent in the immortalized cell lines, in particular the gingival keratinocytes.

3.5.2 Transformed epithelial cells

One of the important clues about the behaviour of cells on microstructured surfaces is the differential behaviour of healthy and cancerous cells grown on these surfaces. However, the cell types used are not easily comparable as they come from different patients and may have differences that are not due solely to the malignancy of the cells studied. In order to remove this uncertainty we used cells that were transformed in the group of William Hahn.[141] These cells are derived from the same healthy parent cell line and have been sequentially transformed so that genes known to be related to cancer are perturbed.

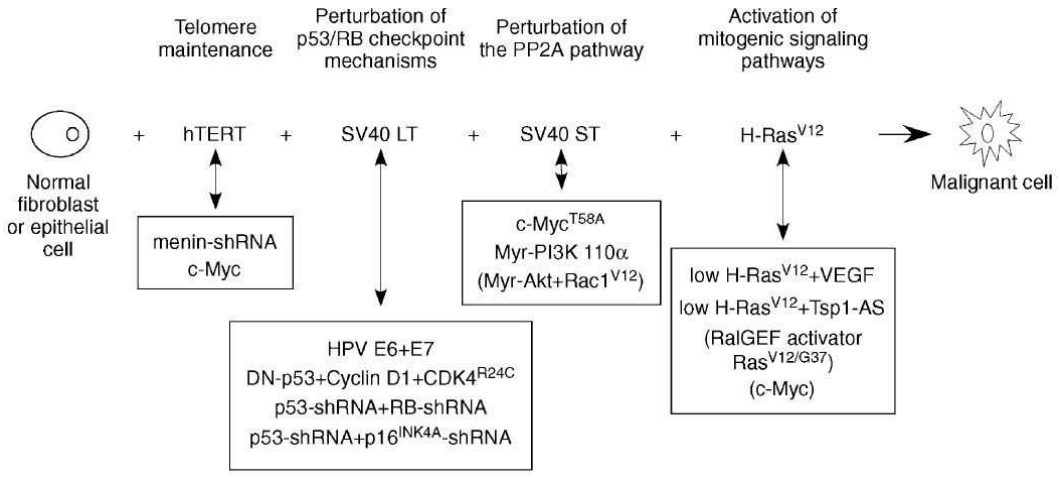

Figure 31: Transformation of cells using oncogenes. Figure reproduced from Boehm et al.[141]

(Figure 31.) We used three types of cells: cells that had an hTERT modification, cells that had hTERT and SV40LT modification, and cells that had hTERT, SV40LT and SV40ST modification.

The cells were seeded on micropillared surfaces and their response was monitored by fluorescence microscopy. The cells showed some deformation of the cells on the surfaces, although it often was not uniform across the cell and not in every cell. Based on our previous experiments we would expect to see some deformation in the cells and increasing deformation with increasing malignancy. However, this trend was not visible in the cells studied. (Figure 32.) It seemed as though the reverse trend was true: the cells that were the most transformed showed the least amount of deformation on the surfaces. This behaviour is surprising given the previous results we have shown on cells of varying malignancies. At present it is difficult to explain this behaviour, although it may point to a difference in the cell mechanics of transformed cells compared to cells that have been harvested from tumours.

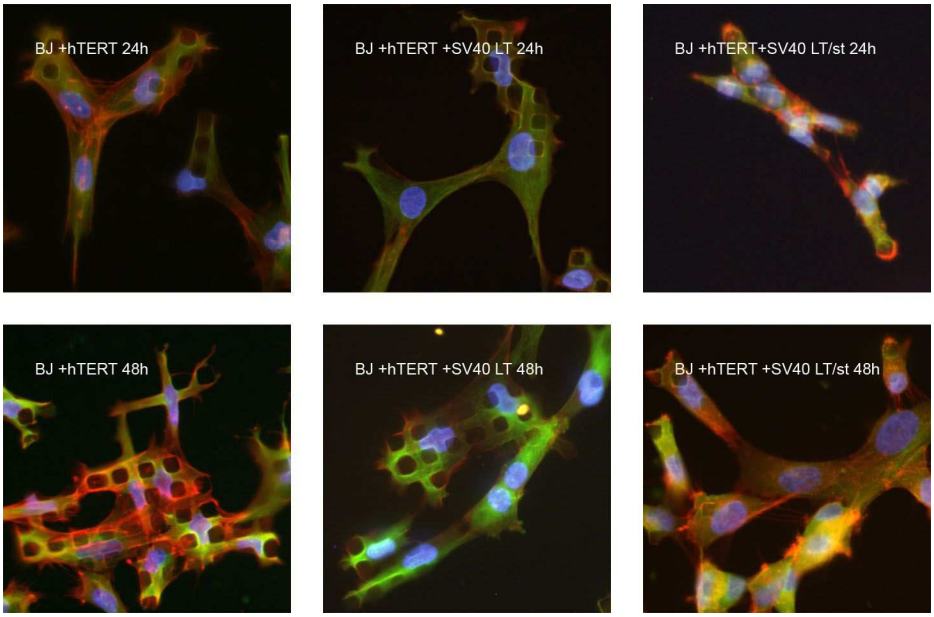

Figure 32: Epithelial cells sequentially transformed seeded on micropillared surfaces. The actin cytoskeleton is labelled in red, the microtubules in green and the nucleus in blue.

3.5.3 Intestinal (adenocarcinoma) cells

Human colon adenocarcinoma cell lines are useful as a model for studying intestinal cells. Healthy

intestinal cells are polarised, have brush border microvilli and tight junctions, produce specific proteins and are capable of vectorial transport. The cell lines available for culture were obtained from tumours and very few have the same properties as healthy intestinal cells. CaCo-2 cells are a widely used model as they spontaneously display properties of differentiated intestinal cells: they form domes in culture (indicative of polarization), form an apical brush border with their associated hydrolases and display enterocytic (absorptive cell) differentiation. Four cell lines were used to test the interaction of colorectal adenocarcinoma with microstructured surfaces: CaCo-2/TC7, HT-29, HCT-116 and SW-480.[142] TC7 cells are a clone of CaCo-2 cells with homogeneous population and high differentiation properties.[143] HT-29 cells are capable of enterocytic differentiation only when grown in the absence of glucose.[142] When grown with glucose the HT-29 cell layer forms intercellular cysts, while when grown in the absence of glucose the cells are polarized with the presence of an apical brush border. Under these conditions HT-29 cells can produce the same enzymes as CaCo-2 cells except for lactase. Neither SW-480 nor HCT-116 form domes in cultures, indicating that they do not form polarized layers.[142] Both CaCo-2/TC7 and SW480 are known to express Cdx-2, a protein that is a homeobox transcription factor that is a marker for gastrointestinal differentiation. Cdx-2 is also known to be involved in oncogeneicity and is believed to be a tumour suppressor gene.[144] Both CaCo-2/TC7 and HT-29 cells express a mutant of p53 which is inactive, HCT116 expresses wild-type p53 and SW480 expresses a mutated p53. Although all intestinal cells that are cultured originate from cancer, it is believed that their malignancy may be related to their ability to polarise, a hallmark of healthy cells. Hence, CaCo-2 and HT29 would be the least malignant cells.

Of the cell types studied the CaCo-2 cells are the most polarised in culture. On the micropillared substrates they deformed readily. (Figure 33.) The deformation was most visible in the actin cytoskeleton, but the nuclei and the microtubule network were also deformed. At longer incubation

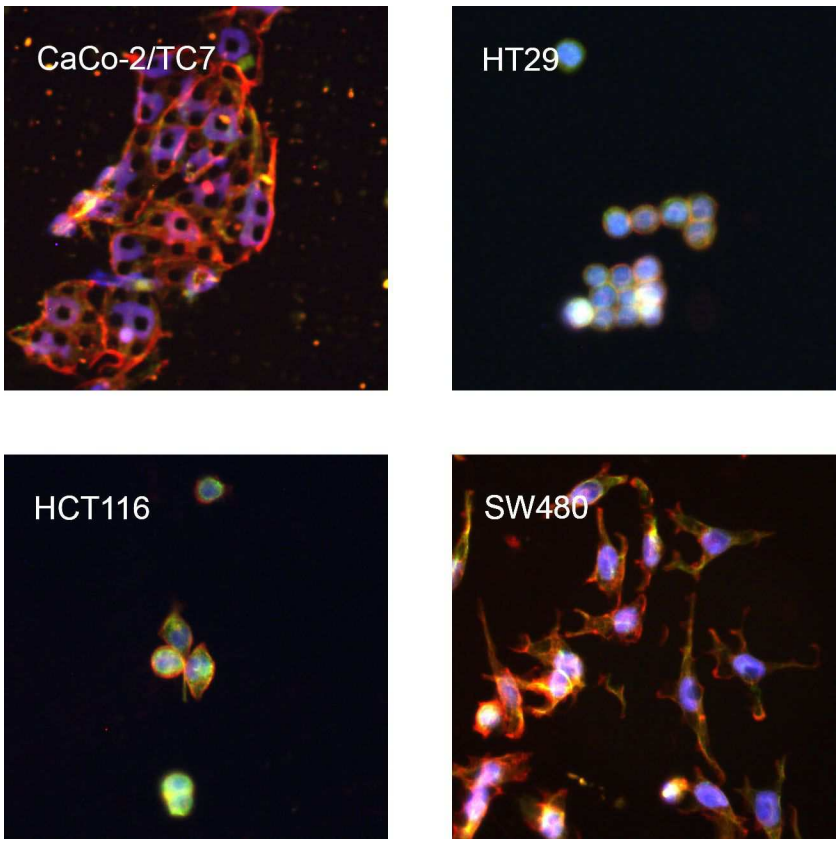

Figure 33: Four adenocarcinoma cell lines grown on micropillared surfaces for 24 hours.

times the cells can form aggregates and the cells in the middle of the aggregates are no longer in contact with the surface and are not deformed.

HT29 cells are cells that are polarized in culture on flat surfaces. When grown on micropillared surfaces they adhere but do not spread very much, possibly indicating that they retain their polarization. In some cases it can be seen that the cells arrange themselves on the top of the pillars and thus show a square close-packing. At longer incubation times the cells form aggregates.

The HCT116 cells are known not to be as polarized as the CaCo-2/TC7 and HT-29 cells. In culture on flat surfaces they do adopt a polarized conformation. When grown on micropillared surfaces they spread more than the HT-29 cells, but seemed to be largely unaffected by the surface structures.

The SW480 cells are the least polarized cells studied. They present a fibroblastic appearance when grown on flat surfaces. On micropillared surfaces they spread and deformed to adopt the surface

structure. Deformation could still be seen clearly even at the longest incubation time as the cells did not form tall aggregates as readily as the other cell lines. At incubation times larger than 24 hours the cell nuclei did not seem to be deformed.

Two of the adenocarcinoma cell lines tested displayed deformation on the mcropillared surfaces: CaCo-2/TC7 and SW-480. Remarkably, these two cells lines were the most and the least polarized cells, excluding a link between polarization/enterocytic differentiation and deformation ability. There was also no clear link between p53 expression and deformation as CaCo-2/TC7 and SW-480 do not express active p53, but neither does HT29. Yet, both deformable cells express Cdx-2, the homeobox enterocytic differentiation gene. The link between cells that express Cdx-2 and their ability to deform on surfaces is of particular interest because this gene has been linked to tumour suppression.[144]

3.5.4 Summary of results on different cell types

The results obtained on cell lines other than cells originating from bone show that the origins of the deformation phenomenon are not simple to explain. In the case of dermal cells we found that there seems to be a link between malignancy and deformation: overall the more malignant cells deformed more than the primary (normal) cells. However, experiments on the transformed cells showed an opposite trend: the cells with the most transformations appeared to be the least deformed. It must be noted that transformed cells and cancerous cells are not the same, and the transformed cells may have different properties than cells that originate from a tumour.

The results obtained on the adenocarcinoma cells show that the deformation is not universal in intestinal carcinoma cells. All of the cells studied originated from tumours, yet only half of them showed deformation on the surfaces. This points to a more complicated mechanism of organisation of adenocarcinoma cells in response to surface topography. Intestinal epithelial cells have a particular organisation that is due to their excretory function. Yet, the ability to deform does not seem to be

related to the cells' ability to perform this function, as the most polarized and least polarized cells deformed on the micropillared surfaces. However, these two cell types do have in common that they express Cdx-2, a homeobox gene that has been linked to malignancy in adenocarcinoma. This property is the subject of an ongoing thesis in our group. In particular, cells in which Cdx-2 expression can be turned on or off will be studied to determine whether this gene has a determining role in the deformation.

3.6 Understanding the deformation

3.6.1 The role of the cytoskeleton

When cells are grown on micropillared surfaces they may adopt the surface topography and this deformation can extend to the interior of the cell. In this manner, we have seen deformation of the cell nucleus to adopt the topography of the surface. This self-driven deformation is surprising given that the nucleus is generally described as a stiff structure (stiffer than the cytosplasm). Experiments on the deformation of the nucleus, using for example micropipette aspiration, have found that forces on the order of 10^{-9}- 10^{-7} N are necessary to deform the nucleus, whereas the force of gravity on an entire cell is only on the order of 10^{-11} N for a typical cell (10^{-9}g).[5] The deformation is therefore certainly due to forces other than gravity. The most likely culprit is the cytoskeleton as it is known to exert considerable forces on its surroundings. There are three known components of the cytoskeleton: actin filaments, microtubules and intermediate filaments. For a description of these systems, please see Chapter 1.

Extensive spontaneous deformation of the nucleus has not yet been described and it is surprising that cellular mechanisms would exist that would encourage this type of behavior. By which mechanism do cancerous cells deform to adopt the shape of the pillars? How is the cell able to reorganize its inner structure in response to the surface topography?

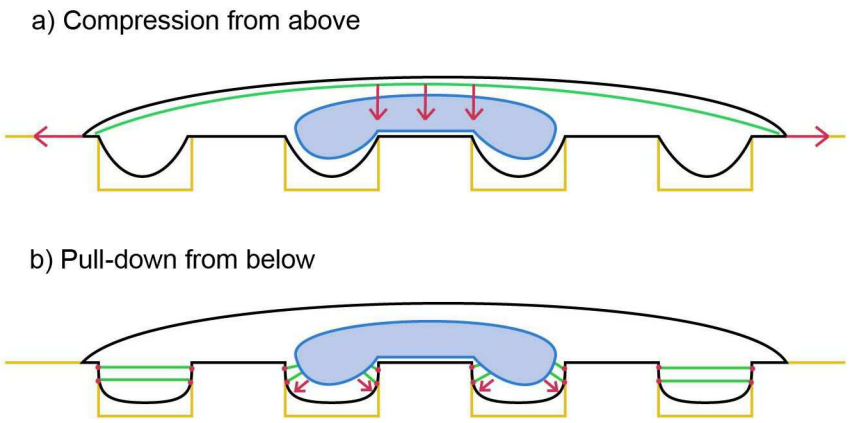

Figure 34: The nucleus is deformed by forces exerted by the cytoskeleton. Proposed mechanisms are shown in which the nucleus is being pushed down through the spreading forces exerted on the cell (a), and the nucleus is pulled down through the focal point-cytoskeleton-nucleus network (b). The cell outline is shown in black, the nucleus in blue, and the cytoskeleton fibres that are the main actors of the deformation are in green. The red arrows represent the forces exerted by the cytoskeletal fibres shown.

To answer these questions we need to better understand the cytoskeleton and the way it may induce such a deformation. The cytoskeleton forms an interconnected network around the cell nucleus.[145] It is connected to the cell wall at the focal contacts and to the nucleus through the LINC complex and lamins.[22] (See also Chapter 1.) In the area close to the cell membrane a layer of actin filaments forms the actin cortex. Based on this knowledge we propose two possible mechanisms to explain how the deformation of the nucleus inside the cell might occur. Both these mechanisms use the same actors (the cytoskeleton and its linkages) and it is possible that both are occurring simultaneously. In the first mechanism proposed in Figure 34 we indicate how the forces occurring during cell spreading may affect the interior of the cell. As the cell spreads, a force is exerted outwards, followed by a contraction of the cytoskeleton.[113] On a flat surface this would result in the flattening of the nucleus that would go from a spherical shape in suspension to a lentoid shape when attached to the surface. On a micropillared surface this may result in a downward force on the cell nucleus, either indirectly because of the stretching of the cell, or directly because of the cortical cytoskeleton filaments that stretch above

the nucleus and contract, exerting a force on the interior of the cell. This mechanism would result in the nucleus being pushed downwards in between the pillars as the cell spreads on the surface (Figure 34a).

The second proposed mechanism involves the pulling down of the nucleus rather than the pushing down from above (Figure 34b). When the cell attaches to the surface it may form attachment sites to the edges and sides of the pillars. As the cell nucleus is connected to the edges of the cell through the cytoskeleton, when the cell wall attaches to the sides of the pillars the nucleus may be pulled down with it.[145] It has been shown that un-adhered cells in suspension have a cytoskeleton scaffold in place,[34] accounting for deformation of the nucleus before the cell has spread over the surface (Figures 18 and 29). This deformation at early stages of spreading is an indication that the second hypothesis could be the right one.

Studies have tried to explain the balance of forces within the cells. In the tensegrity model mechanical changes in the environment (stresses) are transmitted to the cell through the cytoskeleton which consists of pre-stressed fibres at equilibrium.[29] Thus, in our system, an equilibrium state of the cytoskeleton of cancerous cells would be found after deformation between the pillars, in which the cell is in a pre-stressed state. Additional data on the properties of the nucleus-cytoskeleton scaffold should be found in experiments in which modifications to the cytoskeleton scaffold are provoked. Modification of the shape of the nucleus upon release of the cytoskeletal pressure should confirm that the cytoskeleton is an active actor in the deformation of the cell and demonstrate the viscoelastic properties of the nucleus. This can be achieved using cytoskeleton disruptors. Additionally, the use of specific disruptors should provide information on which filaments are responsible and the amount of force they can generate. We will see experiments with cytoskeleton disruptors in section 3.6.1.2.

3.6.1.1 Confocal and scanning electron microscopy

SaOs-2 cells were seeded on micropillared surfaces and their actin and microtubule cytoskeleton

filaments were labelled. Using these sample we are able to monitor the position of the different components of the cytoskeleton relative to each other and to the position of the nucleus.

There are differences that can be observed between cells that are well-deformed (figure 35) and those that have nuclei that are not yet completely inserted in between the pillars (figure 36). In the case of well-deformed cells, actin filaments form well-defined stress fibres in a plane above the nucleus of the cells, with filaments that span the entire length of the cell, uninterrupted. The nucleus is not visible in the same plane as the actin fibres (left-most images, figure 35). In the cell shown, there is also an actin filament that spans the outer edge of two pillars and seems to go through the nucleus, although it is likely that this filament is located below or above the nucleus. (See arrow in bottom row, figure 35.) Below the top surface of the pillars, actin stress fibres can only be found along the side edges of the pillars, a flat surface similar to the top of the pillars.

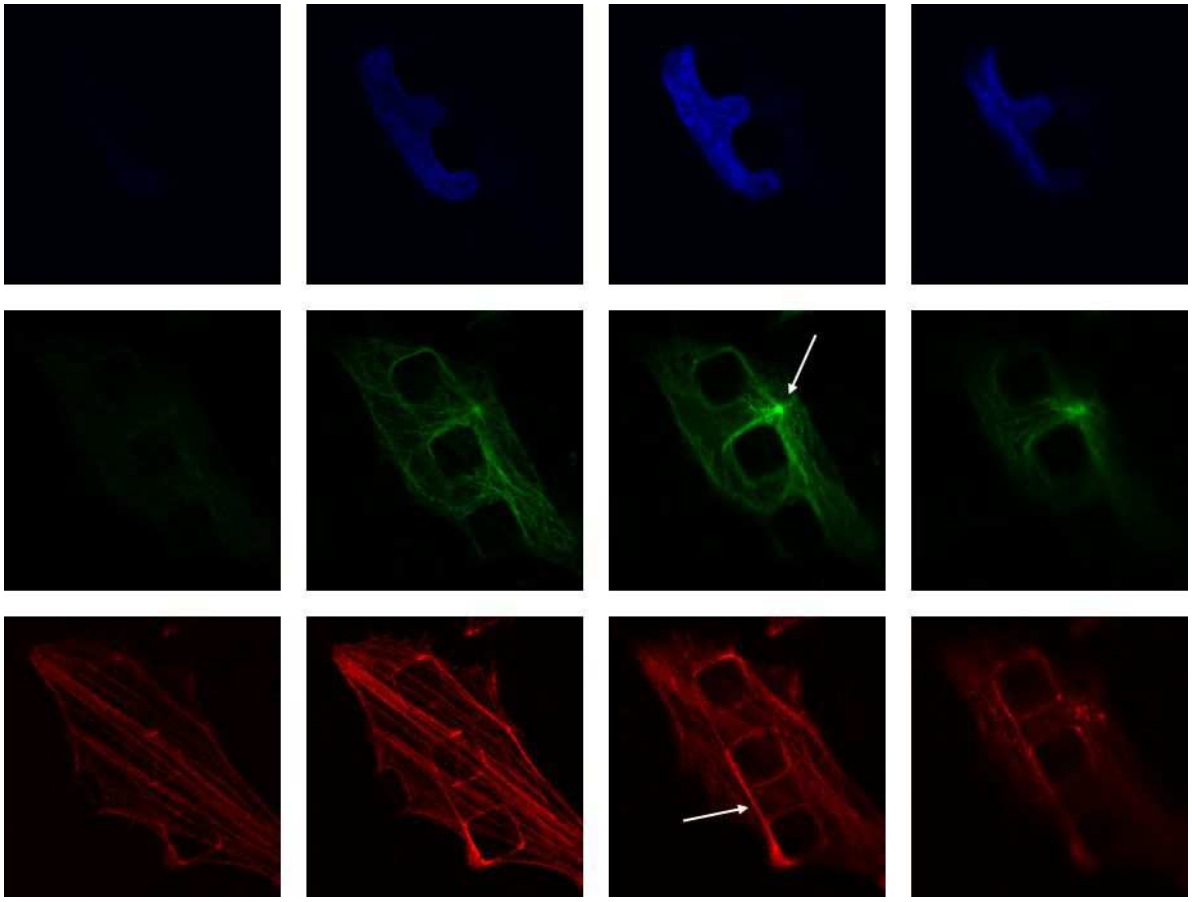

Figure 35: Well-deformed cell grown on micropillars and labelled for the nucleus (blue), microtubule filaments (green) and actin filaments (red). The different images were obtained in different focal planes, each image is in a plane 2 microns above the one to its right.

The microtubules are visible in the same plane as the nucleus. (Figure 35.) In fact, the outline of the nucleus is clearly visible in the organisation of the microtubules. This is not the case for the actin filaments: there is no "hole" corresponding to the shape of the nucleus in the actin labelling images. It thus appears that the nucleus is closely surrounded by the microtubules rather than the actin filaments. The microtubule organisation center (MTOC, or centrosome) is also visible in the images and is located in between the pillars, next to the nucleus. (See arrow in central row, Figure 35.)

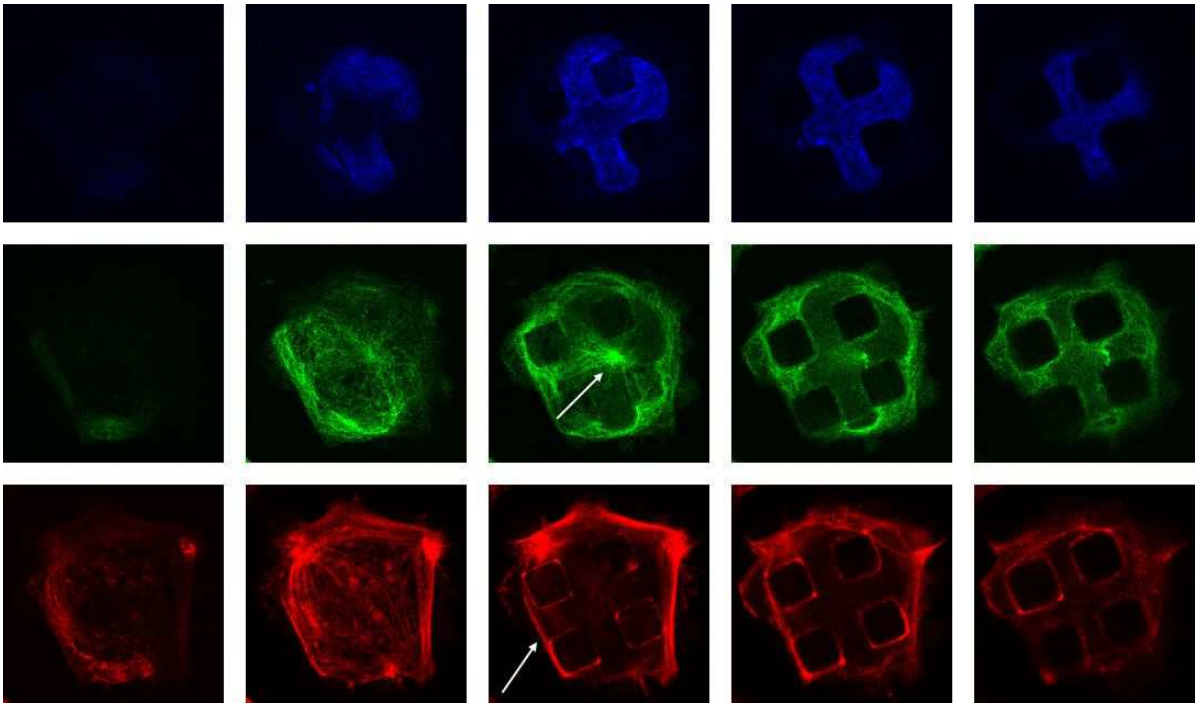

Figure 36: Fluorescence images of a semi-deformed cell on a micropillared surface. The cell's nucleus (blue), microtubules (green) and actin cytoskeleton (red) were labelled. Arrows show the location of the microtubule organisation center (middle row) and stress fibres that grow along the side of the pillars (bottom row). The images from left to right were taken at different focal planes spaced approx. 2 microns apart.

In cells that are not as well-deformed, the nucleus is not inserted completely in between the pillars, it is draped across the top of the pillars and there is some part of the nucleus that hangs in between the pillars. Interestingly, we can see that the top of the nucleus is not flat, but dented in the region between the pillars, adopting a slightly concave shape. The outline of the nucleus is once again clearly visible in the microtubule images. The actin images show some thin actin filaments across the top of the cell, and

some thicker ones around the periphery of the cell. A thick actin filament is also visible spanning two of the pillars in the plane below the top of the pillars. (See arrow in bottom row, Figure 36.) Whereas the MTOC was located in between the pillars in the case of the well-deformed cell, in the case of the partially-deformed cell the MTOC is visible above the nucleus, perhaps an additional indication that the bulk of the cell is not yet inserted in between the pillars. (See arrow in central row, Figure 36.)

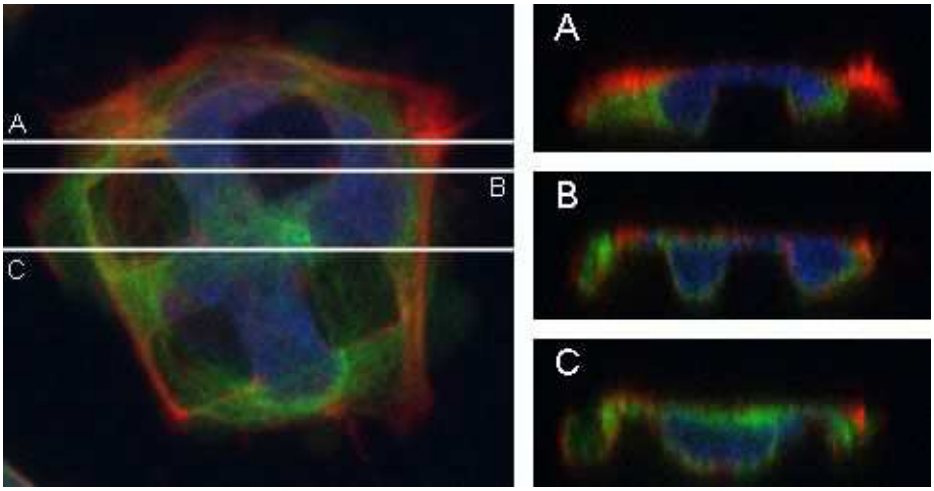

Figure 37: The same cells as in figure 36, showing visual cuts through the cell so that the organisation of the cell can be better visualised. The lines labelled A, B and C in the left image correspond to the area of the slice that is visible in images A, B and C on the right.

The fact that the shape of the nucleus is clearly visible in the microtubule image seems to indicate that the microtubules surround the nucleus more intimately than the actin filaments do. To understand the relative positioning of the different filaments better the images were processed so that we can see the profile of the cell in a plane perpendicular to the surface of the substrates. (Figure 37.)

From the profile images it appears that the microtubules are, in fact, surrounding the nucleus and that the actin filaments are around the periphery of the cell. This is true on the top and the edges of the cell, but also at the interface between the cell and the substrate, especially on the edges of the pillars, where a concentration of actin can be detected. However, the actin seems to be largely concentrated at the top of the cell.

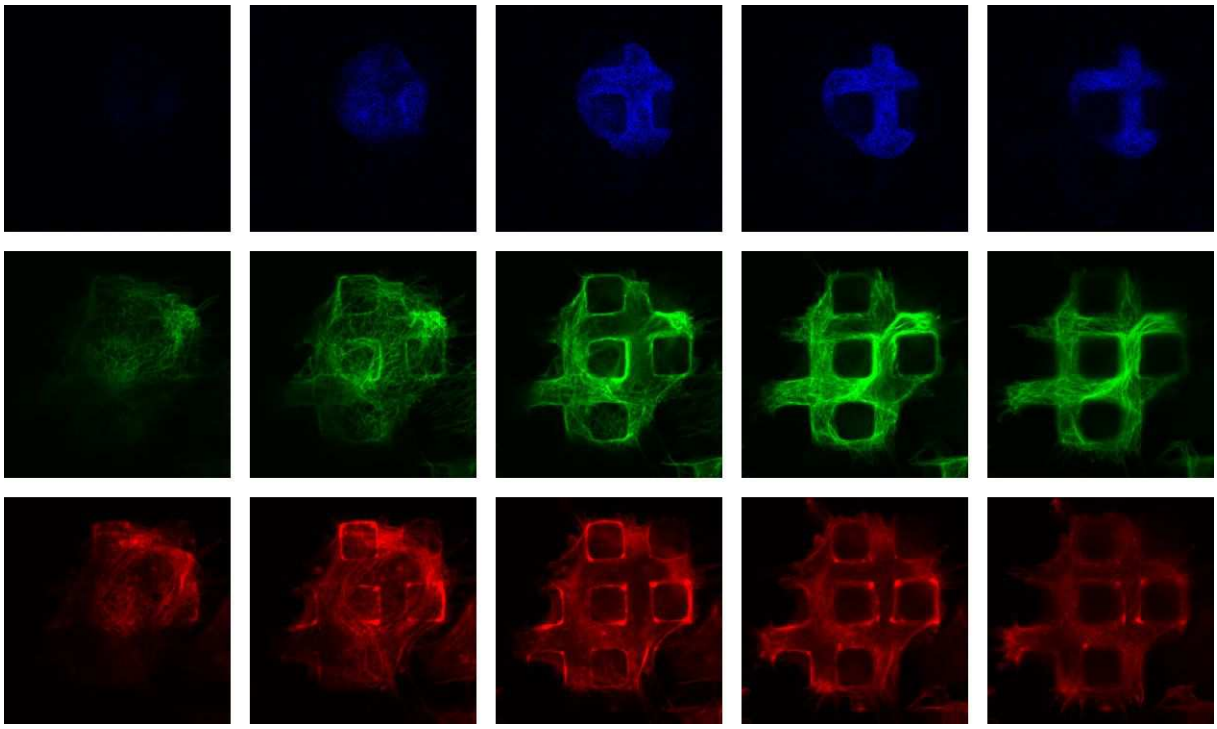

Figure 38: Fluorescence images of a semi-deformed cell on a micropillared surface. The cell's nucleus (blue), microtubules (green) and actin cytoskeleton (red) were labelled. The images from left to right were taken at different focal planes spaced approx. 2 microns apart. The cell is taller in the area above the nucleus and the actin filaments form a circular structure around the top of it. The microtubule filaments appear disorganised above the nucleus but appear to follow the trough in between pillars below the nucleus.

The difference between the two types of organisation of the actin may be related to the actin's role in the deformation. Because bundles of actin filaments are visible across the top of the cell when the cell is well deformed, it may be that the actin has a role in keeping the cell in place rather than deforming the cell. This can also be shown in images where the nucleus is partially deformed, but actin filaments are visible across the top of the cell, in a circle above the nucleus. (Figure 38.) In this manner, the actin filaments maintain the nucleus in place by not allowing it to come back up out of the pillars.

However, the lack of visible stress fibres in the interior of the cells does not necessarily imply that actin filaments do not have a role in deforming the nucleus. There may be much smaller fibres that are not as easy to see in these images connecting the nucleus to the cell surface. As has been discussed in the introduction chapter actin filaments are known to have direct mechanical connections to the cell's

exterior and thus may well have an effect on the nucleus' deformation. Additionally, the high turnover rate of cytoskeletal filaments implies that even if no filament is present at the moment of observation, there is no way of knowing if filaments were present at another point in time.

The presence of thick actin filaments (also called “stress fibres”) only at the surface of the pillars is reminiscent of images of SaOs-2 cells grown on flat substrates. In these cells, the stress fibres appear to be primarily located at the surface of the substrate, underneath the nucleus. Above the nucleus, the actin filaments appear to be less organized. (Figure 39.) The stress fibres underneath the nucleus most likely have a role in motility and keeping the shape of the cell intact (the “footprint” of the cell).

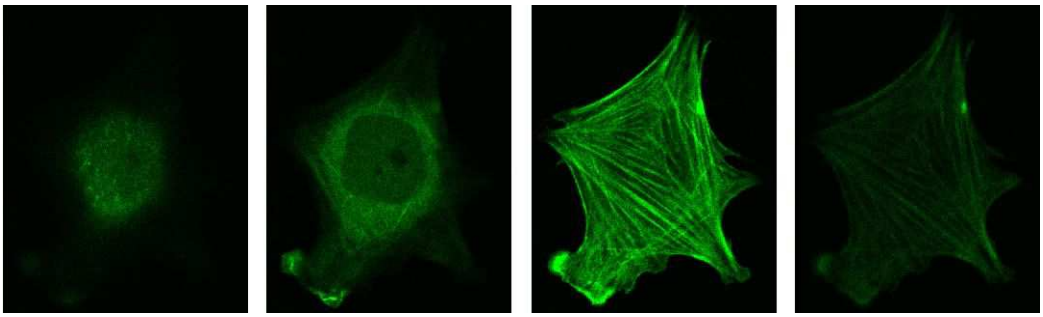

Figure 39: SaOs-2 cell grown on a flat surface, the actin cytoskeleton is labelled in green.

Recent reports have revealed that the actin cytoskeleton is a network of filaments whose architecture changes with its location in the cell.[2] Bundles of actin can be assembled with different types of cross-linking proteins, the assembly can be made up of parallel or orthogonal fibres and myosin can be present to provide contractile function. These differences in actin structure are clear in figure 39, where there is a distinct difference between the organisation of actin fibres above and below the nucleus in cells grown on flat surfaces. It has been reported that the filaments above the nucleus are assembled into highly parallel bundles termed the peri-nuclear actin cap, however this organisation has been reported to be disrupted in two cancerous cell lines (MCF-10A and HeLa).[12] This is not surprising given that cancerous cells are reported to have reduced lamin content and that cells that do not express lamin display no cap or a disorganized one.[12] Hence, SaOs-2 cells may have a disorganized peri-nuclear

actin cap, resulting in modifications in the cytoskeleton management of the nucleus.

Interestingly, the downwards movement of the cell does not appear to be related to a migration of the cell into the space in between the pillars. During migration the centrosome is placed between the leading edge of the cell and the nucleus. In fact, it is believed that the centrosome has an important role in pulling the nucleus in the direction of cell migration.[146] If the cell is migrating towards the space in between the pillars, the centrosome should place itself in between the leading edge and the nucleus, i.e. under the nucleus. However, in the images we have obtained the centrosome is not shown to be placed below the nucleus, but on top (figure 36) or to the side (figure 35). This does not exclude that the cell underwent migration towards the bottom of the pillars, with placement of the centrosome under the nucleus, during the early stages of deformation. An important study would be the relative positioning of the centrosome relative to the cell nucleus during initial deformation. Additionally, the position of the centrosome during cell displacement would allow us to detect whether the cell nucleus is following the centrosome, and is thus being pulled by it.

Scanning electron microscopy (SEM) provides information that is complementary to the information obtained in the confocal microscopy images. Unfortunately, important artefacts result from imaging biological samples in the SEM, due to the dehydration of the sample. In our images, this results in detachment of the cells from the space in between the pillars. However, the information obtained from the SEM images is useful in providing us with a profile of the pillars. It is evident from these images that the embossing process results in a slight tapering of the sides of the pillars, i.e. the sides of the pillars are not orthogonal to the top edge of the pillar. Additionally, the detachment of the cells from the space in between the pillars provides us with qualitative information on the quality of the adhesion of the cells to the spaces in between the pillars: perhaps the cells detach because there is no adhesion or only weak adhesion in the space in between the pillars.

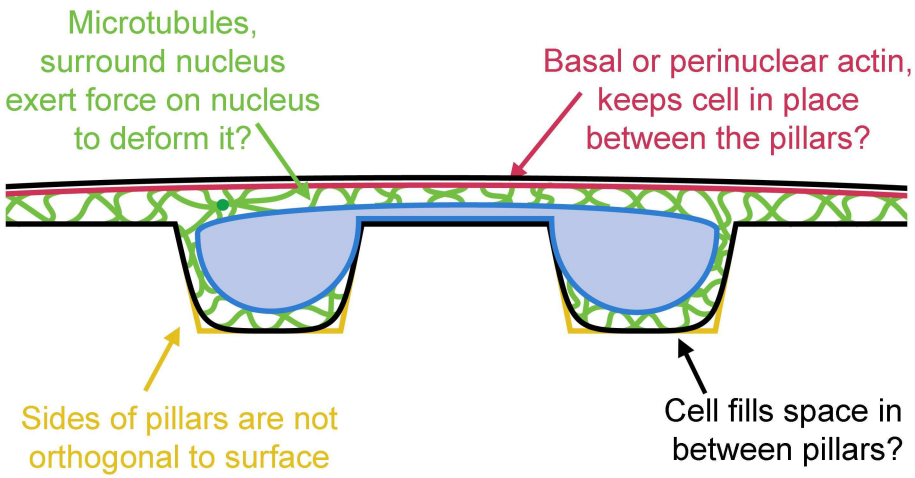

Figure 40: Summary of findings based on confocal microscopy images

Based on our observations of the relative position of the actin and microtubule filaments we propose that the microtubules may play an important role in the deformation of the nucleus, whereas the actin filaments have a role in keeping the nucleus (and the rest of the cell) in place. (Figure 40.) Microtubules are known to be able to displace the nucleus: they are responsible for nucleus rotation.[26] The role of the actin may be fairly active by providing structural rigidity every step of the

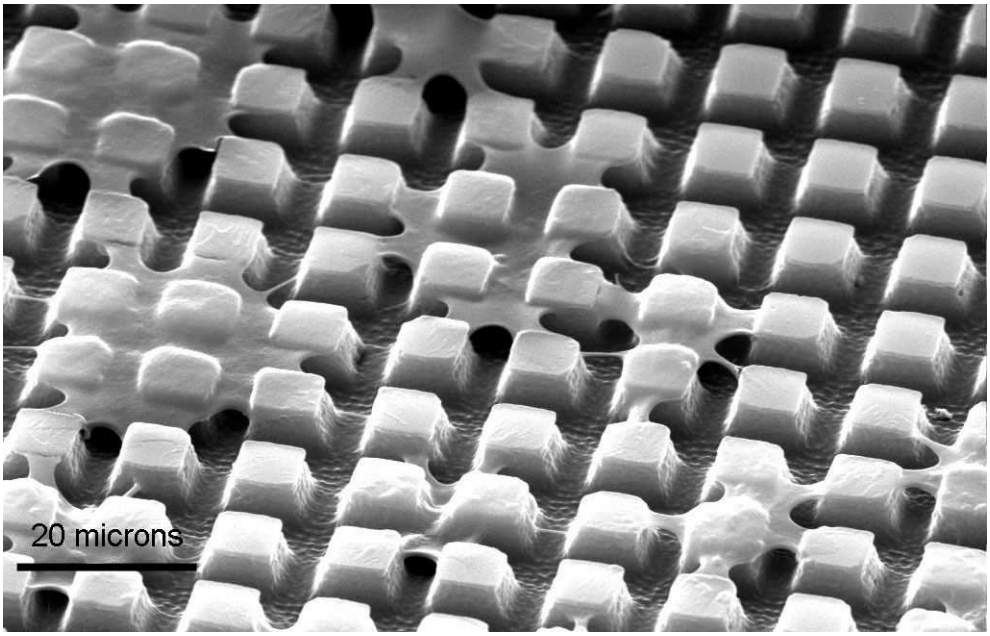

Figure 41: SEM image of the micropillared surface with SaOs-2 cells grown on it. This image shows that the sides of the pillars are not perfectly orthogonal to the surface of the pillars. The cells have detached from the space in between the pillars during the dehydration process. This may be an indication of no or weak attachment to the space between the pillars.

way during the deformation of the cell, by keeping the cell in place after each incremental deformation. This is hinted at in figures 36 and 38, where thin bundles of actin filaments are seen across the top of the nucleus. When the cell has inserted its nucleus entirely in the space between the pillars these filaments become thicker. This is reminiscent of the peri-nuclear actin cap described by Khatau et al.[12] In fact, it has been suggested that the function of this actin cap is to push the nucleus towards the cellular basal surface, resulting in a flattened cell nucleus.[12] On the micropillars, this kind of downwards force on the nucleus could result in it being pushed into the space between the pillars. However, it has been suggested that the peri-nuclear actin cap may be less organized in cancerous cells. Hence, the origin of the deformation may not be due to this specific type of actin organisation.

Images obtained by scanning electron microscopy (SEM) of the surfaces revealed that the sides of the pillars are not perfectly orthogonal to the surface. (Figure 41.) This is the reason that the profile of the cells in between the pillars is tapered at the bottom of the space between the pillars. (Figure 37.) However, it is still difficult to say what the interactions are between the cell and the space in between the pillars. It appears that the cell may be filling the space in between the pillars, but it is not clear whether the cell is forming adhesions in these areas or not. The aspect of the cells upon dehydration suggests that the cells are weakly or not bound to the space in between the pillars.

Selective staining and imaging of the cells in three dimensions provides many clues as to the origin of the deformation. However, imaging cells which have been fixed is not sufficient to understand how forces are distributed in the cell. In order to obtain more information about this further measurements are required on cells while they are alive and exerting forces. This will be the subject of the next two sections.

3.6.1.2 Cytoskeleton inhibitor experiments

In order to verify which component of the cell are responsible for the deformation additional

experiments on the cytoskeleton filaments are necessary. This may be performed by selectively dismantling the different components of the cytoskeleton and observing if any change is detectable in the deformation of the cell. There are three known components of the cytoskeleton: actin filaments, microtubules and intermediate filaments. For each of these types of filaments, two types of inhibitors were chosen (see table 3) and tested on cells grown on flat surfaces. Using these cells it was possible to determine whether the inhibition was specific to the type of filament studied and whether the rest of the cell was affected by the treatment. If the aspect of the cell drastically changes upon addition of the cytoskeleton inhibitor, or if the inhibitor is toxic to the cells, it would be impossible to decouple the effect of cytoskeleton filaments and the effect the inhibitor has on the rest of the cell. The results of these experiments are shown in Appendix A. Following these experiments, appropriate concentrations were chosen for experiments on the micropillars.

Type of filament	Disruptor	Function
Actin	Latrunculin A	Prevents Actin polymerization
	Cytochalasin D	Depolymerizes F-Actin
Microtubules	Nocodazole	Depolymerizes microtubules
	Colchicine	Binds to monomeric tubulin
Intermediate Filaments (Vimentin)	IDPN	Vimentin inhibitor
	Acrylamide	Dissolves Vimentin

Table 5: The cytoskeleton disruptors used and their function.

3.6.1.2.1 Actin filament inhibition

Two cytoskeleton inhibitors were used in experiments on the effect of actin disruption: Latrunculin A and Cytochalasin D. Both are widely used in the literature. Cytochalasin D is able to disrupt polymerized actin, whereas Latrunculin A prevents actin polymerization. These two inhibitors have roughly the same function as actin renewal happens very rapidly.

On the flat surfaces, the effect of latrunculin A is clearly visible in fluorescently labelled cells. (see Appendix A) At low concentrations the cells formed blobs of actin although actin filaments could still be seen. At higher concentrations the cell was no longer spread out but retained its discrete attachment points to which the microtubules seemed to be attached. The concentrations used in experiments were 0.1 µM or 0.3 µM. Cytochalasin D inhibition is immediately visible as the loss of visible stress fibres and the appearance of "blobs" in the cell indicating the aggregation of actin monomers. (See Appendix A.) At higher concentrations the cells are no longer spread out, although they are still anchored to the surface at specific points at which the microtubules (green) still seem to be attached, resulting in a spiky appearance. The concentrations used in experiments on the micropillars were 0.5 µM or 1 µM.

In the experiments performed on the micropillars the cells were allowed to attach to the surfaces for 24 hours or 48 hours before addition of the cytoskeleton disruptor. The cytoskeleton disruptor was not added at the same time the cells were seeded to allow attachment to the surface without perturbations from the disruptors.

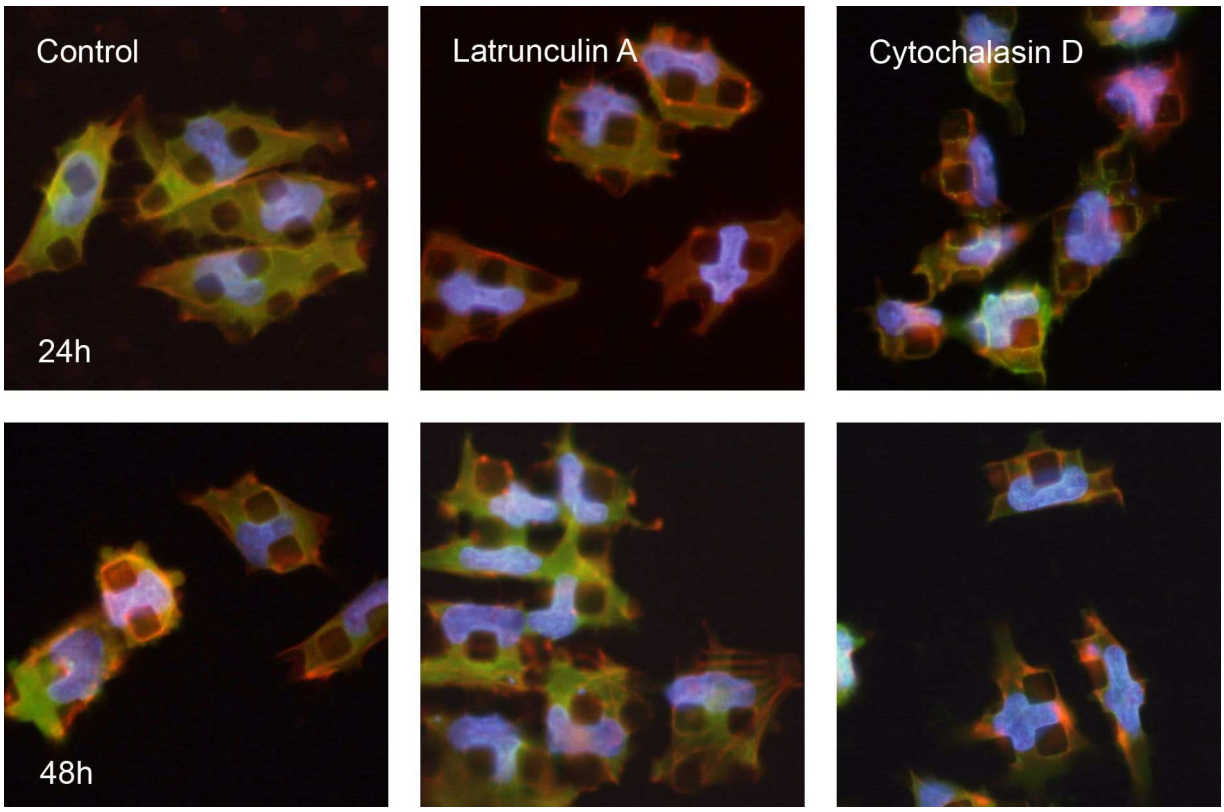

Figure 42: SaOs-2 cells grown on micropillars, with or without actin disruptors.

Actin inhibitor addition after 24 hours did not seem to greatly affect the cells. (Figure 42.) In fact the nuclei appeared to be very deformed and the pillars were clearly visible through the cytoskeleton. It was not clear whether the actin cytoskeleton was sufficiently disrupted by the presence of the inhibitors. In particular, images of samples on which Latrunculin A had been added showed the presence of stress fibres. Similarly, after 48 hours the deformations of the cell nucleus or the cytoskeleton were not affected by the addition of cytoskeleton inhibitors. Greater concentrations of cytoskeleton inhibitors were added in a second experiment. (Figure 43.) However, this did not result in changes to the deformation of the nucleus on the pillars: the shape of the pillars was still clearly visible in the images, even though the actin cytoskeleton was clearly disrupted: both images show red blobs instead of filaments.

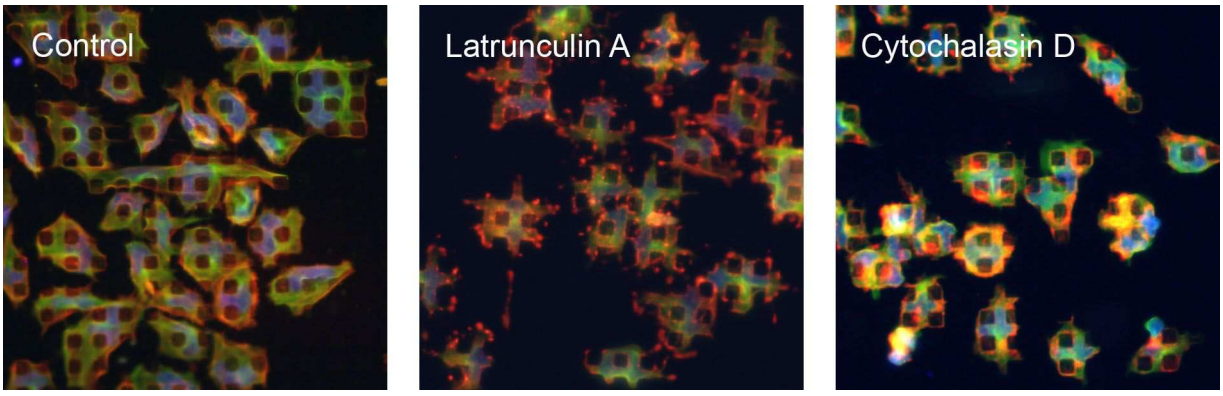

Figure 43: SaOs-2 cells grown on micropillars, with higher concentrations of actin disruptors. The loss of actin organisation is visible as a loss of red filaments and the appearance of red dots.

High resolution imaging confirmed that only the actin filaments were disrupted and not the microtubules: microtubule filaments are clearly visible in the images, as are the centrosomes (organization centers of the microtubules), visible as brighter green spots into which the microtubules are organized. (Figure 44.) The actin appears as red spots in the images instead of the filaments and stress fibres we had seen previously.

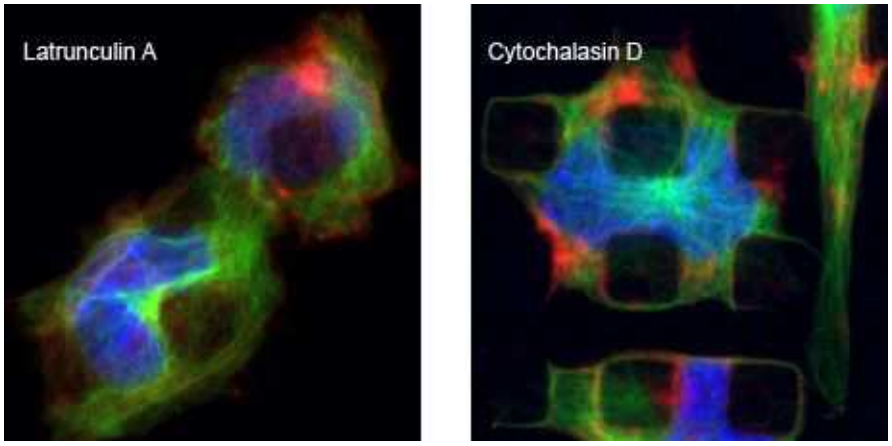

Figure 44: High resolution microscopy of cells grown on micropillars and treated with actin disruptors. The microtubule filaments are intact (green), whereas the actin filaments are clearly disrupted, forming blobs of actin (red).

Confocal imaging showed that the cells appear to be in contact with the bottoms of the space in between the pillars: the height is similar to the control sample and the shape of the profile is "square" (flat bottom). (Figure 45.) Hence, the loss of actin filaments did not result in any noticeable changes in the level of deformation of the cell and it's nucleus.

The actin filament inhibitors did not seem to have any effect on the deformation of the cell and its nucleus. It is thus clear that if the actin filaments are exerting a force on the cell and its nucleus, release of this force does not result in relaxation of the cell to a state in which the cell loses its deformation. This indicates that either the actin filament is not or no longer exerting force on the cell, or that once the cell is deformed, its relaxed state is the deformed state.

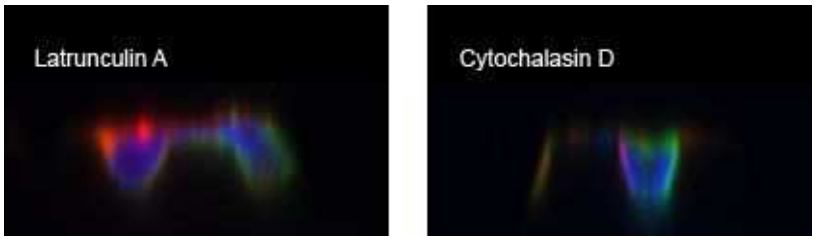

Figure 45: Side profile of cells grown on micropillars and treated with actin disruptors. The cells are still extensively deformed and the cell that has been treated with cytochalasin D appears to have a flat profile at the bottom, indicating contact with the bottom surface.

3.6.1.2.2 Microtubule inhibition

Two microtubule inhibitors were selected for tests, nocodazole and colchicine. Both are well-known in

the literature, nocodazole depolymerizes microtubules[121] and colchicine binds to tubulin (the monomer) to prevent polymerization.[122]

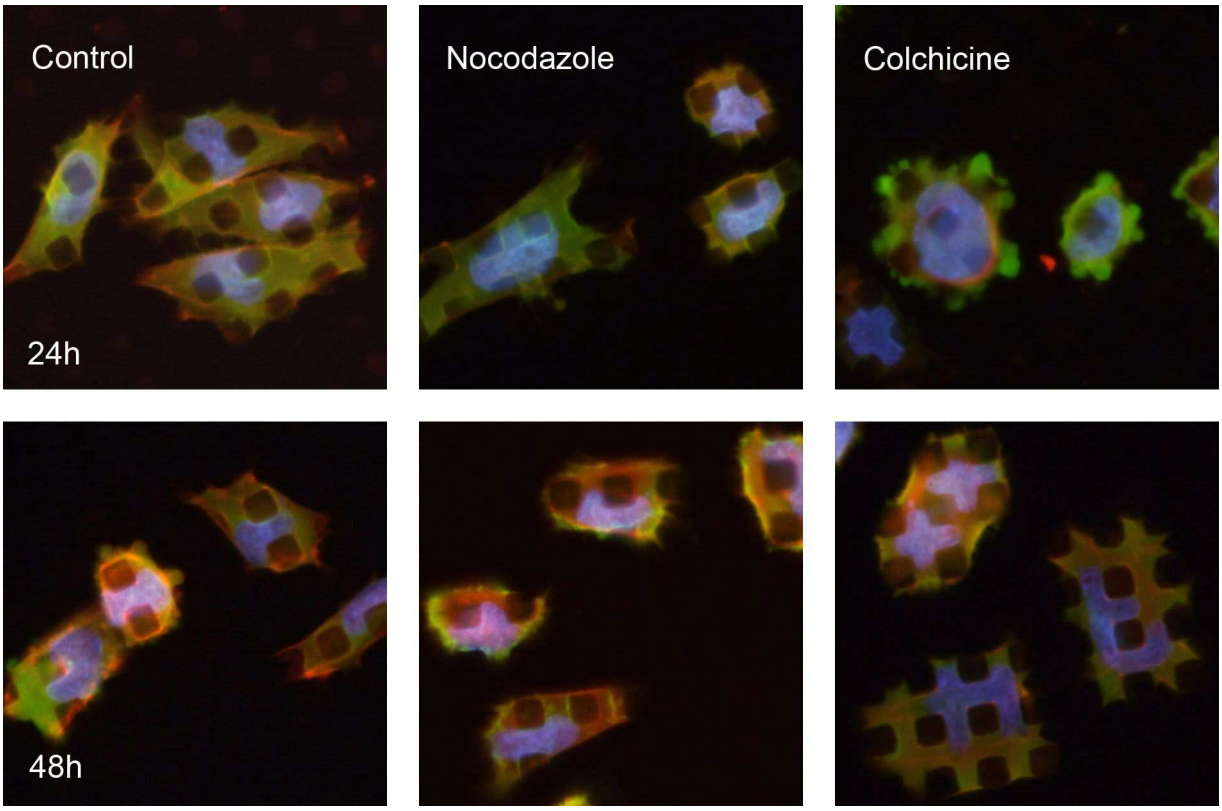

Figure 46: SaOs-2 cells grown on micropillars and treated with microtubule inhibitors

On flat surfaces, nocodazole inhibition is visible as a loss of the filamentous nature of the microtubules and the appearance of blobs in the cells. (See Appendix A.) At low concentrations microtubule filaments are no longer visible inside the cells, and the interior of the cells have an even colouring, indicating loss of structure of the microtubules. Even at higher concentrations the appearance of the cells remain unchanged although the microtubules are depolymerized and unable to provide support to the cell, highlighting that microtubules do not have an important structural role. (In contrast, loss of actin filament support resulted in a very modified appearance of the cell.) The concentration used in the first experiment was 5 μM as at this concentration the microtubules are clearly dissociated but the rest of the cell has kept the same shape. In the second experiment the concentration was increased to 10 μM.

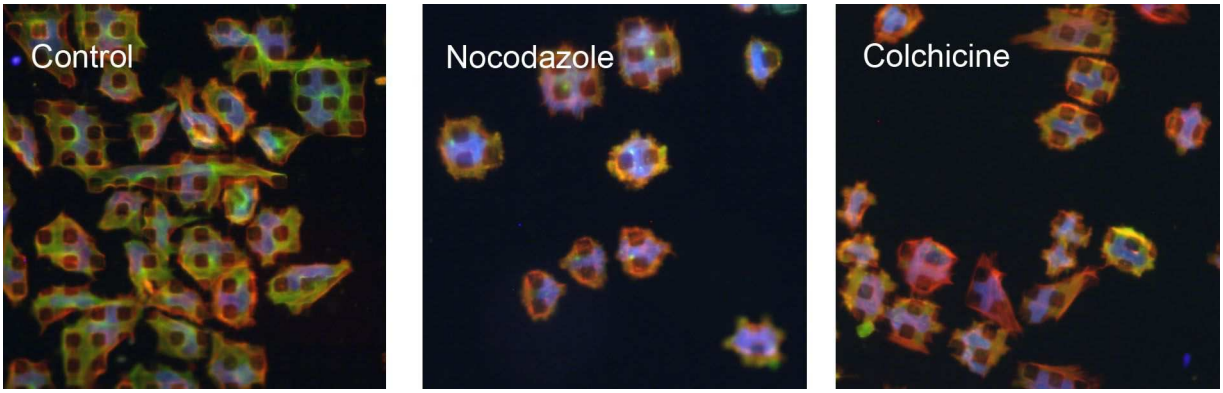

Figure 47: SaOs-2 cells grown on micropillars, with higher concentrations of tubulin disruptors.

The deformation of the cells did not seem to be greatly affected by the presence of microtubule inhibitors. (Figure 46.) The nucleus of the cells is still deformed and the pillars are still visible through the cytoskeleton. Addition of cytoskeleton inhibitors after 48 hours in culture also did not lead to a loss of deformation of the nucleus or the cell. Upon increasing the concentration of the inhibitors, there was no visible effect on the deformation of the cells. (Figure 47.)

In high resolution images the granules of tubulin can be seen, as well as the actin filaments, suggesting that the microtubule inhibitors do not affect the actin filaments greatly. (Figure 48.) The loss of microtubule structure is visible in the images as the loss of green filaments and the appearance of blobs, or an even labelling of the cytoplasm.

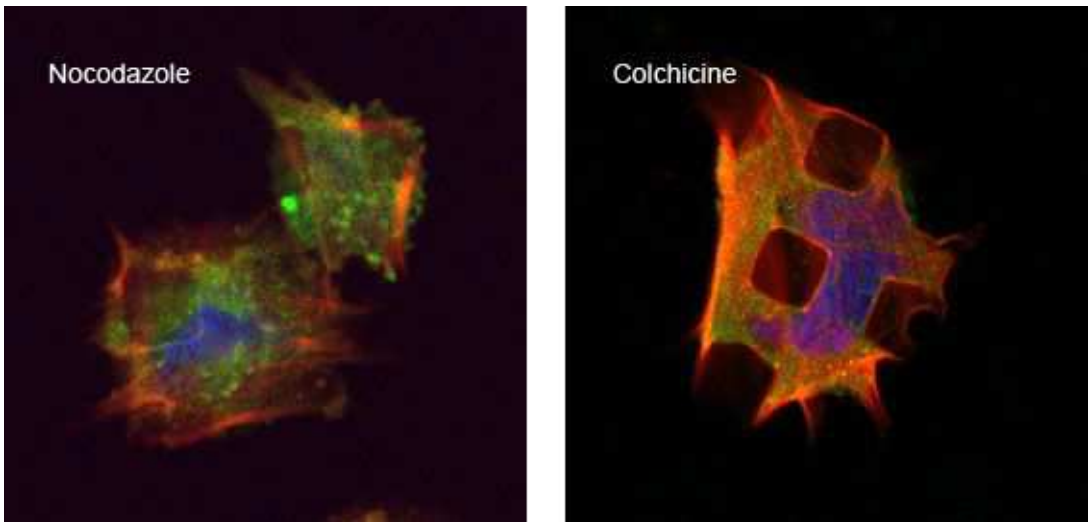

Figure 48: High resolution microscopy of cells grown on micropillars and treated with tubulin disruptors

Confocal imaging confirmed that the cells adopted the shape of the underlying pillars. (Figure 49.) This indicates that the loss of microtubule organisation did not result in loss of the deformation of the cells on the pillars. This may be because the microtubules do not exert significant force on the cells or that the cell is kept in place by the other components of the cytoskeleton. The actin cytoskeleton has an active role in keeping the shape of the cell. (Loss of actin filaments results in loss of the footprint of the cell, even though the cell remains attached to the surface.) Because the rest of the cell remains intact the loss of microtubule forces may not be enough to result in loss of the deformation of the cell.

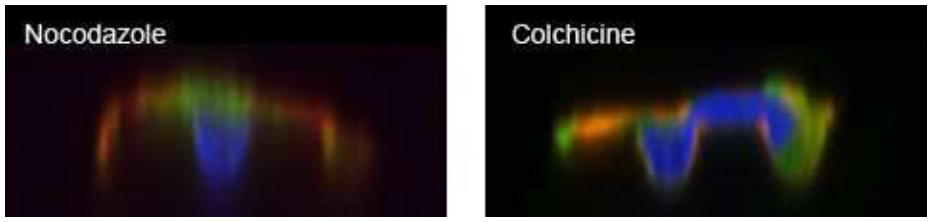

Figure 49: Side profile of cells grown on micropillars and treated with tubulin disruptors.

3.6.1.2.3 Inhibition of intermediate filaments

In osteosarcoma the structural intermediate filaments are predominantly vimentin. Inhibitors that are described in the literature are acrylamide[126] and iminodiproprionitrile (IDPN)[127]. However in control experiments non-toxic concentrations that showed a clear effect on the vimentin filaments could not be found, and at concentrations 5 times greater than the standard concentration of acrylamide reported in the literature (5 mM), no dissociation of the vimentin network was observed.

Experiments were conducted at this high concentration of acrylamide (25 mM) and a concentration of IDPN that was not toxic to the cells. Addition of these inhibitors did not result in noticeable loss of vimentin organisation in the control experiments or loss of deformation of the cells on the pillars. (Data not shown.)

3.6.1.2.4 Cytoskeleton inhibitor result overview and future directions

Cytoskeleton inhibitors were added to cells deformed on micropillared substrates. In the cases of actin

and microtubule inhibition, the cytoskeletal networks were clearly dismantled and could no longer apply force to keep the nucleus deformed. In each case addition of the inhibitors to the deformed cells did not result in any visible change in the deformation of the cells after 2 hours. We believe that this may be due to the plastic properties of the nucleus: once it is deformed, when the tension is released it may not return to its original shape. Experiments performed on cells deformed by micropipette aspiration have shown that the nucleus is a plastic body that does not recover quickly following deformation.[11] Similarly, in the case of the deformation in between the pillars, although force is no longer exerted by the cytoskeleton on the nucleus, because the cell retains its deformed shape, the nucleus may not have sufficient elastic restorative force to adopt a spherical shape.

Alternative tests could be conducted by adding the cytoskeleton inhibitors at an earlier stage in the cell attachment and deformation, although it is unclear whether dismantling cytoskeleton fibres at an early stage of adhesion would not simply halt spreading and result in falsely undeformed nuclei. Experiments performed on cells grown on flat surfaces would need to be performed as a first test. The inhibitors could also be added for longer periods of time, but one must be careful that we are not simply halting cell movement and development.

There may also be different types of actin that are affected upon addition of the inhibitors. It has recently been shown that the architecture and function of actin filaments depends on their location in the cell. In a recent paper low levels of Latrunculin B (80 nM) resulted in a loss of the actin “cap” above the cell's nucleus.[25] This points to different types of actin filaments with varying degrees of organisation that can be more easily disrupted. Hence, disruption of some fundamental actin bundles may require higher concentrations of disruptors than it appears from immunostaining.

Future experiments on the role of the cytoskeleton will look at the possibility of using cytoskeleton inhibitors at different times during the adhesion and for different lengths of time. However, we will also

look at understanding the mechanism of deformation of the cytoskeleton. In figure 34 we had proposed two mechanisms of deformation, one of which relied on cell adhesion at the top of the pillars, and the other which relied on cell adhesion on the sides and edges of the pillars to pull down on the nucleus and the cell. In future experiments we will explore samples in which the region below the tops of the surfaces are passivated so that cells cannot attach to them. This should allow us to verify whether attachment to the sides of the pillars is necessary for cell deformation, or if the cell can deform itself by applying pressure from above. If the cells are not able to do so, they should grow on the micropillared surface in the same way they would on a flat surface.

3.6.2 Live cell imaging

Through fixation and labelling of the different components of the cell a lot of information can be gathered about the interactions of the cells with the surface. However many questions remain about the behaviour of the cell when it is grown on the micropillars. How does a cell move on the surface? Does it need to come out from the space in between the pillars to move or can it move along the surface while being deformed? How does mitosis occur? Can a cell divide when deformed?

Observation was performed on cells that had been transfected so that the actin produced by the cell would be labelled with a fluorescent protein, allowing us to observe the actin cytoskeleton of the cells by fluorescence microscopy. Observation of the cells revealed that they were very dynamic. They were able to move on the surface without much difficulty and the actin cytoskeleton was under constant evolution. In figure 50 we show a cell that was observed for several hours. Images were taken at different focal planes, we are showing here the plane in which the nucleus is situated (just below the top of the pillars) and the plane in which the actin stress fibres are situated (just above the top of the pillars). From these images we can see that above the top of the pillars the actin cytoskeleton is made up of highly organised bundles of actin filaments whereas in the area below the top of the pillars the

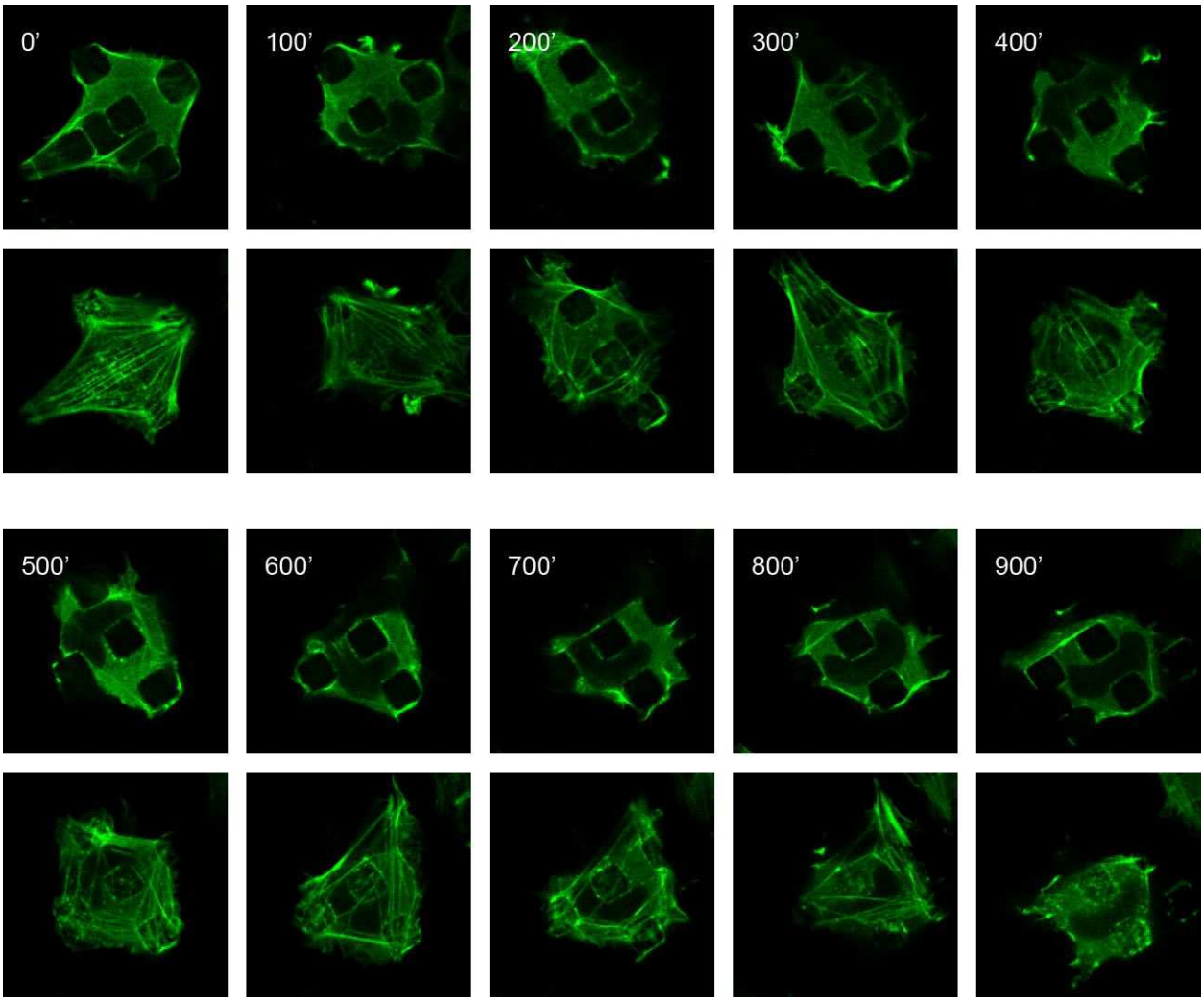

Figure 50: Movement of a live cell on a surface with micropillars. The cell was transfected so that the actin filaments are labelled (green). Two rows of images are shown in which the top row shows a focal plane below the top of the pillars and the bottom image shows a focal plane just above the top of the pillars. The two images are spaced 2 microns apart. The nucleus is distinguishable in the top image, whereas the bottom image shows an abundance of stress fibres in the area just above the top of the pillars.

actin is not organised into visible bundles. The filaments at the top of the pillars, which we believe have similar properties to basal or peri-nuclear actin, are very dynamic and completely rearrange themselves in the time between two subsequent images (100 minutes). Once again, this is reminiscent of the description of the peri-nuclear actin cap, which has been described to be very dynamic.[12]

The nucleus is visible as an area in which there is no fluorescence below the surface of the pillars. It moves quite a bit between images. In fact, during the course of the experiment it underwent a complete

revolution around a pillar. Its displacement was recorded over the duration of the experiment by drawing a path around the pillar and measuring the position of its leading edge and its back edge. (Figure 51.) The total displacement of the front and back edges were then reported in a graph. From this figure we can see that the movement of the cell nucleus is not smooth, and in fact the nucleus is displaced in bursts, similar to a "stick-slip" type of movement. This is most likely due to the barrier provided by the narrow space in between the pillars: the nucleus needs to adapt its shape to the narrow passageway and will only move through the space if there is sufficient force buildup for it to do so.

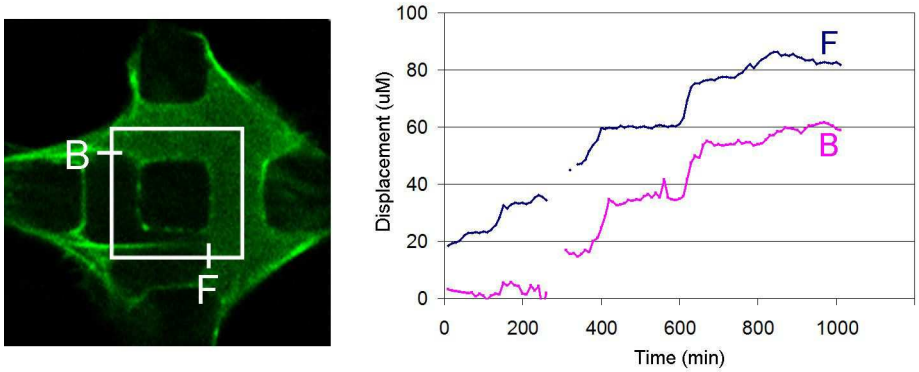

Figure 51: Displacement of the nucleus around a pillar. The position of the front edge (F) and back edge (B) were reported as a measure of the total displacement along the square shown in the left image. The results are reported as a function of time (right). The cell nucleus does not appear to move smoothly, but in a movement similar to "stick-slip". Regions of the graph that are missing are due to time points in which the cell nucleus could not be discerned.

These results are similar to experiments performed on nuclear deformation during migration of cells through pores.[147] In these experiments the cell nucleus is also seen to undergo migration through a pore approx. 5 microns wide in a step-wise fashion. The cell nucleus is described to undergo four phases. The first phase is resistance, during which no deformation is noticeable even though the cell cytoplasm is moving through the pore; local prolaps, in which an initial deformation of the nucleus is visible; compression and gliding, during which the cell nucleus moves at a constant velocity through the pore; and finally rear release: the last part of the nucleus is pushed through the pore at a high velocity. This final phase of high velocity is most likely due to continued pressure from the cytoskeleton and loss of

resistance from the nucleus. In the case of movement of the nucleus between the pillars, similar phenomena may be occurring, although they are most likely occurring simultaneously: while one part of the nucleus is resisting deformation, another part of the nucleus may be gliding through the space between two pillars. This gives rise to the steps of different height in the graph in figure 51.

From these experiments it becomes clear that the cells do not need to come out of the space in between the pillars to move along the surface. There is some barrier to movement of the nucleus, shown by the steps in figure 51, but the cell is eventually able to overcome this. For cell division, this does not appear to be the case. During live cell imaging, several instances of cells undergoing the initial stages of mitosis were recorded. An example is shown in figure 52, in which pictures of the entire cell is shown (a superposition of all the focal planes). In this case, the cell has become less spread on the surface, reducing the surface area it takes up and becoming more round. The preparation for cell division

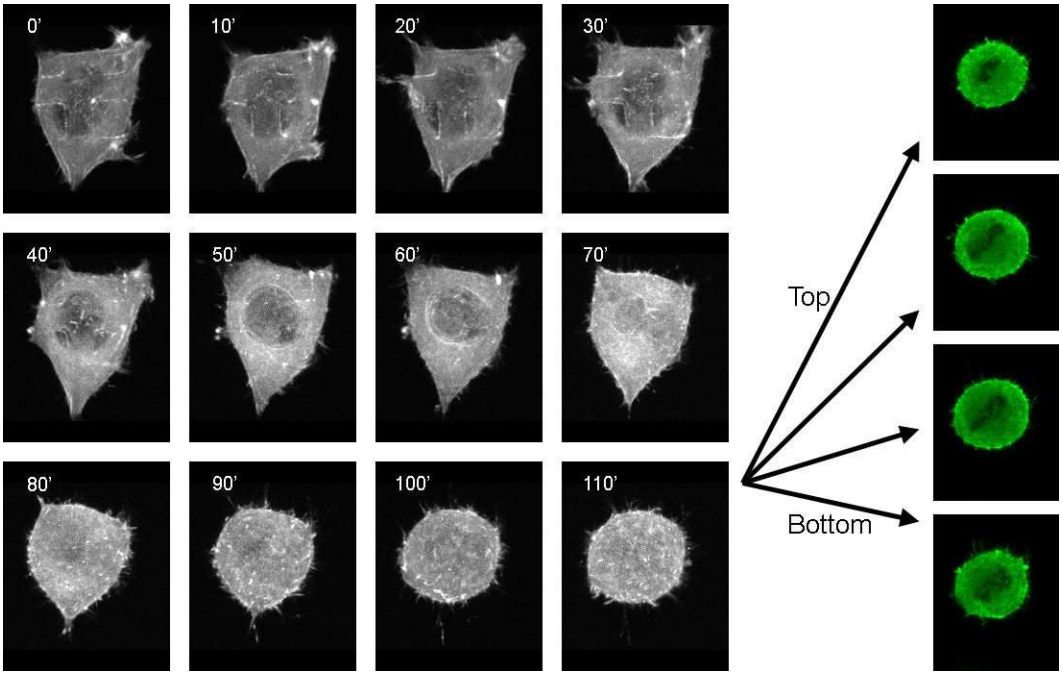

Figure 52: Cell undergoing the first stages of mitosis. In this figure a cell that has been transfected so that its actin is visible under the fluorescence microscope. On the left the cell is shown going from a well-spread conformation on the pillars to a cell that is rounded and tall. In the images on the right we see different sections of the cell showing that the cell's nucleus is no longer round and the DNA has segregated itself to a plane that is almost perpendicular to the surface. This is the mitotic plate.

undergoes several steps. First the cell loses its deformation (from time 0' to time 60') while retaining the overall footprint of the cell intact. The disappearance of the round “hole” indicative of the nucleus between 60 and 70 minutes indicates that the nuclear membrane has been disassembled (prometaphase). Following this, we can see that the footprint of the cell becomes smaller and the cell becomes rounder, gaining height. Observation of the different focal planes at 110' reveals that the DNA has been organised along a mitotic plate, indicating that the cell has entered the metaphase.

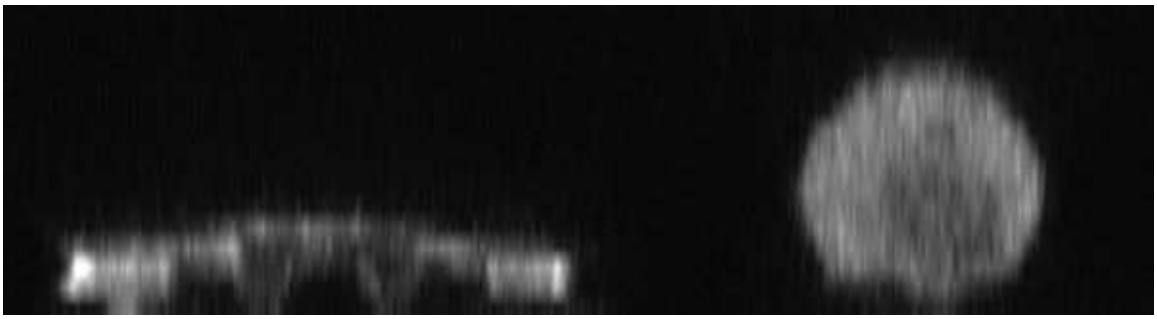

Figure 53: Side-view of a metaphase cell next to a cell that is well-spread on the surface of the pillars. Part of the mitotic plate is visible as a darker area in the metaphase cell on the left.

When the profile of mitotic cells is observed, very little deformation of the cell is visible in metaphase cells, except for slight dents where the cell is resting on the surface. (Figure 53.) The cells undergoing mitosis become rounder, but are also much taller than the cells that are in the interphase, and appear to sit on top of the pillars. (Figure 53.) This is similar to the behaviour of dividing cells on flat surfaces, which become spherical in preparation for cellular division.[148]

Interestingly, the cell's axis of division appears to coincide roughly with the diagonal of the square formed by the four pillars under the cell in its mitotic phase. It has already been shown that surface patterns can orient the cell's axis of division.[149] Surface topography may therefore also be able to orient the cell's mitotic plane. This problem will be the subject of future research.

After mitosis the two newly-formed daughter cells must re-spread on the surface if they are to become deformed once again. This phenomenon was also observed. In figure 54 we show two cells that are initially rounded on the surface but undergo spreading and move. These then become deformed and the

shape of the underlying pillars can clearly be seen in the later images. These images show that once the cell divides, the two daughter cells rapidly adopt the shape of the underlying surface topography. The deformation occurs very quickly, within a few hours, which is a shorter time scale than the initial deformation of the cells upon deposition on the surface. (See Figures 18 and 29.)

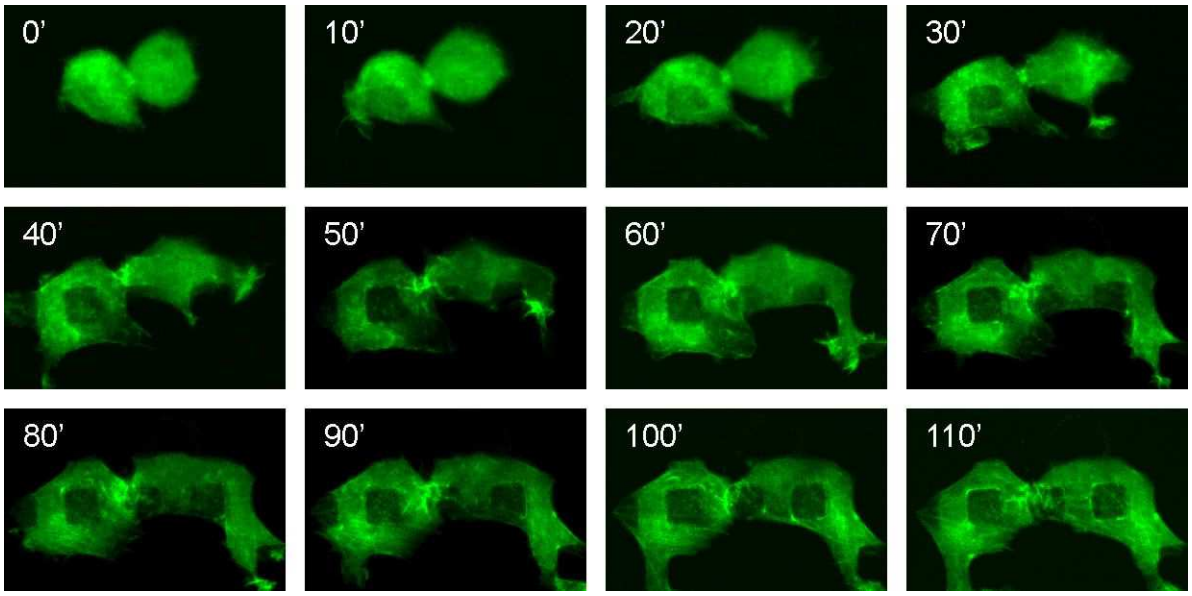

Figure 54: Spreading of two cells after division. Each image is separated from the next by 10 minutes.

This more rapid deformation could be due to adaptation of the cell to its environment. The first time an SaOs-2 cell adheres to the micropillared surface, it may adapt itself to be able to move more fluidly on the pillared surface, for example by adapting the composition of its nuclear membrane. A second explanation could be provided by the attachment points the daughter cells inherit from the mother cell, which may contribute significantly to the increased rate of adhesion to the surface.[150] Interestingly, thick bundles of actin filaments are not visible in the images shown, indicating that the initial stages of deformation do not require this type of actin architecture.

These live cell experiments have shown that the SaOs-2 cells are able to adapt to the micropillared surfaces very well. They are able to move easily on the surfaces, although the surfaces do present a slight barrier to nucleus movement that they are able to overcome. It is likely that the SaOs-2 cells

deform so extensively because they are equipped to adapt to these surfaces, whereas other cell types that do not deform (healthy and immortalized cells) are perhaps not able to move in a deformed state and hence once the cell begins to move across the surface it remains at the top of the pillars.

During mitosis the cells lose their deformation and sit tall on the pillars. This behaviour is similar to the behaviour of cells on flat surfaces: cells lose their polarisation and become spherical. The process of mitosis is a complex phenomenon and thus it is not surprising that the cells would reduce their size to undergo this change. Interestingly, the cells do not appear to have great difficulty in dividing on the pillars, indicating that the attachment to the surface of the pillars is sufficient.

3.6.3 Experiments on a different polymer surface

The deformation of the cell we have seen is most certainly dependent on the interactions of the cell with the surface chemistry. The degree to which the cell is able to adhere to a surface will certainly affect its ability to conform to the surface. Hence, we have studied the behaviour of SaOs-2 cells on a surface produced with a different type of polymer: PDMS. In order to ensure that the cells would be able to adhere to the surface, it was first treated with a solution of fibronectin. In addition to obtaining information about the effect of surface chemistry, using a different type of polymer also enables us to study the effect of surface rigidity. The surfaces we have been using are at room temperature, well below the glass transition temperature of PLLA. This means that the PLLA we are using is vitrified. PDMS, on the other hand, is an elastomer, and should be softer than PLLA.

In the experiments performed PDMS templates of microtopographied surfaces were made from surfaces with pillars 7 microns wide and 4, 5 and 6 micron spacing. SaOs-2 surfaces were grown on these surfaces, as shown in figure 55. Evidently, the cells are able to deform on the surfaces similarly to the PLLA surfaces. One difference that is noticeable is that the cells grown on the PDMS surfaces have more actin buildup on the edges of the pillars. This could be an indication of the response of the cells to

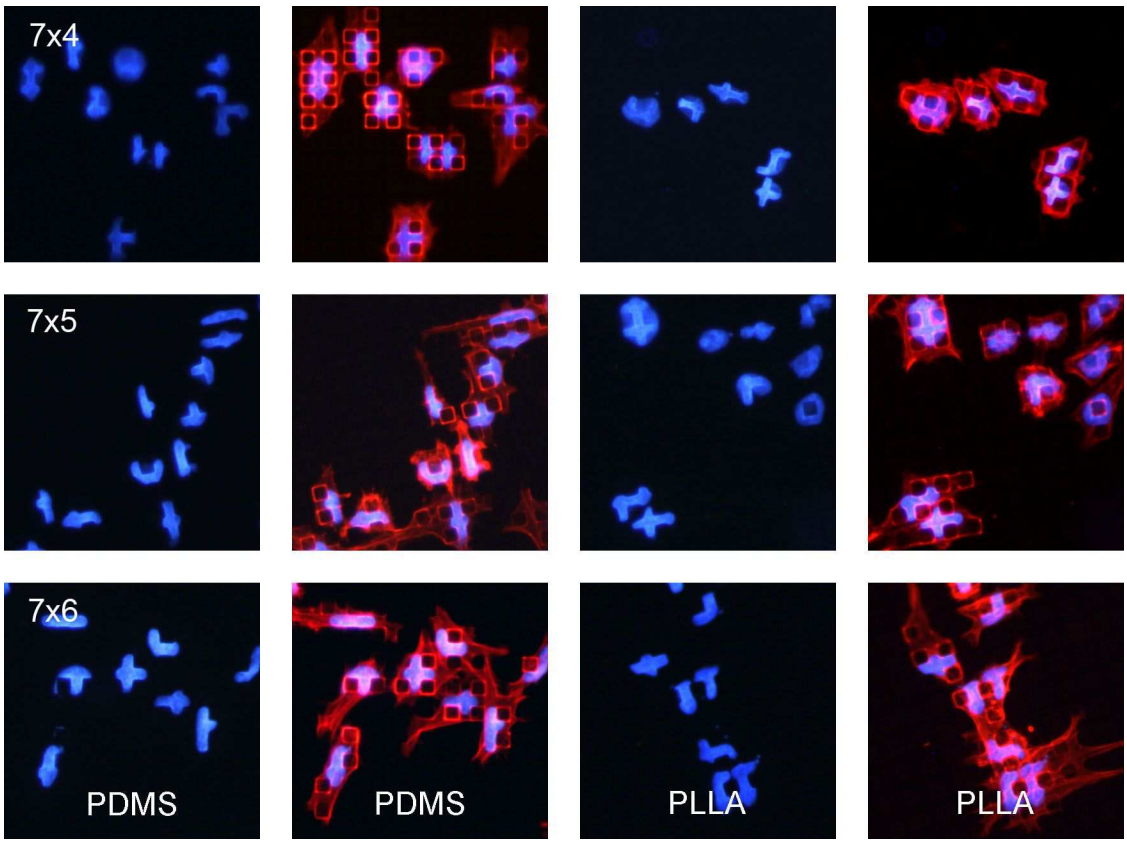

Figure 55: Comparison of the growth of SaOs-2 cells on PDMS (left) or PLLA surfaces (right). In each case the nucleus labelling (blue, left) is shown next to the actin and nucleus labelling superposition for clarity (red and blue, right).

softer pillars. The cells may produce more actin cytoskeleton at the surface of the pillars to compensate for their softness and keep the cell in place.

Several studies have been performed on cells grown on soft surfaces. In particular, an important study has demonstrated that the rigidity of a surface will determine the differentiation of stem cells grown on these.[151] However, both the substrates studied can still be considered to be "hard" when compared to the rigidity of a cell. The rigidity of PDMS surfaces can be altered by changing the amount of cross-linking agent used.[52] Varying the rigidity of the surface topography will enable us to determine the amount of force exerted on the pillars by the cell and the directionality of the force. If the surface pillars are made deformable enough, the force the cell exerts on them should be sufficient to deform them and we should be able to visualize this deformation in live cell imaging experiments. We will also be able to

see whether the deformation is dependent on the rigidity of the surface topography.

3.7 Conclusions and outlook

We have shown that certain types of transformed cells can deform themselves to adopt the surface topography of substrates at the micron scale without undergoing any changes in proliferation rates or viability, and with little change in their differentiation. It is likely that the alterations in mechanical properties of malignant cells are related to this ability to deform on the surfaces: metastatic cancerous cells are able to deform when traveling throughout the body. It is important for these types of cells to be able to undergo such deformation without significantly damaging or altering the cell. Therefore it is not surprising that such types of cells would be able to deform without noticeable effect on their metabolism. It could be thought that this type of behaviour is related to metastatic invasion. Studies on the effect of deformation on the RNA expression of MMPs are necessary to detect whether the deformation can be linked to effort to degrade the matrix, which could occur during invasion.

Several open-ended questions remain. For instance, how is the cell attached to the surface? Is it adhering to the space in between the pillars? Does this have a role in the deformation of the cytoskeleton? Imaging of the focal adhesion points should be able to easily answer these questions but so far attempts to visualize these have been unsuccessful. Continuing efforts will be undertaken using different markers. Other questions relate to the deformation mechanism: how is pressure exerted on the nucleus, which components of the cell are responsible for it? So far, attempts to answer these questions have provided us with clues to the possible mechanisms. The key to these experiments almost certainly lies in live cell imaging, using specific transfection of key components of the cytoskeleton and cytoskeleton disruption in real time. Inactivation of cytoskeleton-associated motors could also provide information on the deformation mechanism.

Remarkably, these experiments have shown us that the cell nucleus is a highly adaptable organelle. Images obtained of the nuclear membrane (figure 17) show that it is a smooth surface when deformed. This is indicative of a fluid adaptive surface, and does not show the folds of a membrane that would have to distort itself to fit in the space available. Live cell imaging studies show that the nucleus is constantly undergoing deformation, indicating its rapid adaptability. This type of property was alluded to in a publication by Dahl et al., who describe the nuclear membrane as a shock absorber: it is able to expand and contract as needed.[8] Additional questions about this remain as well: is this a property of the nucleus in its native state, or does the cell adapt to the microstructured surface by altering its composition, enabling easier migration of the cell nucleus in the space between the pillars? A study on the composition of the nucleus membrane and the expression of nucleus membrane proteins will confirm whether changes occur within the cell to facilitate this deformation.

Further effects of the deformation on the cell remain to be determined. For instance, what is the effect of the deformation on the architecture of the cytoskeleton? We have seen that the actin cytoskeleton forms thick actin bundles across the top of the cell in cases when it is well-deformed. These bundles of actin have been compared to the basal actin fibres present at the base of the cell when grown on a flat surface, but also to peri-nuclear actin. Cancerous cells are thought to have a less organised peri-nuclear actin network, therefore it is unclear whether this type of actin could be of a peri-nuclear type. In the area below the surface of the pillars, the cell does not seem to have this level of organisation: the actin cytoskeleton appears diffuse. This type of actin most likely does not exert considerable force on the cell. More extensive imaging is necessary using markers for different actin cross-linkers and cytoskeleton motors to determine the architecture of the cytoskeleton when deformed on the pillars.

A key technique in future experiments will almost certainly be live cell imaging. This will allow us to determine whether the presence of the micropillars affects the orientation of the axis of division of the

cell. Preliminary experiments could be performed on flat surfaces on which a similar pattern has been imprinted, to determine whether it is the restricted area of attachment or the topography that induces this type of behaviour. Live cell imaging will also be useful to study the mechanical properties of the nucleus.

Chapter 4
General conclusions and outlook

The information presented in this thesis is an overview of the interactions cells can have with nano- and microstructures, and how these interactions differ depending on the cell type. The studies described have highlighted important differences in the way cancerous and healthy cells react to surface structures and, more importantly, in how these cells transmit information to their interior, and in particular their nucleus. Remarkably we have shown an important deformation of the nucleus of cancer cells which had not been shown before. This research has important implications for cell mechanics and cytoskeleton architecture, but also for cancer and metastasis research.

In the chapter on the alignment with surface grooves, we showed how healthy and cancerous cells have different sensitivities to shallow and deep grooves, and differences in how the alignment information is transmitted to the nucleus. The cancerous cells had a greater ability to align and elongate their nucleus than the healthy cells. In the chapter on micron-scale square pillars we presented data on the response of cells grown on structures that are on the size scale of the nucleus. Once again we saw great differences in the behaviour of cancerous and healthy cells on these surfaces: only the cancerous cells were able to deform their nucleus and migrate easily in their deformed state. Remarkably the impact of the deformation on the cancerous cells is very limited: there was no significant effect on the viability, proliferation or differentiation of the cancerous cells. This may thus point to an increased ability of cancer cells to adapt to their environment, even when under significant stress.

These two sets of experiment hint at large differences in the mechanical properties of healthy and cancerous cells, as well as their ability to position and control their nucleus. Despite the insight gained in these studies there are many open-ended questions that remain unanswered:

- Why don't healthy cells deform their nucleus in response to surface topography? We saw that

healthy cells do not elongate their nucleus when the cell becomes elongated and that they do not deform their nucleus on the micropillars. Could this point to different mechanical properties of the cell nucleus or differences in force transduction within the cell?

- What is the nature of the cytoskeleton-nucleus interactions and how do these change for cancerous cells? We have seen that the nucleus is connected to the cytoskeleton, but is this the reason for the deformation observed on the micropillars? Could changes in these connections result in the differences observed between the healthy and the cancerous cells?
- What conclusions can we gather from these results about the mechanics of the cell and its nucleus? If the differences in deformation were related to the mechanics of the nucleus or the cell, could these surfaces be used as diagnostic tools for cell mechanics, in living cells, without exerting outside forces on them?
- Can cell deformation result in semi-permanent changes in the cell? The cancerous cells appear to become more deformed with time in culture, and deformation after cell division is rapid when compared to initial deformation. Could this point to an adaptation of nucleus mechanics or cytoskeleton organisation in response to the surface?
- How are the cells attached on the pillars? Does this have consequences for cell division? If the cells rise above the top of the pillars to divide, are they only adhered at the top of the pillars? Does the presence of the pillars direct the positioning of the cell division axis?

Based on the results we have obtained there are several important research topics on which we may speculate. A first important point is the differences in how healthy and cancerous cells respond to surface structures and how this could relate to metastasis. The cancerous cells do not seem to be greatly affected by the presence of the pillars: these do not greatly alter their viability, proliferation or differentiation characteristics. However, many examples exist in the literature that show that surface

rigidity and topography is an important factor in stem cell differentiation. It would thus seem that there is a difference in the way cancerous and healthy cells transmit information about their environment and react to it. It is very important to identify how the sensitivity of these two types of cells to surfaces differ. The lowered sensitivity of the cancerous cells to changes in surface topography is certainly an important feature during metastasis, in which retaining the cells' phenotype during migration through narrow spaces is essential. Hence, identification of the differences in the way information is transmitted within the cell and converted into changes in gene expression would be pivotal in the fight against cancer: increasing the cancer cells' biological response (or sensitivity) to surface features may help prevent metastatic migration. This is particularly important because, as of yet, differences in transmission of information within healthy and cancerous cells have not been considered. In order to study this, the mechanisms by which information is transmitted from the exterior of the cell and transformed into a cellular response and the differences in cancerous and healthy cells will have to be studied further, and in particular the changes at the level of the cytoskeleton and the connections between the cytoskeleton and the nucleus.

Further study should also concentrate on determining whether the behaviour of the cancerous cells on the surfaces can be related to metastatic migration This can be done by studying the expression of certain proteins, such as matrix metalloproteinases (MMPs), which are enzymes involved in matrix degradation during metastasis. If it is indeed verified that the cells have an increased metastatic migration activity on the surfaces, these surfaces could be used to further study the early stages of metastatic migration. In particular, it would be important to study the changes that occur at the level of the expression of proteins involved in the cytoskeleton-nucleus connection: SUN/KASH proteins, lamins, emerin, etc. This would allow us to understand whether cancerous cells adapt to their environment during metastatic migration to facilitate movement through confined spaces, or whether they are unaffected, as speculated above. A deeper understanding of the changes occurring in metastatic

cells could lead to strategies for reducing metastatic migration, a major challenge in current cancer research.

The surfaces themselves may prove to be useful for studying the mechanical properties of the nuclei of deformable cells. Importantly, these result in useful information without mechanically affecting the cell through manipulation, as is the case with current methods used to test mechanical properties of cells, which involve pulling or pushing on the nucleus (AFM, micropipette aspiration, etc.). Further studies are needed to identify whether the deformation can be directly correlated to properties of the cell (cytoskeleton integrity) or the nucleus (rigidity). The dependence on the latter could be studied through drugs that increase or decrease nucleus rigidity, or by altering the expression of lamins, which have been shown to have a role in the mechanical properties of the nucleus.

We believe this research provides clues to many aspects of cancer research that are very relevant to the current effort to combat cancer and in particular to inhibit metastasis. In particular, this work looks at the problem from the point of view of the cytoskeleton and cell mechanics, which has not be studied extensively, but may prove to be an important factor. There are still many things left to discover on the cytoskeleton architecture, how it is regulated and how this is modified when tumour suppressor-genes are inactived. This also extends to how cytoskeleton-nucleus interactions are affected by changes related to cell malignancy. The work presented here begins to address and provide clues to answer these questions, which opens up exciting new directions for study.

Communication of the work

Publications

The interaction of cells and bacteria with surfaces structured at the nanometre scale (review)
K. Anselme, P. M. Davidson, A.M. Popa, M. Giazzon, M. Liley, L. Ploux, *Acta Biomater.* 6, 10, 3824-46 (2010)

Topographically induced self-deformation of the nuclei of cells: dependence on cell type and proposed mechanisms
P. M. Davidson, O. Fromigué, P. J. Marie, V. Hasirci, G. Reiter, K. Anselme, *J. Mater. Sci.: Mater. Med.* 21, 939–946 (2010)

Definition of a simple statistical parameter for the quantification of orientation in two dimensions: Application to cells on grooves of nanometric depths
P. M. Davidson, M. Bigerelle, B. Bounichane, M. Giazzon, K. Anselme, *Acta Biomater.* 6, 7, 2590-8 (2010)

Microstructured Surfaces Cause Severe but Non-Detrimental Deformation of the Cell Nucleus
P. M. Davidson, H. Özçelik, V. Hasirci, G. Reiter, and K. Anselme, *Adv. Mater.* 21, 3586–3590 (2009)

Presentations

April 2011 — Invited Seminar: *Exploring cell mechanics through cell-surface interactions*
Kansai Advanced ICT Research Center, Kobe, Japan

April 2011 — Invited Seminar: *The plasticity of cancerous cells and the cell nucleus: cell-surface interactions*
Freiburg University, Soft Matter Science IRTG

March 2011 — Poster: *The plasticity of cancerous cells and the cell nucleus.*
Annual meeting of the Biophysical Society, Baltimore, USA

Sept 2010 — Conference presentation: *The plasticity of cancerous cells and the cell nucleus.*
Poster: *Cancerous cells on grooved surfaces*
European Materials Research Society meeting, Strasbourg

July 2010 — Student presentation: *Microstructured Surfaces Cause Severe but Non-Detrimental Deformation of the Cell Nucleus*
Osaka University Frontier Biosciences Summer Program, Osaka, Japan

June 2010 — Invited Seminar: *Microstructured Surfaces Cause Severe but Non-Detrimental Deformation of the Cell Nucleus*
Kansai Advanced ICT Research Center, Kobe, Japan

Oct 2009 Invited Seminar: *Microstructured Surfaces Cause Severe but Non-Detrimental Deformation of the Cell Nucleus*
Institute for New Materials, Saarbrucken, Germany

Sept 2009 Selected Poster Presentation: *Microstructured Surfaces Cause Severe but Non-Detrimental Deformation of the Cell Nucleus*
Physics of Cells conference, Primosten, Croatia

March 2009 Conference presentation: *Bootstrap protocol to characterize the contact guidance angle of cell orientation*
International Conference on Bioengineering and Biomaterials, Meknes, Morocco

Sept 2008 Presentation: *Cell Responses to Topography*
Biopolysurf Research Training Network final meeting, Majorca

Abbreviations

AFM	Atomic force microscope
BMP-2	Bone morphogenic protein 2
BrdU	Bromo deoxyuridine
C_{GDE}	Cell groove depth effect
DAPI	4',6-diamidino-2-phenylindole
DIC	Differential interference contrast microscopy
HOP	Human osteoprogenitor
HPV	Human papilloma virus
IDPN	Imino diproprio nitrile
INM	Inner nuclear membrane
LINC	Linker of nucleoskeleton and cytoskeleton
MMP	Matrix metalloproteinase
MTOC	Microtubule organisation center
MTT	3-(4,5-Dimethylthiazol-2-yl)-2,5-diphenyltetrazolium bromide
NMP	Nuclear membrane protein
ONM	Outer nuclear membrane
PCR	Polymerase chain reaction
PDMS	Polydimethylsiloxane
PLLA	Poly-L-lactic acid
SEM	Scanning electron microscopy

Résumé substantiel

Le sujet de cette thèse est l'étude de la réponse de cellules saines et cancéreuses à la topographie de surface. Nous allons tout d'abord brièvement introduire les concepts biologiques nécessaires à la compréhension de ce travail et discuter de ce qui est connu dans le domaine de l'interaction entre les cellules et la topographie de surface. Ensuite nous discuterons des résultats obtenus sur les stries de profondeur nanométrique et les piliers de taille micrométrique et nous présenterons une conclusion générale des résultats.

Chapitre 1: Introduction

Biologie de la cellule eucaryote

Les cellules sont les unités de base de la vie. Elles sont entourées d'une membrane cytoplasmique et contiennent, entre autres, un noyau et un cytosquelette. Le noyau de la cellule est son organite (compartiment cellulaire entouré d'une membrane) principal. Celui-ci contient l'ADN et est entouré d'une couche de protéines (les lamines) à la surface intérieure d'une membrane double, ce qui lui confère une plus grande rigidité par rapport au reste de la cellule. Le cytosquelette sert à exercer des forces à l'intérieur de la cellule: il est responsable du trafic intracellulaire et du mouvement de la cellule elle-même. Il est composé de trois classes de filaments protéiniques: l'actine, les microtubules et la famille des filaments intermédiaires (dont les lamines). Chacun de ces types de filaments ont un rôle précis pour la cellule.[1] Lorsque les cellules sont adhérées à une surface, elles forment des points d'attache, les points focaux, qui sont des complexes de protéines, dont les intégrines, des protéines trans-membranaires qui détectent la présence de motifs protéiniques spécifiques dans la matrice extracellulaire. A l'intérieur de la cellule, toutes ces entités sont reliées: les filaments du cytosquelette sont attachés aux points focaux, et il existe plusieurs liens entre le noyau et les composants du cytosquelette.[15,16,20] Ainsi, le noyau de la cellule est relié mécaniquement à l'extérieur de la cellule.

Il existe plusieurs types de cellule, et parmi ces types il peut y avoir aussi des différences qui sont dues à des mutations de la cellule. Ces mutations peuvent causer une transformation maligne de la cellule. Les lignées cellulaires utilisées couramment dans le domaine des biomatériaux sont surtout des lignées cancéreuses issues de tumeurs ou des lignées des cellules saines qui ont été immortalisées: ces dernières ont subi un traitement qui leur permet de se multiplier plus rapidement que les cellules normales. Ceci a des conséquences connues sur l'organisation et la mécanique de la cellule: les cellules immortalisées sont plus déformables, ont un cytosquelette moins organisé et produisent moins de cytosquelette. [32-34]

Interactions des cellules humaines avec la topographie de surface

Plusieurs découvertes importantes ont été faites grâce à l'étude de la réponse des cellules à la topographie de surface. A l'échelle nanométrique, il a été montré que des structures d'une hauteur d'une dizaine de microns peuvent influencer l'étalement, la prolifération et le cytosquelette de cellules.[53] La différentiation d'une cellule souche en cellule osseuse peut aussi être induite par l'organisation de nanotopographies.[61] De plus, il a été montré qu'il y a une distance minimale entre les intégrines[3] et une taille minimale de surface d'adhesion[68] pour la formation d'un point focal stable.

A l'échelle du micron, la topographie de surface a été utilisée pour étudier les forces cellulaires, grâce à des piliers déformables.[113] L'adhésion de cellules à l'intérieur de micro-puits a permis de montrer l'effet de l'architecture tri-dimensionnelle de la cellule sur l'organisation de son cytosquelette.[52] Des études ont montré que l'étalement de la cellule, déterminé par la taille du patch sur lequel elle peut adhérer, détermine sa différenciation: les cellules peu étalées se transforment en adipocytes (stockage de graisse) et celles qui sont très étalées se transforment en cellules osseuses.[63]

Chapitre 2: L'interaction de cellules avec des stries de profondeur nanométrique

L'alignement de cellules saines et cancéreuses avec des stries a été déterminé par des marquages du cytosquelette et du noyau des cellules. Plusieurs conditions ont été testées: 4 profondeurs différentes (30 nm, 100 nm, 200 nm, 500nm) et 5 délais d'incubation différents (4h, 24h, 48h, 72h et 120h). La densité d'inoculation des cellules saines a aussi été modifiée pour tester l'effet de la coopération entre cellules et obtenir des valeurs de densité de surface similaire à la densité des cellules cancéreuses, qui s'étalent moins.

Les valeurs de l'alignement sont présentées sous forme d'histogrammes, et ceux-ci décrivent une courbe gaussienne. Pour obtenir une valeur quantitative de l'alignement des cellules, l'écart-type des valeurs de l'angle des cellules pour chaque échantillon a été calculé. A partir de ces valeurs, des graphiques ont permis d'établir la relation entre l'écart-type et la profondeur pour chaque délai, qui se présente sous la forme:

$$\sigma = \alpha_{inf} + \frac{\sigma_0 - \alpha_{inf}}{1 + aR} \tag{7}$$

Où α_{inf} représente la limite d'alignement des cellules pour des profondeurs infinies, σ représente l'écart-type, σ_0 représente l'écart-type de cellules non-alignées (52 degrés), R représente la profondeur, et a est une constante qui est déterminée par ajustement de courbe. A partir de cette valeur, la sensibilité des cellules aux stries peu profondes peut être déterminée grâce à l'équation 7, ci-dessous.

$$C_{GDE} = (52 - \alpha_{inf}) * a \tag{8}$$

Cette valeur représente l'asymptote à la courbe à R=0. Ainsi, des valeurs de la sensibilité des cellules aux stries peuvent être déterminées qui sont indépendantes de la profondeur des stries.

Limite de l'alignement pour des stries infiniment profondes

L'analyse des courbes révèle que les cellules saines sont capables de s'aligner plus fortement sur des stries profondes: la valeur de la limite à l'infini est beaucoup plus petite pour les cellules saines (0 degrés) que pour les cellules cancéreuses (23 degrés). Ainsi, même lorsque les conditions d'alignement sont très favorables, les cellules cancéreuses gardent une large dispersion dans leurs alignement sur les stries. Nous pouvons expliquer ce phénomène grâce au comportement de ces cellules. Premièrement, les cellules cancéreuses ont tendance à proliférer beaucoup plus rapidement que les cellules saines. Pendant chaque division, les cellules deviennent rondes et ainsi perdent leur alignement. Puisque ce phénomène est plus fréquent chez les cellules cancéreuses, elle seraient moins alignées en moyenne. Deuxièmement, le cytosquelette des cellules cancéreuses, qui est responsable du déplacement de la cellule, est modifié par rapport au cytosquelette des cellules saines: les cellules cancéreuses produisent moins de cytosquelette et celui-ci est moins organisé. Dans le cas de cellules saines l'alignement sur des stries profondes est surement régi par le placement de longs filopodes sur les surfaces striées, ce qui a comme conséquence d'aligner les cellules efficacement. Les cellules cancéreuses, à cause de leur cytosquelette moins organisé, produisent peu de filopodes et ainsi ne sont pas aussi limitées dans leurs mouvements.

Sensibilité aux stries peu profondes

Les valeurs de sensibilité aux stries peu profondes démontrent qu'il dépend fortement de la coopérativité des cellules: une augmentation de 30% de la densité initiale résulte en un doublement de la sensibilité. Ce phénomène a déjà été décrit dans la littérature.[74]

Les valeurs de sensibilité des cellules cancéreuses sont intermédiaires entre les valeurs de sensibilité des cellules saines aux deux densités d'inoculation. Par contre, la densité de couverture de la surface des cellules cancéreuses est plus proche des cellules saines moins denses. (Ces valeurs sont même

inférieures pour les temps de culture étudiés.) Si on prend en compte l'effet de la coopération entre cellules, les cellules cancéreuses seraient donc plus sensibles aux stries peu profondes que les cellules saines. Une hypothèse pour expliquer l'alignement des cellules avec les stries est reliée à la formation de points d'attache à la surface (les points focaux). Ceux-ci sont des complexes de protéines à l'interface de la cellule et de la surface. A cette interface se trouvent les intégrines qui sont assemblées avec une distance minimale d'environ 60 nm. Ainsi, une marche de 30 nm causerait une perturbation de l'assemblement des points focaux. Puisque les cellules cancéreuses sont plus mobiles que les cellules saines elles rencontrent plus souvent des différences de hauteur qui les inciteraient à s'aligner avec les stries.

Dans chacun des cas la sensibilité croît avec le temps en culture, jusqu'à atteindre un plateau qui pourrait être dû à la confluence des cellules (difficulté à se déplacer) ou à un comblement des structures par la synthèse de matrice extra-cellulaire.

Alignement et élongation du noyau

Lorsque l'analyse est effectuée sur l'alignement des noyaux des cellules, la sensibilité des noyaux de cellules cancéreuses est plus grande que la sensibilité de noyaux de cellules saines, aux deux densités d'inoculation. La comparaison des valeurs de l'alignement des corps cellulaires et de l'alignement des noyaux révèle que l'alignement des noyaux suit l'alignement des corps cellulaires dans le cas des cellules cancéreuses, même pour les cellules qui ne sont pas alignées avec les stries. Dans le cas des cellules saines la corrélation n'est pas aussi nette. La forme du noyau a aussi été analysée en calculant le rapport longueur/largeur. Ceci a permis de démontrer que les cellules cancéreuses sont capables d'étirer leur noyau en réponse aux stries de manière plus importante que les cellules saines. On trouve des rapports allant jusqu'à des valeurs de 2 et très peu entre 2 et 3 pour les cellules saines, même pour des cellules bien alignées, alors que les valeurs pour les cellules cancéreuses vont jusqu'à 5 et

quelquefois au-dessus de 5. Dans ce dernier cas on voit une forte corrélation entre l'alignement avec les stries et l'élongation du noyau.

Ces résultats peuvent être expliqués par la modification des propriétés mécaniques des noyaux des cellules. Il a été montré que la composition de la membrane nucléaire est modifiée dans les cellules cancéreuses et que la rigidité des noyaux changent avec le niveau de différentiation de la cellule (relié à la production de lamines de la membrane nucléaire).[11]

Chapitre 3: Interactions des cellules avec des piliers micrométriques

La réponse de cellules aux structures de surface à la taille du micron ne sont pas bien connues. Il est souvent pensé que les cellules passent au-dessus des structures et ne sont pas grandement affectées par cette structure. Cependant, les surfaces que nous utilisons ont des tailles qui sont à l'échelle des organites à l'intérieur de la cellule. On peut imaginer que si les cellules adhèrent aux structures fortement on peut obtenir une déformation de la cellule en réponse à la topographie de surface.

Cellules de l'os

Lorsque des cellules d'ostéosarcome sont inoculées sur une surface polymère bio-compatible comportant des piliers carrés de diamètre 7 microns, d'espacement 7 microns et de hauteur 4 microns, une déformation nette du noyau se produit. Celui-ci est introduit par la cellule dans l'espace entre les piliers et adopte une forme qui n'a jamais été observée avant. La viabilité et la prolifération de ces cellules a été testée mais de manière surprenante, cette déformation ne provoque pas d'effet significatif. La différenciation de ces cellules issues de l'os a aussi été testée en mesurant l'activité d'une enzyme spécifique de l'os (pas de différence) et l'expression de trois gènes spécifiques de l'os (une faible différence). D'autres lignées d'ostéosarcomes ont été testées sur ces surfaces et elles se déforment aussi. Par contre, des tests sur des surfaces avec des espacements entre piliers réduits montrent des

différences de capacité à déformer leur noyau entre lignées d'ostéosarcome.

Puisque ces cellules sont cancéreuses et que celles-ci ont une capacité de déformation plus grande que les cellules saines, d'autres lignées issues de l'os ont été testées sur ces surfaces. Des cellules immortalisées ont d'abord été testées. Celles-ci sont des cellules saines qui ont été inoculées avec un oncovirus qui leur confère certaines propriétés des cellules cancéreuses: prolifération plus rapide, immortalité. Cependant elles ne sont pas considérées comme des cellules malignes. Elles ont donc un caractère intermédiaire entre les cellules saines et les cellules cancéreuses. De plus elles sont plus déformables que les cellules saines. Lorsque celles-ci sont inoculées sur les surfaces comportant des piliers, ces cellules montrent très peu de déformation. Une des lignées est déformée faiblement et une autre ne montre aucune déformation de la cellule, sauf à l'extrémité des filopodes des cellules, qui servent de points d'ancrage aux piliers.

Un autre type de cellule testé sont des cellules saines issues directement de la moelle de patients. Sur ces échantillons très peu de cellules montraient une déformation en réponse à la surface. Une étude plus poussée de l'adhésion des cellules saines à des temps courts a montré qu'elles se déforment durant la phase initiale d'adhésion, mais perdent leur déformation progressivement pendant les premières 48 heures d'incubation. Au contraire, les cellules cancéreuses présentent une déformation qui augmente avec le temps. Ceci indique des différences importantes dans l'interaction de cellules saines et cancéreuses avec les surfaces. Il est possible que les cellules saines nécessitent la perte de la déformation pour pouvoir se déplacer sur la surface, et donc qu'elles remontent au-dessus des piliers après la première phase d'adhésion.

Autres types cellulaires

D'autres lignées issues de différents tissus ont aussi été étudiées sur ces surfaces. Des lignées de keratinocytes saines, immortalisées et cancéreuses montrent une tendance similaire aux cellules

osseuses. Une lignée de cellules épithéliales ayant subit plusieurs transformations successives pour obtenir une gamme de malignité montre très peu de déformation sur les piliers, et un effet faible qui est inverse à celui des cellules osseuses. Quatre lignées d'adénocarcinomes ont été testées et deux d'entre elles présentent une déformation. Ceci n'est pas relié à leur polarisation mais pourrait être lié à leur capacité à exprimer un gène particulier: Cdx-2.

Mécanisme de la déformation

Nous avons attribué cette déformation du noyau à une pression exercée par le cytosquelette sur l'intérieur de la cellule. Celle-ci pourrait s'appliquer au-dessus du noyau par une contraction des fibres de stress ou autre composantes du cytosquelette, ou en dessous du noyau, si les cellules sont adhérées sur les parois des piliers ou dans les espaces entre les piliers. Des études avec un microscope confocal ont été entreprises pour voir si une de ces hypothèses pouvait être juste. Celles-ci ont révélé qu'il y a effectivement des fibres de stress qui passent au-dessus du noyau, mais celles-ci sont présentes surtout dans des cellules qui sont bien déformées et leur rôle serait donc plutôt de garder en place le noyau déformé. Des filaments d'actine sont aussi présents sur les bords des piliers, ce qui pourrait indiquer la présence de points d'attache, nécessaires à la traction depuis le bas. Alors que les filaments d'actine se trouvent plutôt à la périphérie de la cellule, les microtubules englobent le noyau de la cellule. Il serait donc aussi possible que les forces exercées proviennent des microtubules, qui sont placés plus près du noyau. Malheureusement des études statiques ne sont pas suffisantes pour comprendre d'où proviennent les forces.

Les études d'imagerie en vivant ont permis d'observer le comportement des cellules et de répondre à plusieurs questions. Une transfection a été effectuée pour rendre les filaments d'actine fluorescents. L'observation des cellules d'ostéosarcome sur plusieurs heures a permis de montrer que ces cellules se déplacent librement sur les surfaces, même lorsqu'elles sont complètement déformées. Il est aussi

observé que le noyau des cellules se faufilent assez facilement entre les piliers, en réponse au déplacement de la cellule. Cependant le mouvement se fait par étapes: le noyau ne se déplace pas de façon complètement fluide, mais plutôt de façon séquentielle, certainement dû à la résistance du noyau au confinement entre piliers.

La mitose a aussi été observée sur ces cellules. Il a ainsi été trouvé que les cellules s'arrondissent au début de la mitose et montent au-dessus des piliers en perdant leur déformation. Après la division les deux cellules filles se déforment plus rapidement que pendant la période d'adhésion initiale des cellules. Ceci peut être expliqué soit grâce aux points d'attache à la surface que les cellules filles ont hérité de la cellule mère, qui facilite l'étalement et ainsi la déformation, mais aussi par une adaptation possible de la cellule à la surface, rendant les cellules plus souples. Ceci devra être étudié plus profondément à l'avenir.

Le ou les acteurs responsables de la déformation ont été recherchés en utilisant des inhibiteurs de cytosquelette. Des concentrations ont été déterminées auxquelles il n'y a pas d'incidence forte sur l'aspect des cellules mais où le démantèlement du réseau du cytosquelette est clairement observé. Malheureusement, l'addition d'inhibiteurs à ces concentrations n'a pas abouti à une perte de la déformation du noyau. Ceci peut être expliqué par la nature plastique plutôt qu'élastique du noyau.[11] Ainsi, une perte de la force exercée sur le noyau ne résulterait en une récupération de sa forme sphérique que s'il y avait une force restauratrice qui pouvait contrer l'organisation interne de la cellule déjà en place. Cependant, des tests plus poussés seront effectués dans l'avenir à différentes concentrations et à différents moments pendant l'adhésion des cellules pour voir si un effet peut être détecté.

Conclusions

Les résultats présentés dans cette thèse représentent une large étude de la réponse de cellules à la

topographie de surface, et en particulier aux effets qui peuvent se produire à l'intérieur de la cellule. Nous avons vu plusieurs exemples de différences notables dans les mécanismes de réponse aux surfaces et dans la capacité à organiser l'intérieur de la cellule, et notamment le positionnement du noyau.

Plusieurs questions restent ouvertes. Pourquoi les cellules saines ne déforment-elles pas leurs noyaux, ni sur les stries, ni sur les piliers? Quelle est la nature de l'interaction entre le cytosquelette et le noyau et comment change-t-elle pour les cellules cancéreuses? Quelles conclusions peut-on tirer sur la mécanique de la cellule et du noyau? La déformation de cellules peut-elle engendrer un changement semi-permanent des cellules? (Composition de la membrane nucleaire, etc.) Toutes ces questions sont importantes et permettrait de faire avancer de plusieurs pas notre compréhension des cellules.

References

1. Suresh, S. Biomechanics and biophysics of cancer cells. *Acta biomaterialia* **3**, 413-38(2007).

2. Wirtz, D. & Khatau, S.B. Protein filaments: Bundles from boundaries. *Nature materials* **9**, 788-90(2010).

3. Arnold, M., Cavalcanti-Adam, E.A., Glass, R., Blümmel, J., Eck, W., Kantlehner, M., Kessler, H. & Spatz, J.P. Activation of integrin function by nanopatterned adhesive interfaces. *Chemphyschem : a European journal of chemical physics and physical chemistry* **5**, 383-8(2004).

4. Fujita, S., Ohshima, M. & Iwata, H. Time-lapse observation of cell alignment on nanogrooved patterns. *Journal of the Royal Society, Interface / the Royal Society* **6 Suppl 3**, S269-77(2009).

5. Rowat, A.C., Lammerding, J., Herrmann, H. & Aebi, U. Towards an integrated understanding of the structure and mechanics of the cell nucleus. *BioEssays : news and reviews in molecular, cellular and developmental biology* **30**, 226-36(2008).

6. Guilak, F., Tedrow, J.R. & Burgkart, R. Viscoelastic properties of the cell nucleus. *Biochemical and biophysical research communications* **269**, 781-6(2000).

7. Mazumder, A., Roopa, T., Basu, A., Mahadevan, L. & Shivashankar, G.V. Dynamics of chromatin decondensation reveals the structural integrity of a mechanically prestressed nucleus. *Biophysical journal* **95**, 3028-35(2008).

8. Dahl, K.N., Kahn, S.M., Wilson, K.L. & Discher, D.E. The nuclear envelope lamina network has elasticity and a compressibility limit suggestive of a molecular shock absorber. *Journal of cell science* **117**, 4779-86(2004).

9. Lammerding, J., Schulze, P.C., Takahashi, T., Kozlov, S., Sullivan, T., Kamm, R.D., Stewart, C.L. & Lee, R.T. Lamin A/C deficiency causes defective nuclear mechanics and mechanotransduction. *Journal of Clinical Investigation* **113**, 370–378(2004).

10. Lee, J.S.H., Hale, C.M., Panorchan, P., Khatau, S.B., George, J.P., Tseng, Y., Stewart, C.L., Hodzic, D. & Wirtz, D. Nuclear lamin A/C deficiency induces defects in cell mechanics, polarization, and migration. *Biophysical journal* **93**, 2542-52(2007).

11. Pajerowski, J.D., Dahl, K.N., Zhong, F.L., Sammak, P.J. & Discher, D.E. Physical plasticity of the nucleus in stem cell differentiation. *Proceedings of the National Academy of Sciences* **104**, 15619-15624(2007).

12. Khatau, S.B., Kim, D.-H., Hale, C.M., Bloom, R.J. & Wirtz, D. The perinuclear actin cap in health and disease. *Nucleus (Austin, Tex.)* **1**, 337-342(2010).

13. Fuhrmann, a, Staunton, J.R., Nandakumar, V., Banyai, N., Davies, P.C.W. & Ros, R. AFM stiffness nanotomography of normal, metaplastic and dysplastic human esophageal cells. *Physical biology* **8**, 015007(2011).

14. Konety, B.R. & Getzenberg, R.H. Nuclear structural proteins as biomarkers of cancer. *Journal of Cellular Biochemistry* **75**, 183–191(1999).

15. Kaverina, I., Krylyshkina, O. & Small, J.V. Regulation of substrate adhesion dynamics during cell motility. *The international journal of biochemistry & cell biology* **34**, 746-61(2002).

16. Qin, Z., Buehler, M.J. & Kreplak, L. A multi-scale approach to understand the mechanobiology of intermediate filaments. *Journal of biomechanics* **43**, 15-22(2010).

17. Bhattacharya, R., Gonzalez, A.M., Debiase, P.J., Trejo, H.E., Goldman, R.D., Flitney, F.W. & Jones, J.C.R. Recruitment of vimentin to the cell surface by beta3 integrin and plectin mediates adhesion strength. *Journal of cell science* **122**, 1390-400(2009).

18. Small, J.V., Geiger, B., Kaverina, I. & Bershadsky, A.D. How do microtubules guide migrating cells? *Nature reviews. Molecular cell biology* **3**, 957-64(2002).

19. Ezratty, E.J., Partridge, M. a & Gundersen, G.G. Microtubule-induced focal adhesion disassembly is mediated by dynamin and focal adhesion kinase. *Nature cell biology* **7**, 581-90(2005).

20. Starr, D. a Communication between the cytoskeleton and the nuclear envelope to position the nucleus. *Molecular bioSystems* **3**, 583-9(2007).

21. Burke, B. & Roux, K.J. Nuclei take a position: managing nuclear location. *Developmental cell* **17**, 587-97(2009).

22. Wang, N., Tytell, J.D. & Ingber, D.E. Mechanotransduction at a distance: mechanically coupling the extracellular matrix with the nucleus. *Nature reviews. Molecular cell biology* **10**, 75-82(2009).

23. Starr, D. a A nuclear-envelope bridge positions nuclei and moves chromosomes. *Journal of cell science* **122**, 577-86(2009).

24. Jaalouk, D.E. & Lammerding, J. Mechanotransduction gone awry. *Nature reviews. Molecular cell biology* **10**, 63-73(2009).

25. Khatau, S.B., Hale, C.M., Stewart-Hutchinson, P.J., Patel, M.S., Stewart, C.L., Searson, P.C., Hodzic, D. & Wirtz, D. A perinuclear actin cap regulates nuclear shape. *Proceedings of the National Academy of Sciences of the United States of America* **106**, 19017-22(2009).

26. Wu, J., Lee, K.C., Dickinson, R.B. & Lele, T.P. How dynein and microtubules rotate the nucleus. *Journal of cellular physiology* (2010).doi:10.1002/jcp.22616

27. Starr, D. a & Fridolfsson, H.N. Interactions Between Nuclei and the Cytoskeleton Are Mediated by SUN-KASH Nuclear-Envelope Bridges. *Annual review of cell and developmental biology* (2010).doi:10.1146/annurev-cellbio-100109-104037

28. Forgacs, G. On the possible role of cytoskeletal filamentous networks in intracellular signaling: an approach based on percolation. *Journal of cell science* **108**, 2131-43(1995).

29. Ingber, D.E. Tensegrity: the architectural basis of cellular mechanotransduction. *Annual review of physiology* **59**, 575-99(1997).

30. Ali, S.H. & DeCaprio, J. a Cellular transformation by SV40 large T antigen: interaction with host proteins. *Seminars in cancer biology* **11**, 15-23(2001).

31. Steinberg, T., Schulz, S., Spatz, J.P., Grabe, N., Müssig, E., Kohl, A., Komposch, G. & Tomakidi, P. Early keratinocyte differentiation on micropillar interfaces. *Nano letters* **7**, 287-94(2007).

32. Comer, K. a, Dennis, P. a, Armstrong, L., Catino, J.J., Kastan, M.B. & Kumar, C.C. Human smooth muscle alpha-actin gene is a transcriptional target of the p53 tumor suppressor protein. *Oncogene* **16**, 1299-308(1998).

33. Ben-ze'ev, A. The cytoskeleton in cancer cells. *Biochimica et Biophysica Acta* **780**, 197-212(1985).

34. Guck, J., Schinkinger, S., Lincoln, B., Wottawah, F., et al. Optical deformability as an inherent cell marker for testing malignant transformation and metastatic competence. *Biophysical journal* **88**, 3689-98(2005).

35. Blättler, T., Huwiler, C., Ochsner, M., Städler, B., Solak, H., Vörös, J. & Grandin, H.M. Nanopatterns with Biological Functions. *Journal of Nanoscience and Nanotechnology* **6**, 2237-2264(2006).

36. Yang, S.-M., Jang, S.G., Choi, D.-G., Kim, S. & Yu, H.K. Nanomachining by colloidal lithography. *Small (Weinheim an der Bergstrasse, Germany)* **2**, 458-75(2006).

37. Wood, M. a Colloidal lithography and current fabrication techniques producing in-plane nanotopography for biological applications. *Journal of the Royal Society, Interface / the Royal Society* **4**, 1-17(2007).

38. Meli, M.-V., Badia, A., Grütter, P. & Lennox, R.B. Self-Assembled Masks for the Transfer of Nanometer-Scale Patterns into Surfaces: Characterization by AFM and LFM. *Nano Letters* **2**, 131-135(2002).

39. Wen, G., Chung, B. & Chang, T. Effect of spreading solvents on Langmuir monolayers and Langmuir–Blodgett films of PS-b-P2VP. *Polymer* **47**, 8575-8582(2006).

40. Cox, J.K., Eisenberg, A. & Lennox, R.B. Patterned surfaces via self-assembly Juliet K Cox, Adi Eisenberg" and R Bruce Lennoxt. *Current Opinion in Colloid & Interface Science* 52-59

41. Krishnamoorthy, S., Pugin, R., Brugger, J., Heinzelmann, H. & Hinderling, C. Tuning the Dimensions and Periodicities of Nanostructures Starting from the Same Polystyrene-block-poly(2-vinylpyridine) Diblock Copolymer. *Advanced Functional Materials* **16**, 1469-1475(2006).

42. Spatz, J., Herzog, T., Mößmer, S., Ziemann, P. & Möller, M. Micellar inorganic-polymer hybrid systems-a tool for nanolithography. *Advanced Materials* **11**, 149–153(1999).

43. Truskett, V.N. & Watts, M.P.C. Trends in imprint lithography for biological applications. *Trends in biotechnology* **24**, 312-7(2006).

44. Dalby, M.J., Riehle, M.O., Johnstone, H.J.H., Affrossman, S. & Curtis, A.S.G. In vitro reaction of endothelial cells to polymer demixed nanotopography. *Biomaterials* **23**, 2945-54(2002).

45. Dalby, M.J. Rapid fibroblast adhesion to 27nm high polymer demixed nano-topography. *Biomaterials* **25**, 77-83(2004).

46. Teo, W.-E. & Ramakrishna, S. A review on electrospinning design and nanofibre assemblies. *Nanotechnology* **17**, R89-R106(2006).

47. Teo, W.-E., He, W. & Ramakrishna, S. Electrospun scaffold tailored for tissue-specific extracellular matrix. *Biotechnology journal* **1**, 918-29(2006).

48. Anselme, K., Davidson, P., Popa, a M., Giazzon, M., Liley, M. & Ploux, L. The interaction of cells and bacteria with surfaces structured at the nanometre scale. *Acta biomaterialia* **6**, 3824-46(2010).

49. Dugina, V., Fontao, L., Chaponnier, C., Vasiliev, J. & Gabbiani, G. Focal adhesion features during myofibroblastic differentiation are controlled by intracellular and extracellular factors. *Journal of cell science* **114**, 3285-96(2001).

50. Nakatsuji, N. & Nagata, I. Paradoxical perpendicular contact guidance displayed by mouse cerebellar granule cell neurons in vitro. *Development (Cambridge, England)* **106**, 441-7(1989).

51. Dusseiller, M.R., Smith, M.L., Vogel, V. & Textor, M. Microfabricated three-dimensional environments for single cell studies. *Biointerphases* **1**, P1(2006).

52. Ochsner, M., Textor, M., Vogel, V. & Smith, M.L. Dimensionality controls cytoskeleton assembly and metabolism of fibroblast cells in response to rigidity and shape. *PloS one* **5**, e9445(2010).

53. Dalby, M.J., Pasqui, D. & Affrossman, S. Cell response to nano-islands produced by polymer demixing: a brief review. *IEE proceedings. Nanobiotechnology* **151**, 53-61(2004).

54. Dalby, M.J., Yarwood, S.J., Riehle, M.O., Johnstone, H.J.H., Affrossman, S. & Curtis, A.S.G. Increasing fibroblast response to materials using nanotopography: morphological and genetic measurements of cell response to 13-nm-high polymer demixed islands. *Experimental cell research* **276**, 1-9(2002).

55. Dalby, M.J., Riehle, M.O., Johnstone, H.J.H., Affrossman, S. & Curtis, A.S.G. Investigating the limits of filopodial sensing: a brief report using SEM to image the interaction between 10 nm high nano-topography and fibroblast filopodia. *Cell biology international* **28**, 229-36(2004).

56. Washburn, N.R., Yamada, K.M., Simon, C.G., Kennedy, S.B. & Amis, E.J. High-throughput investigation of osteoblast response to polymer crystallinity: influence of nanometer-scale roughness on proliferation. *Biomaterials* **25**, 1215-24

57. Oh, S., Brammer, K.S., Li, Y.S.J., Teng, D., Engler, A.J., Chien, S. & Jin, S. Stem cell fate dictated solely by altered nanotube dimension. *Proceedings of the National Academy of Sciences of the United States of America* **106**, 2130-5(2009).

58. Brammer, K.S., Oh, S., Cobb, C.J., Bjursten, L.M., Heyde, H. van der & Jin, S. Improved bone-forming functionality on diameter-controlled TiO(2) nanotube surface. *Acta biomaterialia* **5**, 3215-23(2009).

59. Park, J., Bauer, S., Mark, K. von der & Schmuki, P. Nanosize and vitality: TiO2 nanotube diameter directs cell fate. *Nano letters* **7**, 1686-91(2007).

60. Park, J., Bauer, S., Schlegel, K.A., Neukam, F.W., Mark, K. von der & Schmuki, P. TiO2 nanotube surfaces: 15 nm--an optimal length scale of surface topography for cell adhesion and differentiation. *Small (Weinheim an der Bergstrasse, Germany)* **5**, 666-71(2009).

61. Dalby, M.J., Gadegaard, N., Tare, R., Andar, A., Riehle, M.O., Herzyk, P., Wilkinson, C.D.W. & Oreffo, R.O.C. The control of human mesenchymal cell differentiation using nanoscale symmetry and disorder. *Nature materials* **6**, 997-1003(2007).

62. Chen, C.S. Geometric Control of Cell Life and Death. *Science* **276**, 1425-1428(1997).

63. McBeath, R., Pirone, D.M., Nelson, C.M., Bhadriraju, K. & Chen, C.S. Cell shape, cytoskeletal tension, and RhoA regulate stem cell lineage commitment. *Developmental cell* **6**, 483-95(2004).

64. Théry, M., Racine, V., Pépin, A., Piel, M., Chen, Y., Sibarita, J.-B. & Bornens, M. The extracellular matrix guides the orientation of the cell division axis. *Nature cell biology* **7**, 947-53(2005).

65. Théry, M., Racine, V., Piel, M., Pépin, A., Dimitrov, A., Chen, Y., Sibarita, J.-B. & Bornens, M. Anisotropy of cell adhesive microenvironment governs cell internal organization and orientation of polarity. *Proceedings of the National Academy of Sciences of the United States of America* **103**, 19771-6(2006).

66. Slater, J.H. & Frey, W. Nanopatterning of fibronectin and the influence of integrin clustering on

endothelial cell spreading and proliferation. *Journal of biomedical materials research. Part A* **87**, 176-95(2008).

67. Arnold, M., Schwieder, M., Blümmel, J., Cavalcanti-Adam, E.A., López-García, M., Kessler, H., Geiger, B. & Spatz, J.P. Cell interactions with hierarchically structured nano-patterned adhesive surfaces. *Soft Matter* **5**, 72(2009).

68. Berry, C.C., Curtis, A.S.G., Oreffo, R.O.C., Agheli, H. & Sutherland, D.S. Human fibroblast and human bone marrow cell response to lithographically nanopatterned adhesive domains on protein rejecting substrates. *IEEE transactions on nanobioscience* **6**, 201-9(2007).

69. Davidson, P.M., Bigerelle, M., Bounichane, B., Giazzon, M. & Anselme, K. Definition of a simple statistical parameter for the quantification of orientation in two dimensions: application to cells on grooves of nanometric depths. *Acta biomaterialia* **6**, 2590-8(2010).

70. Davidson, P.M., Özçelik, H., Hasirci, V., Reiter, G. & Anselme, K. Microstructured Surfaces Cause Severe but Non-Detrimental Deformation of the Cell Nucleus. *Advanced Materials* **21**, 3586-3590(2009).

71. Davidson, P.M., Fromigué, O., Marie, P.J., Hasirci, V., Reiter, G. & Anselme, K. Topographically induced self-deformation of the nuclei of cells: dependence on cell type and proposed mechanisms. *Journal of materials science. Materials in medicine* **21**, 939-46(2010).

72. Boyan, B. Role of material surfaces in regulating bone and cartilage cell response. *Biomaterials* **17**, 137-146(1996).

73. Yang, J.-Y., Ting, Y.-C., Lai, J.-Y., Liu, H.-L., Fang, H.-W. & Tsai, W.-B. Quantitative analysis of osteoblast-like cells (MG63) morphology on nanogrooved substrata with various groove and ridge dimensions. *Journal of biomedical materials research. Part A* **90**, 629-40(2009).

74. Sutherland, J., Denyer, M. & Britland, S. Contact guidance in human dermal fibroblasts is modulated by population pressure. *Journal of anatomy* **206**, 581-7(2005).

75. Lee, C.H., Shin, H.J., Cho, I.H., Kang, Y.-M., Kim, I.A., Park, K.-D. & Shin, J.-W. Nanofiber alignment and direction of mechanical strain affect the ECM production of human ACL fibroblast. *Biomaterials* **26**, 1261-70(2005).

76. Crouch, A.S., Miller, D., Luebke, K.J. & Hu, W. Correlation of anisotropic cell behaviors with topographic aspect ratio. *Biomaterials* **30**, 1560-7(2009).

77. Teixeira, A.I., Abrams, G. a, Bertics, P.J., Murphy, C.J. & Nealey, P.F. Epithelial contact guidance on well-defined micro- and nanostructured substrates. *Journal of cell science* **116**, 1881-92(2003).

78. Andersson, a Nanoscale features influence epithelial cell morphology and cytokine production. *Biomaterials* **24**, 3427-3436(2003).

79. Lenhert, S., Meier, M.-B., Meyer, U., Chi, L. & Wiesmann, H.P. Osteoblast alignment, elongation and migration on grooved polystyrene surfaces patterned by Langmuir-Blodgett lithography. *Biomaterials* **26**, 563-70(2005).

80. Meyle, J., Gültig, K. & Nisch, W. Variation in contact guidance by human cells on a microstructured surface. *Journal of biomedical materials research* **29**, 81-8(1995).

81. McCartney, M.D. & Buck, R.C. Comparison of the degree of contact guidance between tumor cells and normal cells in vitro. *Cancer research* **41**, 3046-51(1981).

82. Chen, C. Cell shape provides global control of focal adhesion assembly. *Biochemical and Biophysical Research Communications* **307**, 355-361(2003).

83. Folkman, J. & Moscona, A. Role of cell shape in growth control. *Nature* **273**, 345-349(1978).

84. Kooten, T.G. van, Whitesides, J.F. & Recum, A.F. von Influence of silicone (PDMS) surface texture on human skin fibroblast proliferation as determined by cell cycle analysis. *Journal of Biomedical Materials Research* **43**, 1-14(1998).

85. Perizzolo, D., Lacefield, W.R. & Brunette, D.M. Interaction between topography and coating in the formation of bone nodules in culture for hydroxyapatite- and titanium-coated micromachined surfaces. *Journal of biomedical materials research* **56**, 494-503(2001).

86. Matsuzaka, K., Yoshinari, M., Shimono, M. & Inoue, T. Effects of multigrooved surfaces on osteoblast-like cells in vitro: scanning electron microscopic observation and mRNA expression of osteopontin and osteocalcin. *Journal of biomedical materials research. Part A* **68**, 227-34(2004).

87. Khakbaznejad, A., Chehroudi, B. & Brunette, D.M. Effects of titanium-coated micromachined grooved substrata on orienting layers of osteoblast-like cells and collagen fibers in culture. *Journal of biomedical materials research. Part A* **70**, 206-18(2004).

88. Flemming, R.G., Murphy, C.J., Abrams, G. a, Goodman, S.L. & Nealey, P.F. Effects of synthetic micro- and nano-structured surfaces on cell behavior. *Biomaterials* **20**, 573-88(1999).

89. Loesberg, W. a, Riet, J. te, Delft, F.C.M.J.M. van, Schön, P., Figdor, C.G., Speller, S., Loon, J.J.W. a van, Walboomers, X.F. & Jansen, J. a The threshold at which substrate nanogroove dimensions may influence fibroblast alignment and adhesion. *Biomaterials* **28**, 3944-51(2007).

90. Yim, E.K.F., Reano, R.M., Pang, S.W., Yee, A.F., Chen, C.S. & Leong, K.W. Nanopattern-induced changes in morphology and motility of smooth muscle cells. *Biomaterials* **26**, 5405-13(2005).

91. Biggs, M.J.P., Richards, R.G., McFarlane, S., Wilkinson, C.D.W., Oreffo, R.O.C. & Dalby, M.J. Adhesion formation of primary human osteoblasts and the functional response of mesenchymal stem cells to 330nm deep microgrooves. *Journal of the Royal Society, Interface / the Royal Society* **5**, 1231-42(2008).

92. Fujita, S., Ono, D., Ohshima, M. & Iwata, H. Supercritical CO2-assisted embossing for studying cell behaviour on microtextured surfaces. *Biomaterials* **29**, 4494-500(2008).

93. Lu, X. & Leng, Y. Quantitative analysis of osteoblast behavior on microgrooved hydroxyapatite and titanium substrata. *Journal of biomedical materials research. Part A* **66**, 677-87(2003).

94. Tzvetkova-Chevolleau, T., Stéphanou, A., Fuard, D., Ohayon, J., Schiavone, P. & Tracqui, P. The motility of normal and cancer cells in response to the combined influence of the substrate rigidity and anisotropic microstructure. *Biomaterials* **29**, 1541-51(2008).

95. Anselme, K., Broux, O., Noel, B., Bouxin, B., Bascoulergue, G., Dudermel, A.-F., Bianchi, F., Jeanfils, J. & Hardouin, P. In vitro control of human bone marrow stromal cells for bone tissue engineering. *Tissue engineering* **8**, 941-53(2002).

96. Dunn, G. a & Brown, a F. Alignment of fibroblasts on grooved surfaces described by a simple geometric transformation. *Journal of cell science* **83**, 313-40(1986).

97. Lomri, a, Marie, P.J., Escurat, M. & Portier, M.M. Cytoskeletal protein synthesis and organization in cultured mouse osteoblastic cells. Effects of cell density. *FEBS letters* **222**, 311-6(1987).

98. Clark, P., Connolly, P., Curtis, A.S.G., Dow, J. a & Wilkinson, C.D.W. Cell guidance by ultrafine topography in vitro. *Journal of cell science* **99 (Pt 1)**, 73-7(1991).

99. Farley, J.R., Hall, S.L., Herring, S., Tarbaux, N.M., Matsuyama, T. & Wergedal, J.E. Skeletal alkaline phosphatase specific activity is an index of the osteoblastic phenotype in subpopulations of the human osteosarcoma cell line SaOS-2☆. *Metabolism* **40**, 664-671(1991).

100. Kasperk, C.H., Faehling, K., Börcsök, I. & Ziegler, R. Effects of androgens on subpopulations of the human osteosarcoma cell line SaOS2. *Calcified Tissue International* **58**, 376-382(1996).

101. Dey, P. Cancer nucleus: Morphology and beyond. *Diagnostic Cytopathology* **38**, 382–390(2010).

102. Docheva, D., Padula, D., Popov, C., Mutschler, W., Clausen-Schaumann, H. & Schieker, M. Researching into the cellular shape, volume and elasticity of mesenchymal stem cells, osteoblasts and osteosarcoma cells by atomic force microscopy. *Journal of cellular and molecular medicine* **12**, 537-52(2008).

103. Reinsch, S. & Gönczy, P. Mechanisms of nuclear positioning. *Journal of cell science* **111**, 2283-95(1998).

104. Ellenbroek, S.I.J. & Collard, J.G. Rho GTPases: functions and association with cancer. *Clinical & experimental metastasis* **24**, 657-72(2007).

105. Carley, W.W., Barak, L.S. & Webb, W.W. F-actin aggregates in transformed cells. *The Journal of cell biology* **90**, 797-802(1981).

106. Katsantonis, J., Tosca, a, Koukouritaki, S.B., Theodoropoulos, P. a, Gravanis, a & Stournaras, C. Differences in the G/total actin ratio and microfilament stability between normal and malignant human keratinocytes. *Cell biochemistry and function* **12**, 267-74(1994).

107. Lee, J.S.H., Chang, M.I., Tseng, Y. & Wirtz, D. Cdc42 mediates nucleus movement and MTOC polarization in Swiss 3T3 fibroblasts under mechanical shear stress. *Molecular biology of the cell* **16**, 871-80(2005).

108. Su, W.-T., Chu, I.-M., Yang, J.-Y. & Lin, C.-D. The geometric pattern of a pillared substrate influences the cell-process distribution and shapes of fibroblasts. *Micron (Oxford, England : 1993)* **37**, 699-706(2006).

109. Matschegewski, C., Staehlke, S., Loeffler, R., Lange, R., Chai, F., Kern, D.P., Beck, U. & Nebe, B.J. Cell architecture-cell function dependencies on titanium arrays with regular geometry. *Biomaterials* **31**, 5729-40(2010).

110. Steinberg, T., Schulz, S., Spatz, J.P., Grabe, N., Müssig, E., Kohl, A., Komposch, G. & Tomakidi, P. Early keratinocyte differentiation on micropillar interfaces. *Nano letters* **7**, 287-94(2007).

111. Mussig, E., Steinberg, T., Schulz, S., Spatz, J.P., Ulmer, J., Grabe, N., Kohl, A., Komposch, G. & Tomakidi, P. Connective-Tissue Fibroblasts Established on Micropillar Interfaces are Pivotal for Epithelial-Tissue Morphogenesis. *Advanced Functional Materials* **18**, 2919–2929(2008).

112. Thakar, R.G., Chown, M.G., Patel, A., Peng, L., Kumar, S. & Desai, T. a Contractility-dependent modulation of cell proliferation and adhesion by microscale topographical cues. *Small (Weinheim an der Bergstrasse, Germany)* **4**, 1416-24(2008).

113. Tan, J.L., Tien, J., Pirone, D.M., Gray, D.S., Bhadriraju, K. & Chen, C.S. Cells lying on a bed of microneedles: an approach to isolate mechanical force. *Proceedings of the National Academy of*

Sciences of the United States of America **100**, 1484-9(2003).

114. Bischofs, I.B., Schmidt, S. & Schwarz, U. Effect of Adhesion Geometry and Rigidity on Cellular Force Distributions. *Physical Review Letters* **103**, 1-4(2009).

115. Tsai, W.-B., Ting, Y.-C., Yang, J.-Y., Lai, J.-Y. & Liu, H.-L. Fibronectin modulates the morphology of osteoblast-like cells (MG-63) on nano-grooved substrates. *Journal of materials science. Materials in medicine* **20**, 1367-78(2009).

116. Dalby, M.J., Riehle, M.O., Yarwood, S.J., Wilkinson, C.D.W. & Curtis, A.S.G. Nucleus alignment and cell signaling in fibroblasts: response to a micro-grooved topography. *Experimental Cell Research* **284**, 272-280(2003).

117. Oyajobi, B.O., Lomri, a, Hott, M. & Marie, P.J. Isolation and characterization of human clonogenic osteoblast progenitors immunoselected from fetal bone marrow stroma using STRO-1 monoclonal antibody. *Journal of bone and mineral research : the official journal of the American Society for Bone and Mineral Research* **14**, 351-61(1999).

118. Fromigué, O., Kheddoumi, N., Lomri, a, Marie, P.J. & Body, J.J. Breast cancer cells release factors that induced apoptosis in human bone marrow stromal cells. *Journal of bone and mineral research : the official journal of the American Society for Bone and Mineral Research* **16**, 1600-10(2001).

119. Rodan, S.B., Imai, Y., Thiede, M. a, Wesolowski, G., Thompson, D., Bar-Shavit, Z., Shull, S., Mann, K. & Rodan, G. a Characterization of a human osteosarcoma cell line (Saos-2) with osteoblastic properties. *Cancer research* **47**, 4961-6(1987).

120. Myers, K. a, Rattner, J.B., Shrive, N.G. & Hart, D. a Osteoblast-like cells and fluid flow: cytoskeleton-dependent shear sensitivity. *Biochemical and biophysical research communications* **364**, 214-9(2007).

121. Weder, G., Vörös, J., Giazzon, M., Matthey, N., Heinzelmann, H. & Liley, M. Measuring cell adhesion forces during the cell cycle by force spectroscopy. *Biointerphases* **4**, 27-34(2009).

122. Mansell, J.P., Farrar, D., Jones, S. & Nowghani, M. Cytoskeletal reorganisation, 1alpha,25-dihydroxy vitamin D3 and human MG63 osteoblast maturation. *Molecular and cellular endocrinology* **305**, 38-46(2009).

123. Keller, H., Zadeh, A.D. & Eggli, P. Localised depletion of polymerised actin at the front of Walker carcinosarcoma cells increases the speed of locomotion. *Cell motility and the cytoskeleton* **53**, 189-202(2002).

124. Norvell, S.M., Ponik, S.M., Bowen, D.K., Gerard, R. & Pavalko, F.M. Fluid shear stress induction of COX-2 protein and prostaglandin release in cultured MC3T3-E1 osteoblasts does not require intact microfilaments or microtubules. *Journal of applied physiology (Bethesda, Md. : 1985)* **96**, 957-66(2004).

125. Parreno, J., Buckley-Herd, G., de-Hemptinne, I. & Hart, D. a Osteoblastic MG-63 cell differentiation, contraction, and mRNA expression in stress-relaxed 3D collagen I gels. *Molecular and cellular biochemistry* **317**, 21-32(2008).

126. Wang, N. Mechanical interactions among cytoskeletal filaments. *Hypertension* **32**, 162-5(1998).

127. Galigniana, M.D., Scruggs, J.L., Herrington, J., Welsh, M.J., Carter-Su, C., Housley, P.R. & Pratt, W.B. Heat shock protein 90-dependent (geldanamycin-inhibited) movement of the glucocorticoid

receptor through the cytoplasm to the nucleus requires intact cytoskeleton. *Molecular endocrinology (Baltimore, Md.)* **12**, 1903-13(1998).

128. Kumar, N., Robidoux, J., Daniel, K.W., Guzman, G., Floering, L.M. & Collins, S. Requirement of vimentin filament assembly for beta3-adrenergic receptor activation of ERK MAP kinase and lipolysis. *The Journal of biological chemistry* **282**, 9244-50(2007).

129. Fukuda, K., Iwasaka, T., Hachisuga, T., Sugimori, H., Tsugitomi, H. & Mutoh, F. Immunocytochemical detection of S-phase cells in normal and neoplastic cervical epithelium by anti-BrdU monoclonal antibody. *Analytical and quantitative cytology and histology / the International Academy of Cytology [and] American Society of Cytology* **12**, 135-8(1990).

130. Taddei, A., Hediger, F., Neumann, F.R. & Gasser, S.M. The function of nuclear architecture: a genetic approach. *Annual review of genetics* **38**, 305-45(2004).

131. Reddy, K.L., Zullo, J.M., Bertolino, E. & Singh, H. Transcriptional repression mediated by repositioning of genes to the nuclear lamina. *Nature* **452**, 243-7(2008).

132. Martin, J.Y., Schwartz, Z., Hummert, T.W., Schraub, D.M., Simpson, J., Lankford, J., Dean, D.D., Cochran, D.L. & Boyan, B.D. Effect of titanium surface roughness on proliferation, differentiation, and protein synthesis of human osteoblast-like cells (MG63). *Journal of biomedical materials research* **29**, 389-401(1995).

133. Jäger, M., Zilkens, C., Zanger, K. & Krauspe, R. Significance of nano- and microtopography for cell-surface interactions in orthopaedic implants. *Journal of biomedicine & biotechnology* **2007**, 69036(2007).

134. Philip, J.T. & Dahl, K.N. Nuclear mechanotransduction: response of the lamina to extracellular stress with implications in aging. *Journal of biomechanics* **41**, 3164-70(2008).

135. Heessen, S., Leonchiks, A., Issaeva, N., Sharipo, A., Selivanova, G., Masucci, M.G. & Dantuma, N.P. Functional p53 chimeras containing the Epstein-Barr virus Gly-Ala repeat are protected from Mdm2- and HPV-E6-induced proteolysis. *Proceedings of the National Academy of Sciences of the United States of America* **99**, 1532-7(2002).

136. Ochalek, T., Nordt, F.J., Tullberg, K. & Burger, M.M. Correlation between cell deformability and metastatic potential in B16-F1 melanoma cell variants. *Cancer research* **48**, 5124-8(1988).

137. Tzanakakis, G.N., Nikitovic, D., Katonis, P., Kanakis, I. & Karamanos, N.K. Expression and distribution of N-acetyl and N- glycolylneuraminic acids in secreted and cell-associated glycoconjugates by two human osteosarcoma cell lines. *Biomedical Chromatography* **21**, 406-409(2007).

138. Pautke, C., Schieker, M., Tischer, T., Kolk, A., Neth, P., Mutschler, W. & Milz, S. Characterization of osteosarcoma cell lines MG-63, Saos-2 and U-2 OS in comparison to human osteoblasts. *Anticancer research* **24**, 3743-8

139. Frolov, V.A. & Zimmerberg, J. Membranes: Shaping biological matter. *Nature materials* **8**, 173-4(2009).

140. He, S., Dunn, K.L., Espino, P.S., Drobic, B., et al. Chromatin organization and nuclear microenvironments in cancer cells. *Journal of cellular biochemistry* **104**, 2004-15(2008).

141. Boehm, J.S. & Hahn, W.C. Immortalized cells as experimental models to study cancer. *Cytotechnology* **45**, 47-59(2004).

142. Chantret, I., Barbat, a, Dussaulx, E., Brattain, M.G. & Zweibaum, a Epithelial polarity, villin expression, and enterocytic differentiation of cultured human colon carcinoma cells: a survey of twenty cell lines. *Cancer research* **48**, 1936-42(1988).

143. Violante, G. Da, Zerrouk, N., Richard, I., Frendo, J.-L., et al. Short term Caco-2/TC7 cell culture: comparison between conventional 21-d and a commercially available 3-d system. *Biological & pharmaceutical bulletin* **27**, 1986-92(2004).

144. Bonhomme, C., Duluc, I., Martin, E., Chawengsaksophak, K., Chenard, M.-P., Kedinger, M., Beck, F., Freund, J.-N. & Domon-Dell, C. The Cdx2 homeobox gene has a tumour suppressor function in the distal colon in addition to a homeotic role during gut development. *Gut* **52**, 1465-71(2003).

145. Bidwell, J.P., Alvarez, M., Feister, H., Onyia, J. & Hock, J. Nuclear matrix proteins and osteoblast gene expression. *Journal of bone and mineral research : the official journal of the American Society for Bone and Mineral Research* **13**, 155-67(1998).

146. Gerlitz, G. & Bustin, M. The role of chromatin structure in cell migration. *Trends in cell biology* **21**, 6-11(2010).

147. Friedl, P., Wolf, K. & Lammerding, J. Nuclear mechanics during cell migration. *Current opinion in cell biology* **23**, 55-64(2010).

148. Théry, M. & Bornens, M. Get round and stiff for mitosis. *HFSP journal* **2**, 65-71(2008).

149. Théry, M., Jiménez-Dalmaroni, A., Racine, V., Bornens, M. & Jülicher, F. Experimental and theoretical study of mitotic spindle orientation. *Nature* **447**, 493-6(2007).

150. Théry, M. & Bornens, M. Cell shape and cell division. *Current opinion in cell biology* **18**, 648-57(2006).

151. Engler, A.J., Sen, S., Sweeney, H.L. & Discher, D.E. Matrix elasticity directs stem cell lineage specification. *Cell* **126**, 677-89(2006).